University of Alberta

Fundamental Behaviour of Composite Tailings

by

Juliana Tang ©

A thesis submitted to the Faculty of Graduate Studies and Research in partial fulfilment

of the requirements for the degree of *Master of Science*

in

Geoenvironmental Engineering

Department of Civil & Environmental Engineering

Edmonton, Alberta

Fall 1997

National Library
of Canada

Acquisitions and
Bibliographic Services

395 Wellington Street
Ottawa ON K1A 0N4
Canada

Bibliothèque nationale
du Canada

Acquisitions et
services bibliographiques

395, rue Wellington
Ottawa ON K1A 0N4
Canada

Your file Votre référence

Our file Notre référence

The author has granted a non-exclusive licence allowing the National Library of Canada to reproduce, loan, distribute or sell copies of this thesis in microform, paper or electronic formats.

The author retains ownership of the copyright in this thesis. Neither the thesis nor substantial extracts from it may be printed or otherwise reproduced without the author's permission.

L'auteur a accordé une licence non exclusive permettant à la Bibliothèque nationale du Canada de reproduire, prêter, distribuer ou vendre des copies de cette thèse sous la forme de microfiche/film, de reproduction sur papier ou sur format électronique.

L'auteur conserve la propriété du droit d'auteur qui protège cette thèse. Ni la thèse ni des extraits substantiels de celle-ci ne doivent être imprimés ou autrement reproduits sans son autorisation.

0-612-22680-8

Canada

University of Alberta

Library Release Form

Name of Author: *Juliana Tang*

Title of Thesis: *Fundamental Behaviour of Composite Tailings*

Degree: *Master of Science*

Year this Degree Granted: *1997*

Permission is hereby granted to the University of Alberta Library to reproduce single copies of this thesis and to lend or sell such copies for private, scholarly, or scientific research purposes only.

The author reserves all other publication and other rights in association with the copyright in the thesis, and except as herein before provided, neither the thesis nor any substantial portion thereof may be printed or otherwise reproduced in any material form whatever without the author's prior written permission.

Juliana Tang
1512-48th Street
Edmonton, Alberta
T6L 6H9

October 3, 1997
Date submitted to FGSR

University of Alberta

Faculty of Graduate Studies and Research

The undersigned certify that they have read, and recommend to the Faculty of Graduate Studies and Research for acceptance, a thesis entitled, *Fundamental Behaviour of Composite Tailings* submitted by *Juliana Tang* in partial fulfillment of the requirements for the degree of Master of Science in Geoenvironmental Engineering.

Kevin Biggar
Dr. K.W. Biggar
Supervisor

D Sego
Dr. D.C. Sego
Supervisor

J. D. Scott
Dr. J.D. Scott
Co-Supervisor

M.J. Dudas
Dr. J.M. Dudas
External Examiner

Dr. S.J. Stanley
External Examiner

Date: Oct 3/97

ABSTRACT

The thesis research had two main purposes, an introductory and a principal study. The introductory study examined how the MFT card-house structure is formed and determined what chemicals in the MFT pore water contribute to the formation of the structure. Examination of the clay structure using a Scanning Electron Microscope suggested that bicarbonate, sodium hydroxide, bitumen and the *strongly bound* organic matter may contribute to the formation of the *card-house* structure. Sodium naphthenates appeared to have no effect on the structure. High temperature used in the bitumen extraction process appeared to enhance the structure, and the addition of laboratory grade gypsum (LGG) strengthened the structure.

The principal study examined the effects of varying clay contents (<2μm) in MFT on the segregation and consolidation behaviour of composite tailings (CT). Standpipe tests performed on tailings with 36%, 55%, and 70% clay content MFT treated with 900g/m^3 of LGG showed that the *clay:water* ratio at the segregation boundaries were 0.085, 0.090, and 0.118 respectively. It is found that tailings with lower clay content MFT required higher solids content to form CT. A unique segregation boundary which relates the initial void ratio, clay mineral fraction of tailings, and clay to clay-water (C/(C+W)) ratio was generated for all the test samples. The initial consolidation behaviour of CT was found to be more dependent on the bitumen content in the MFT than the MFT's clay content. It was found that the higher the bitumen content, the lower the initial consolidation rate of CT.

Acknowledgements

I would like to thank my supervisors, Dr. K.W. Biggar, Dr. J.D. Scott, and Dr. D.C. Sego for their encouragement and guidance throughout the coarse of this study. Their technical and financial support, patience, and attention are deeply appreciated. This has been an extremely valuable experience for me and I am very thankful that they were there to assist and guide me. Special thanks to Nagula Suthaker and Gilbert Wong who have also assisted me in the study.

I would also like to extend my extreme gratitude to the geotechnical technicians, Christine Hereygers, Steve Gamble, and Gerry Cyre. Especially to Christine who has endured many days of my interruptions, bad jokes, and assisted me in fixing those annoying filters.

Special thanks to all my friends and colleagues who made this journey more interesting and less stressful.

Most importantly, I would like to thank my beloved family, and the Turner family for their never ending love and support.

TABLE OF CONTENTS

Abstract

1.0 Introduction 1

- 1.1 Problem Statement 1
- 1.2 Research Objectives 3
- 1.3 Scope of Thesis 4
- 1.4 Organisation of Thesis 5

2.0 Overview of Oil Sands Operation and Tailings Management 7

- 2.1 Oil Sands Operation at Syncrude Canada Limited 7
- 2.2 Characteristics of MFT 10
  - 2.2.1 Geotechnical Properties 10
  - 2.2.2 Water Chemistry Properties 13
    - 2.2.2.1 Organic Compounds in MFT Pore Water 13
    - 2.2.2.2 Inorganic Compounds in MFT Pore Water 15
- 2.3 Tailings Management Techniques 15

3.0 Examination of MFT Microstructure Using Scanning Electron Microscope 29

- 3.1 Literature Review 29
  - 3.1.1 Flocculation and Dispersion of Clays in Colloidal Solution 29
  - 3.1.2 Theories Developed to Explain the Structure of MFT 33
  - 3.1.3 The Functions of a Scanning Electron Microscope (SEM) 35
  - 3.1.4 Issues on Artefact Observed in Cryogenically Prepared Samples 37
- 3.2 Experimental Procedures and Sample Preparation 39
  - 3.2.1 Index Tests 39
  - 3.2.2 Cavity Expansion Test 42
  - 3.2.3 Slurry Samples Preparation Procedures for a Scanning Electron Microscope 44

3.2.3.1 Freeze-drying/fracturing Method 46

3.3 Results and Discussion 47

3.3.1 Material Properties 47

3.3.2 Is the Observed Clay Structure an Artefact of the SEM Preparation Procedure? 51

3.3.3 Effects of Various Pore Water Chemicals on the MFT Structure 54

3.3.4 Settling of Clay Particles Observed in the SEM Samples 60

3.3.5 Engineering Applications 61

3.4 Summary 63

4.0 Effects of Varying Clay Content on Composite Tailings Behaviour 88

4.1 Literature Review 88

4.1.1 Fine Tailings Deposition Problem 88

4.1.2 Slurry Property Diagram 90

4.1.3 Composite Tailings Background 91

4.2 Definitions 98

4.3 Experimental Procedures and Design 100

4.3.1 Material Preparation 101

4.3.2 Index Tests 104

4.3.3 Slurry Samples Preparation for SEM 106

4.3.4 Experimental Program for Standpipe Tests 106

4.3.5 Standpipe Tests 108

4.4 Results 110

4.4.1 Material Properties 110

4.4.2 Scanning Electron Micro-graphs of CT 112

4.4.3 Standpipe Tests Results for Tailings with 36%, 55%, and 70% Clay Content MFT 114

4.5 Discussion 117

4.5.1 Material Properties 117

4.5.2 Composite Tailings Micro-structure Examination 120

4.5.3 Segregation Boundary 121
4.5.4 Initial Consolidation Behaviour 125
4.5.5 Engineering Application 129
4.6 Summary 130

5.0 Conclusion and Recommendations 183
5.1 Conclusions to the Introductory Study (Chapter 3) 184
5.2 Conclusion to the Principal Study (Chapter 4) 185
5.3 Recommendations 188
5.3.1 Recommendations for Field Operations 188
5.3.2 Recommendations for Future Research 189

6.0 References 191
Appendix 1: Sample Calculations 196

LIST OF TABLES

Table 2.1: Major inorganic icons in a water sample from Syncrude's MFT 19

Table 3.1: Samples prepared for scanning electron microscopy 67

Table 3.2: The results of Atterberg limits of MFT samples and kaolinite samples 68

Table 3.3: MFT properties 68

Table 3.4: MFT water analysis 68

Table 3.5: MFT water analysis of diluted pore water 69

Table 4.1: Samples collected for SEM. 134

Table 4.2: Solids, fines, clay, bitumen contents of MFT, sands, and pond water used in CT. 134

Table 4.3: Atterberg limits test results for 36% clay content MFT, and 70% clay content MFT. 135

Table 4.4: Colloidal properties of the 36% clay content MFT, MFT-55, and 70% clay content MFT. 135

Table 4.5: The comparison between the clay mineral fraction (CMF) obtained from hydrometer test and methylene blue test. 136

Table 4.6: Water chemistry analysis results for the 36%, and 70% clay content MFT. 136

Table 4.7: *Clay:water* ratios for 36%, 55%, and 70% clay content MFT. The shaded and italised *clay:water* ratios were chosen for standpipe tests. 137

Table 4.8: Summary data of the sedimentation test for tailings samples with 36% clay content MFT. 138

Table 4.9: Determination of a segregated or non-segregated mix using segregation index and fines captured parameters for 36% clay content in MFT. 139

Table 4.10: Summary data of sedimentation test for tailings samples with 55% clay content MFT. 140

Table 4.11: Determination of a segregated or non-segregated mix using segregation index and fines captured parameters for 55% clay content in MFT. 141

Table 4.12: Summary data of sedimentation test for tailings samples with 70% clay content MFT. 142

Table 4.13: Determination of a segregated or non-segregated mix using segregation index and fines captured parameters for 70% clay content in MFT. 143

Table 4.14: Comparison between the initial void ratios, CMF, and the consolidation behaviour for CT with 36%, 55%, or 70% clay content MFT. 144

LIST OF FIGURES

Figure 2.1: A simplified cross-section of the geology near the Syncrude Canada mine site 20

Figure 2.2: Map showing the locations of the Athabasca oil sands deposits and the Syncrude and Suncor extraction operations 21

Figure 2.3: Diagram showing the oil sands operation at the Syncrdue mine site 22

Figure 2.4: A model of the Athabasca oil sands 23

Figure 2.5: Schematic of the oils sands extraction process 24

Figure 2.6: Plan view of Syncrude site 25

Figure 2.7: A typical size distribution of oil sands fine tailings 26

Figure 2.8: Plasticity of various mine waste sludges 27

Figure 2.9: Cross section of the interface of the fine tailings zone and the water capping layer. The detrital zone of high benthic and microbial activity at the interface is shown. 28

Figure 3.1: a) Repulsion and attraction forces between platelike clay particles represented as quadrupoles
b) Cardhouse structure due to quadrupole interactions
c) Chain spatial arrangement of dipole 70

Figure 3.2 : A schematic of a scanning electron microscope column 71

Figure 3.3: The experimental set-up for the cavity expansion test 72

Figure 3.4: Grain size distibution for MFT (SY-22), kaolinite clay and silica flour 73

Figure 3.5: a) MFT exposed to fast freezing rate
b) MFT exposed to slow freezing rate 74

Figure 3.6: MFT (SY-22) 75

Figure 3.7: a) Kaolinite slurry with ESR near 2.0
b) Silica flour slurry with ESR near 2.0 76

Figure 3.8: Confocal micrograph of a MFT sample that was unfrozen and observed using the confocal optical technique 77

Figure 3.9: Electron micrograph of a MFT sample that was vibrated to destroy the floc structure and allowed to sit for only a short time before rapidly frozen 78

Figure 3.10: Electron micrograph of a MFT sample that was vibrated and then frozen immediately 79

Figure 3.11: Kaolinite clay mixed with deionized water 80
Figure 3.12: Kaolinite clay mixed with MFT pond water 81
Figure 3.13: Kaolinite clay mixed with deionized water and bicarbonate 82
Figure 3.14: Kaolinite clay mixed with deionized water and NaOH 83
Figure 3.15: Kaolinite clay mixed with sodium naphthenate solution 84
Figure 3.16: MFT was cnetrifuged twice and the pore water was replaced with deionized water 85
Figure 3.17: MFT mixed with 2500ppm of laboratory grade gypsum 86
Figure 3.18: Kaolinite clay mixed with MFT pond water and heated to 80°C 87

Figure 4.1: Grain size distrubution of tailings stream, clay-shale fines, and oil sands 145
Figure 4.2: Slurry Property Diagram for Syncrude Tailings 146
Figure 4.3: Segregation of CaO tailings 147
Figure 4.4: Segregation boundaries for Syncrude tailings stream and CaO treated tailings (modified) 148
Figure 4.5: Segregation boundary for Syncrude Composite Tailings 149
Figure 4.6: Schematic of the separated layers. 150
Figure 4.7: Filtering tube used during the separation process 151
Figure 4.8: Suncor segregation test results for 600ppm of agricultured grade gyspum 152
Figure 4.9: Segregation boundary obtained from data in Figure 4.8 153
Figure 4.10: Flow chart illustrating the experimental program 154
Figure 4.11: Blade used for mixing CT 155
Figure 4.12: Grain size distribution of low clay content MFT, MFT-55 (SY-22) and high clay content MFT 156
Figure 4.13: Grain size distribution of beach sand 157
Figure 4.14: a) 36% clay content MFT
b) 70% clay content MFT 158
Figure 4.15: 36% clay content MFT mixed with 2500g/m^3 of laboratory grade gypsum 159

Figure 4.16: 70% clay content mixed with 2500g/m^3 of laboratory grade gypsum 160

Figure 4.17: CT with 36% clay content MFT mixed with 2500g/m^3 of laboratory grade gypsum (Magnification at 200X) 161

Figure 4.18: CT with 55% clay content MFT mixed with 2500g/m^3 of laboratory grade gypsum (Magnification at 200X) 162

Figure 4.19: CT with 70% clay content MFT mixed with 2500g/m^3 of laboratory grade gypsum (Magnification at 200X) 163

Figure 4.20: CT with 36% clay content MFT mixed with 2500g/m^3 of laboratory grade gypsum (Magnification at 500X) 164

Figure 4.21: CT with 55% clay content MFT mixed with 2500g/m^3 of laboratory grade gypsum (Magnification at 500X) 165

Figure 4.22: CT with 70% clay content MFT mixed with 2500g/m^3 of laboratory grade gypsum (Magnification at 500X) 166

Figure 4.23: Clay/Water ratio boundary for tailings with 36% clay content MFT 167

Figure 4.24: Fines vs. Initial Void Ratio and F/(F+W) for tailings with 36% clay content MFT 168

Figure 4.25: Solids content profile for tailings with 36% clay content MFT 169

Figure 4.26: Standpipe testing progress for tailings with 36% clay content MFT 170

Figure 4.27: Clay/Water ratio boundary for tailings with 55% clay content MFT 171

Figure 4.28: Fines vs. Initial Void Ratio and F/(F+W) for tailings with 55% clay content MFT 172

Figure 4.29: Solids content profile for tailings with 55% clay content MFT 173

Figure 4.30: Standpipe testing progress for tailings with 55% clay content MFT 174

Figure 4.31: Clay/Water ratio boundary for tailings with 70% clay content MFT 175

Figure 4.32: Fines vs. Initial Void Ratio and F/(F+W) for tailings with 70% clay content MFT 176

Figure 4.33: Solids content profile for tailings with 70% clay content MFT 177

Figure 4.34: Standpipe testing progress for tailings with 70% clay content MFT 178

Figure 4.35: Segregation boundaries for tailings with 36%, 55%, and 70% clay content MFT 179

Figure 4.36: Segregation boundaries for tailings with 36%, 55%, and 70% clay content MFT 180

Figure 4.37: Segregation boundary for tailings treated with 900g/m^3 of laboratory grade gypsum 181

Figure 4.38: Segregation boundaries for tailings treated with laboratory grade, and agricultured grade gypsum 182

Figure A-1: Output data for Cavity Expansion test on two day old MFT (SY-22) 206

Figure A-2: Output data for cavity Expansion test on MFT treated with 2500g/m^3 of LGG 207

1.0 INTRODUCTION

1.1 Problem Statement

The oil sands tailings discharged from the Syncrude Canada Limited (SCL) bitumen extraction plant is a segregating mix. The mix is the separation of fine grained material from the sands when discharged into a conventional disposal area. The fine grained material which is referred to as the fine tailings consists mainly of silt, clay, water, various chemicals and residual quantities of bitumen. Through self-weight consolidation, the freshly deposited fine tailings achieves a void ratio of approximately 6 (30% solids content) during the first two years. The denser fine tailings (void ratio < 6) is referred to as mature fine tailings (MFT).

It is not environmentally acceptable to discharge this waste into neighbouring river systems, therefore it is stored on site in the vicinity of the extraction plant. There are presently approximately 400 million cubic metres of MFT in storage on the oil sands leases. Many issues surround the method of storage of MFT and the eventual reclamation of sites chosen to store MFT. Geoenvironmental issues include the management of this immense volume of waste product, and the chemicals in tailings water that has both adverse acute and chronic effects on aquatic organisms and wildlife in areas surrounding the storage site.

The fluid-like nature of MFT can be explained by its unique clay structure called the *card-house* structure. The structure which develops is a function of the pore water chemistry, specifically the pH levels of the pore water, and the amount of mineral surfaces exposed. Consequently, the vast amount of fine tailings generated, combined with the slow consolidation process of the MFT, create a challenging task for waste management and land reclamation.

One of the mine waste management techniques is to create a nonsegregating mixture or composite tailings (CT) that will accelerate the dewatering process resulting in a higher consolidation rate of the fine tailings. A nonsegregating tailings can be achieved by increasing the solids content (includes all soil minerals), fines content (particles that are < 45μm in size), changing the grain size of the fine tailings or by adding chemicals. In a CT, the types and amount of chemicals used, and the amount of fines content in the tailings can affect its segregation and initial consolidation characteristics. Whether or not a CT can be created also depends on the amount of clay minerals in the fine tailings or MFT reacting with the added chemicals.

Previous experiments performed by Suncor Oil Sands Group (SOSG) have shown that the nonsegregating boundary of CT mixed with 600 ppm of agricultural grade gypsum is equivalent to a *clay mineral:water* ratio of 0.1 (SOSG, 1996). The parameter *clay mineral* describes the amount of clay mineral surface area found in fine tailings obtained from methylene blue testing, and *water* describes the amount of water in the CT. Their report stated that CT with a *clay mineral:water* ratio greater than 0.1 will not segregate. However these findings required further investigation and verification to examine the effects of the varying amount of clay content in the tailings on the segregation and initial consolidation behaviour of CT. This is the topic of the thesis, and the objectives of this study are described in the following section.

1.2 Research Objectives

The purpose of this research work, herein identified as the principal study, was to examine the effects of varying amounts of clay content in MFT on the segregation and initial consolidation behaviour of CT. In order to comprehend the interactions between the chemical additives and the clay particles in CT that affect the aforementioned behaviour, it was necessary to first study the interactions between the clay minerals and various pore water chemistry in the MFT. Thus, the introductory study examined how the MFT *card-house* structure is formed and determined what chemicals are responsible for the structure formation. The study involved the use of a Scanning Electron Microscope (SEM) to qualitatively examine the structure of MFT. The objectives of this introductory study were:

1. to justify that the clay structure of the cryogenically treated samples prepared for a SEM are not artefacts of the preparation method,
2. to identify and examine the organic and inorganic compounds in the MFT pore water that are responsible for the structure that develops in MFT, and
3. to examine the effects of gypsum and the processing temperature on the structure of MFT.

The principal objectives of the thesis were:

1. to qualitatively examine the laboratory grade gypsum (LGG) treated MFT structures at different clay contents and compare the structures to the untreated ones,
2. to examine the CT structures,

3. to verify if the *clay:water* ratio of 0.1 is a valid boundary in describing the segregation behaviour of CT by performing standpipe tests on tailings with varying clay content in MFT, and
4. to study how varying clay contents in MFT affect the segregating and initial consolidating behaviour of CT.

1.3 Scope of Thesis

A SEM was used to examine the clay structures of MFT, CT and kaolinite slurries. Before examining the clay structure, the problems related to the cryogenically prepared SEM samples were identified. This thesis discusses these issues and explains that careful preparation of the slurry samples does not produce large ice crystals that may distort the clay structure of the samples. Experiments were carried out to compare the structure of a kaolinite clay-water system to a finely ground Ottawa sand-water system with the same chemicals and concentrations. Evidence provided by other researchers who argue that the frozen structure observed by the SEM is not an artefact of the preparation method is also presented. The examination of MFT structure is then presented considering that the cryogenic preparation process has successfully preserved the clay structure of the slurry samples.

In order to analyse the effects of these MFT pore water chemicals on the MFT *card-house* structure, a simplified MFT model, kaolinite clay slurry, was used. The HCO_3^-, NaOH, or sodium naphthenates were added to the kaolinite clay-water system to examine the type of clay structures that would formed. MFT samples were also prepared by isolating the bitumen and the *strongly bound* organic matter in the MFT solids to examine its effect on the MFT *card-house* structure. Furthermore, the influence of processing temperature on the structure of MFT were examined by comparing the structure of a heated kaolinite clay-MFT pore water slurry to an unheated one.

The effects of LGG on the MFT clay structure were studied to assist in the understanding of how a CT is formed. This was done by comparing the structure and the thixotropic strength of MFT treated with LGG to the untreated ones. The structures of both LGG treated and untreated MFT that had 36%, 55%, or 70% clay contents were also studied. The effects of varying clay content in MFT on the segregation and initial consolidation behaviour of CT were then studied by performing standpipe tests on tailings that consisted of MFT with 36%, 55% or 70% clay content.

1.4 Organisation of Thesis

Chapter 2 gives a brief description of geological events contributing to oil sands formation followed by the review of the oil sands operation at Syncrude Canada Limited (SCL). The geotechnical and the chemical properties of MFT, and the reclamation techniques used in the fine tailings management are then reviewed.

Chapter 3 pertains to the examination of MFT structure using a SEM. It contains a literature review, experimental procedures and sample preparation, and a discussion on artefacts. This is followed by a discussion on the effects of the pore water chemistry on the clay structure, and then concludes with engineering applications of these findings.

Chapter 4 begins with a literature review on the deposition problem of the fine tailings, and an overview of the composite tailings (CT). The review is followed by the experimental procedure and experimental design which presents a flow chart illustrating the approach of the experimental program. The results of the material properties, sedimentation tests, and the SEM micro-graphs of CT clay structures are reported. The discussion includes the material properties, the characteristics MFT and CT clay structure at different clay contents, the effects of the varying clay content on the segregation boundary, and the initial consolidation behaviour of CT. The engineering application of these findings are summarised in the next section followed by a summary that highlights the major findings of the study.

The final chapter, *Chapter 5*, summarises the findings of this research and makes recommendations for future work based on this study.

2.0 OVERVIEW OF OIL SANDS OPERATION AND TAILINGS MANAGEMENT

2.1 Oil Sands Operation at Syncrude Canada Limited

Oil sands are sandstone deposits which contain a very heavy hydrocarbon, bitumen. The oil sands deposits in Alberta occurred in the early Cretaceous age. Parent material for these sediments originated in the Rocky Mountains to the west and the Canadian Shield to the east. In northern Alberta, most of the sediments were transported and deposited in a fluvial environment while some occurred in a marine environment. Marine water conditions covered most of Alberta due to the merging of the Boreal and the Gulfian Sea which were created by more active tectonic events in the early Cretaceous.

The oil sands are found in the McMurray Formation. This formation is overlain by varying thickness of non-oil bearing marine shales and underlain by limestone. Figure 2.1 illustrates a simplified cross-section of the geology at the Sycrude Canada Limited (SCL) site. The McMurray Formation was created in a drainage basin where alternate deposition of estuarine and fluvial deposits resulted in a number of distinct layers. The clay minerals in the upper and lower McMurray Formation are predominantly kaolinite and illite, although a large amount of smectites are found in the upper formation whereas the vermiculite and mixed-layer clays are found in the lower formation. Consequently, the oil-bearing sands in this deposit have a great variability in their compositions and properties.

The Athabasca deposit located in northern Alberta is presently the largest known oil sands deposit in the world. It is estimated that this deposit can yield approximately 600 billion barrels of bitumen but only about 60 billion can be recovered by surface mining. Presently, SCL and Suncor Oil Sands Group are operating in the Athabasca oil sands deposit. The locations of these oil sands operations are shown on Figure 2.2. These companies use the open pit mining technique to retrieve the oil sands ore. At the SCL mine site, approximately 30m of overburden must be removed before the oil sand is mined. As shown on Figure 2.3, draglines excavate the oil sand from an open pit, and the mined oil sands are dumped to form windrows. Bucketwheels then load the oil sands onto belt conveyors which transfer the sands to a surge pile and dump pockets. From there, the oil sands are fed into tumblers in the extraction plant at a uniform rate.

The Athabasca oil sands are commonly found to be water-wet and are illustrated in Figure 2.4. The bitumen is not in direct contact with the sand but separated by a thin film of water. Hot water floatation is therefore a suitable method for recovering the bitumen from the minerals. In the process plant, the bitumen extraction process is called the Clark Hot Water Extraction process. The bitumen is separated by digesting and conditioning the oil sands with added caustic soda and hot water. Figure 2.5 illustrates the extraction operation. The oil sands, hot water and caustic soda are fed into a tumbler and the material is mixed for 4 minutes at about 80°C. The slurry is then removed from the tumbler and mixed with hot water while the large particles are removed by screening. The diluted slurry is transported into settling vessels where the bitumen floats as the primary froth and the sands settle as the primary tailings. The middle portion of the settling vessels, referred to as the middlings, consists of suspended fines and some bitumen. Both the sand and middlings are treated again to recover more bitumen. The waste is then discharged as total tailings into the settling basins. SCL currently processes approximately 150×10^6 tonnes of oil sand annually and from this yields approximately 74×10^6 barrels of Sweet Blend Crude Oil (List and Lord, 1997).

The Southwest Sand Storage Facility was developed in 1991 as a sand storage facility, while the fine tailings and water are transported back to the settling basin, Mildred Lake Settling Basin (MLSB) for consolidation (List and Lord, 1997). Figure 2.6 illustrates the plan view of both storage area at the SCL oil sands processing site.

The deposition behaviour of total tailings is classified as a segregation process. Upon deposition, the coarser grained material separates from the finer grained material forming dykes and beaches while the finer material flows into the pond. The fine grained material, referred to as fine tailings, consists mainly of silt, clay, water, various chemicals and residual quantities of bitumen. This mixture has a pH ranging between 8 and 9. Once the fine tailings has been deposited into the pond, it begins to consolidate under self-weight. When the fine tailings has achieved a void ratio of approximately 6 (after two years), the consolidation process slows down considerably (FTFC, 1995*a*), and it is referred to as mature fine tailings (MFT). The released water at the top of the pond is returned to the extraction plant for further reuse in the extraction process.

2.2 Characteristics of MFT

2.2.1 Geotechnical Properties

The clay minerals found in the fine tailings come from clay bands in the McMurray Formation. The clays are predominantly kaolinite which makes up to 80% of the clay minerals (FTFC, 1995*a*). The other clay minerals are illite, smectite, chlorite, and mixed layers.

A typical range of grain size distribution of the MFT is shown on Figure 2.7. The grain size analysis shows that the material consists of mostly silt and clay size minerals. From this figure, the clay size material ranges from 40% to 60% of the MFT.

Since the MFT material is mainly silt and kaolinite clay, the properties of a low plastic clay would be expected. However, the presence of the bitumen appears to have an effect on the characteristics of the MFT. Scott and Dusseault (1982) found that the liquid limit of a MFT sample dropped from 65% to 50% after the bitumen was extracted from the MFT. This suggested that the bitumen can be treated as a solid because bitumen is at least 10^6 times as viscous as water, and it cannot be considered a mobile phase with respect to the fluid being expelled (Scott *et al.*, 1985). The higher the amount of bitumen and fine grained material, the higher the Atterberg limits. The MFT liquid limit range from 40% to 75% indicates that the material is intermediate to highly plastic. The plastic limit ranges from 10% to 25%. Figure 2.8 shows the plasticity characteristics of various mine waste sludge. The geotechnical parameter that quantifies the mass of bitumen in MFT is called the bitumen content. It is expressed in percentage and defined as:

$$\text{Bitumen content (\%)}, b = \frac{M_b}{M_s} x100\% \tag{2.1}$$

M_b *and* M_s represent the mass of bitumen and the total mass of solids respectively. Mass of solids includes the bitumen, fines and sands of the tailings. The bitumen content in MFT typically ranges from 2% to 10% (FTFC, 1995*a*).

The solids content is a term used for quantifying the amount of solids in a sample of MFT. The formula is written as follows:

$$\text{Solids Content (\%)}, s = \frac{M_s}{M} x100\% \ , \tag{2.2}$$

where M_s and M are the mass of total mass of solids and the total mass of tailings respectively. The solids contents of MFT can range from 25% to 60% but usually occur at about 30%. The initial void ratio of MFT based on the solids content ranges between 1.7 and 7.5. It is written as:

$$\text{Initial Void Ratio } (e_i) = \frac{G_{fb}(100\% - s)}{s} \tag{2.3}$$

The specific gravity of the solids (mineral plus bitumen) in the MFT is defined as G_{fb} , and the solid content as s. A G_{fb} value of 2.5 was used in the above formula to calculate the void ratio. A specific gravity formula based on a weighted average of the bitumen and the mineral particles is:

$$G_{fb} = \frac{M_b + M_m}{\frac{M_b}{G_b} + \frac{M_m}{G_m}}, \tag{2.4}$$

G_b and G_m are specific gravity of bitumen and minerals respectively. The remaining parameters have been identified above.

The fines content of MFT has been defined as the amount of mineral that is finer than 45μm (<#325 sieve). The average fines content of MFT is approximately 90%.

The fundamental geotechnical behaviour of SCL's MFT were characterised by Suthaker (1995). She found that the compressibility of MFT was dependent on its initial void ratio. The change in void ratio was the largest at low effective stresses until the stresses increased to 100kPa after which the void ratio became constant. Suthaker (1995) has also shown that the hydraulic conductivity of MFT is independent of the initial void ratio but is dependent on the bitumen content. In that study, hydraulic conductivity decreased as the bitumen content increased. This was confirmed by Scott *et al.* (1985) that the bitumen-clay-water system was at least 10 to 100 times less permeable than the equivalent material without bitumen. They explained that the bitumen blocked pore throats, and therefore increased the tortuosity of the flow paths decreasing the hydraulic conductivity.

MFT also exhibits a thixotropic behaviour. A geotechnical definition of thixotropic behaviour is given by Mitchell (1960) as: a process of softening caused by remoulding followed by a time-dependent return to a harder state at a constant water content and constant porosity. Water content is defined as the mass of water divided by the mass of total dry solids of tailings. Banas (1991) found that the oil sands tailings is a highly thixotropic soil that has higher relative thixotropic gain in strength than other typical clay minerals. The effect of thixotropy in the tailings was found to be highly dependent on water content; the lower the water content, the higher the thixotropic strength. Banas (1991) also showed that the rate of hardening was the highest in the first several hours after mixing for all water contents. The undrained shear strength doubled within 6 hours and then the rate of strength gain decreased with time. Suthaker (1995) showed that the rate of thixotropic strength gain was also dependent on the water content of MFT. A sample with a 100% gravimetric water content increased in strength from 500Pa to 2450Pa after 460 days. For comparison, a MFT with 233% water content gained from 160Pa to 600Pa after 460 days.

2.2.2 Water Chemistry Properties

2.2.2.1 Organic Compounds in MFT Pore Water

The organic material in the MFT can be divided into three categories: residual bitumen, soluble compounds, and mineral-associated compounds. At SCL, 0.3 to 0.5 percent weight of the tailings stream is bitumen. In general, the bitumen content of MFT varies from 2% to 10% depending on the depth of the MFT in the containment pond. Majid *et al*. (1990) found that the bitumen extracted from the MFT was lower in molar mass and asphaltene content than the bitumen extracted from the oil sands. They concluded that the asphaltene are tightly bounded to the clay particles in the tailings and therefore cannot be easily extracted.

Soluble organic compounds are defined as the organic compounds that dissolve in water during the hot water extraction process (Kasperski, 1992). These compounds in the MFT are mostly polar organics such as humic and fulvic acids. Other compounds are phenols, alkyl phenols, polyphenolic aromatics, and polycyclic aromatic hydrocarbons. The soluble organic compounds also include the natural surfactants, naphthenate and sulfonates (FTFC, 1995*b*). The acid form of naphthenate is called the naphthenic acids.

These acids are a natural component of bitumen that are liberated from the bitumen during the Clark extraction process. The addition of NaOH during the extraction process accelerates the release of naphthenic acids into the process water. It was found that the concentration of naphthenic acid in the slurry correlated to the amount of NaOH added during the extraction process (FTFC, 1995*b*).

The naphthenic acids are also responsible for the toxicity in the process water. These acids in the process water do not exist as an acid but as sodium salts called sodium naphthenates. The naphthenic acids can be extracted with methylene chloride by lowering the pH to 3. At pH of 3, the naphthenates are in its acid form and also soluble in methylene chloride (FTCT, 1995*c*). The concentration of naphthenic acids in the MLSB are approximately 112 ppm (FTFC, 1995*b*).

Ignasiak *et al.* (1985) defined the mineral-associated compounds as organic matter that are strongly adhered to the minerals and cannot be extracted using toluene or dicholoromethane. Infrared spectroscopy indicated that the compounds consist of carboxylic acids, polymeric phenols, alcohols, chelated ketones in the humic acid fraction, and mostly phenolic and carboxylic acids in the fulvic acids similar to the same fractions from soil (Kapserski, 1992). Furthermore, Yong and Sethi (1978) reported fine fractions (<44μm) containing an average of approximately 4% amorphous Fe_2O_3, and less than 0.1% amorphous Al_2O_3 and SiO_3.

2.2.2.2 Inorganic Compounds in MFT Pore Water

The inorganic compounds found in MFT come from three sources: oil sand connate water, water from the Athabasca River, and chemicals added during the Clark extraction process (Kasperski, 1992). Connate water is defined as the pore water found between the oil sand grains in the McMurray formation. Table 2.1 lists the cations and anions which the FTFC (1995*b*) has categorised as the major inorganic constituents the Syncrude MLSB. The concentrations of these inorganic constituents vary depending on the sampling location. The most abundant cation is Na^+. The connate water in Syncrude oil sands has about 1.7 to 5.8 g/L of NaCl and small amounts of K^+, Ca^{2+}, Mg^{2+} and SO_4^{2-}. The high concentration of Na^+ in the tailings water is also due to the addition of NaOH during the extraction process. The most abundant anion in the tailings water is HCO_3^- which also comes from the oil sands connate water and the Athabasca River. The secondary source of HCO_3^- is the adsorption of CO_2 during the aeration process in the plant and, to a lesser extent, the absorption via the surface into the tailings pond.

2.3 Tailings Management Techniques

The objective of the reclamation program is to acquire a self-sustaining environment that is geotechnically stable, requires minimal maintenance, and can exist with the neighbouring and regional environment. Due to the immense volume of tailings, the reclamation program should also be efficient and cost effective. It is therefore favourable to use natural processes such as freezing and thawing, evaporation, evapotranspiration, infiltration of water, and vegetation to consolidate the fine tailings.

The reclamation program developed for SCL mine tailings can be divided into three categories: *dry* landscape, *wet* landscape, and wetlands. The *dry* approach involves a dewatering process wherein the water content in the tailings is significantly reduced producing a solid deposit that is strong enough to be capped with soil (FTFC, 1995*d*). The land will be reclaimed as a land surface. Some examples of the dry landscape techniques used in the oil sands tailings management are: cyclic freeze-thaw consolidation, composite tailings, drainage/infiltration, evaporation, and evapotransporation.

Composite tailings is presently implemented at the SCL to increase the consolidation rate of the oil sands tailings. The MFT has a weak fluid-like structure which cannot support the sand grains within its clay matrix. Hence, chemicals are added to alter the clay structure of MFT to form a nonsegregating mixture with the sands. At SCL, this mixture is termed as the composite tailings (CT). The sand grains create an internal surcharge within the MFT which accelerates the self-weight consolidation process of MFT. The chemicals that are found to be successful in forming CT are lime, sulphuric acid and lime, phosphogysum, and agriculture grade gypsum. Further densification of MFT can be enhanced by evaporation during the summer season, and freezing-drying in the winter season.

The purpose of *wet* landscape reclamation technique is to create a productive aquatic ecosystem that can exist with the surrounding landscape and the climatic conditions. The *wet* landscape method disposes the MFT as a fluid over which a layer of water is placed. The principle of the wet landscape approach is based on the rheological properties of MFT. Its low permeability, high density and relatively high viscosity are conducive for the water capping plan. The layer of water should have a sufficient depth to isolate the fine tailings from the surrounding environment. The proposed capping depth is at least 5m. The potential sources of water include local rivers, runoff, drainage water from the dry landscape reclamation method, and or process-affected waters.

It is anticipated that within one to two years of capping, the concentration of the organic compounds released from the MFT into the surface water will be reduced to a level that is not acutely toxic to the aquatic organisms (FTFC, 1995*e*). Gully and MacKinnon (1993) explained that the water released from the MFT into the overlying water will not be detrimental to the ecosystem because the rate of water release is slow enough for natural detoxification to occur. The natural build up of detritus layer between the MFT and the water cap will provide a barrier for potential mixing in the above layer of water and the biological degradation active zone for the MFT below. Figure 2.9 illustrates the cross-section of a wet landscape.

The use of both natural and constructed wetlands have been used to treat polluted waters including domestic wastewater, agricultural and urban storm runoff, acid rock drainage, mine waters, industrial discharges, and landfill leachates. In tailings management, they function as a buffer zone between the deposited tailings and the adjacent environment. The wetland will receive water discharging from dry landscape via groundwater discharge as a part of the hydrological cycle, and from the lake system via infiltration to the surrounding land surfaces (Gully and MacKinnon, 1993). It is also possible to utilise wetlands as a primary water treatment system for CT release water. The wetland is therefore an integral component of the *dry* and *wet* landscape techniques.

Nevertheless, the implementation of all the above reclamation methods requires careful consideration of the ecological compatibility with the surroundings, and its long-term environmental impacts. Hence it is imperative to evaluate and monitor their performance to ensure that no adverse effects will result in the devastation of the regional ecosystem.

Table 2.1: Major inorganic ions in a water sample from Syncrude's MFT (Mikula et al., 1996a).

Components	mg/L
Ca^{2+}	3-6
Mg^{2+}	2-4
Na^{+}	450-500
K^{+}	9-12
F^{-}	7
Cl^{-}	140-160
SO_4^{2-}	2-10
HCO_3^{-}	950-1050

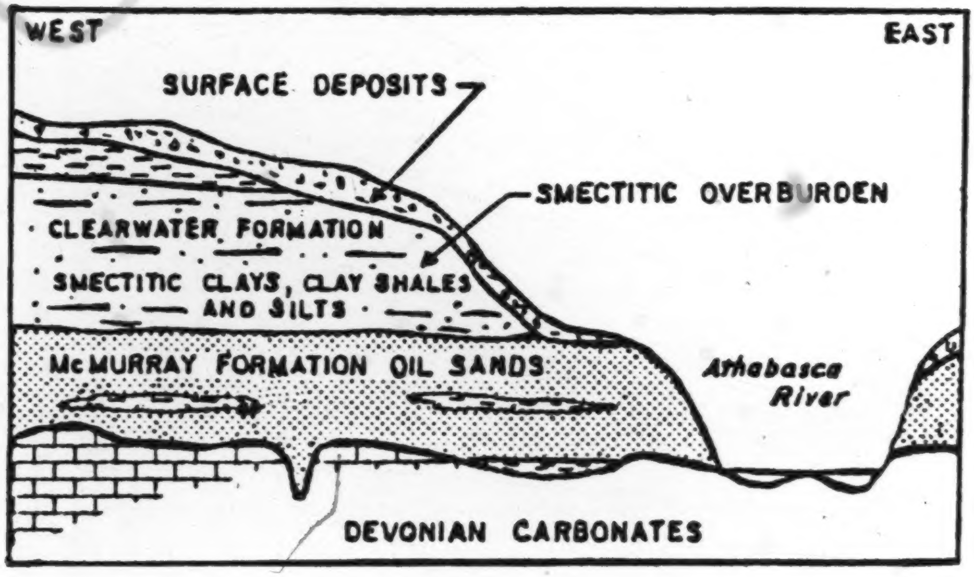
WEST
EAST
SURFACE DEPOSITS
SMECTITIC OVERBURDEN
CLEARWATER FORMATION
SMECTITIC CLAYS, CLAY SHALES
AND SILTS
McMURRAY FORMATION OIL SANDS
Athabasca
River
DEVONIAN CARBONATES

Figure 2.1: A simplified cross-section of the geology near the Syncrude Canada Limited mine site (Dusseault *et al.*, 1984)

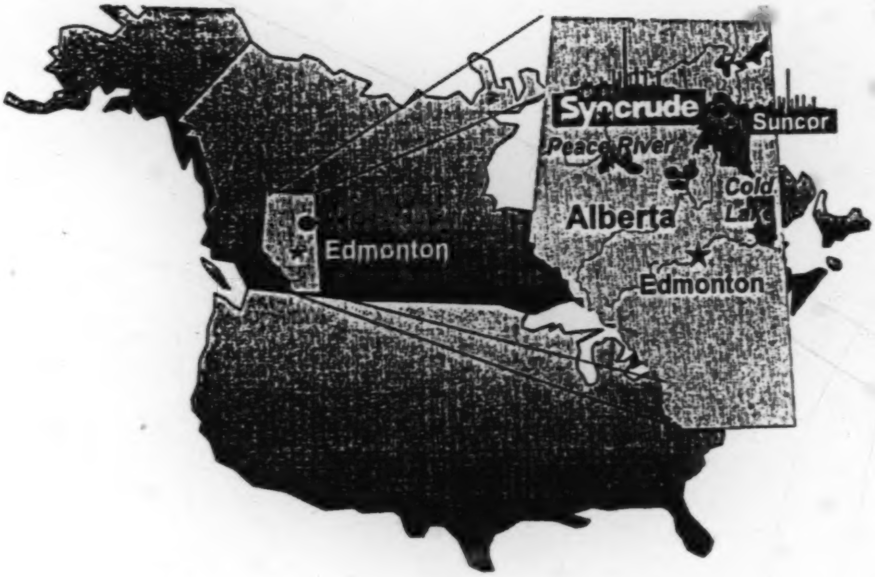
Syncrude
Suncor
Peace River
Cold Lake
Alberta
Edmonton
Edmonton

Figure 2.2: Map showing the locations of the Athabasca oil sands deposits and the Syncrude and Suncor extraction operations (Shaw *et al.*, 1996)

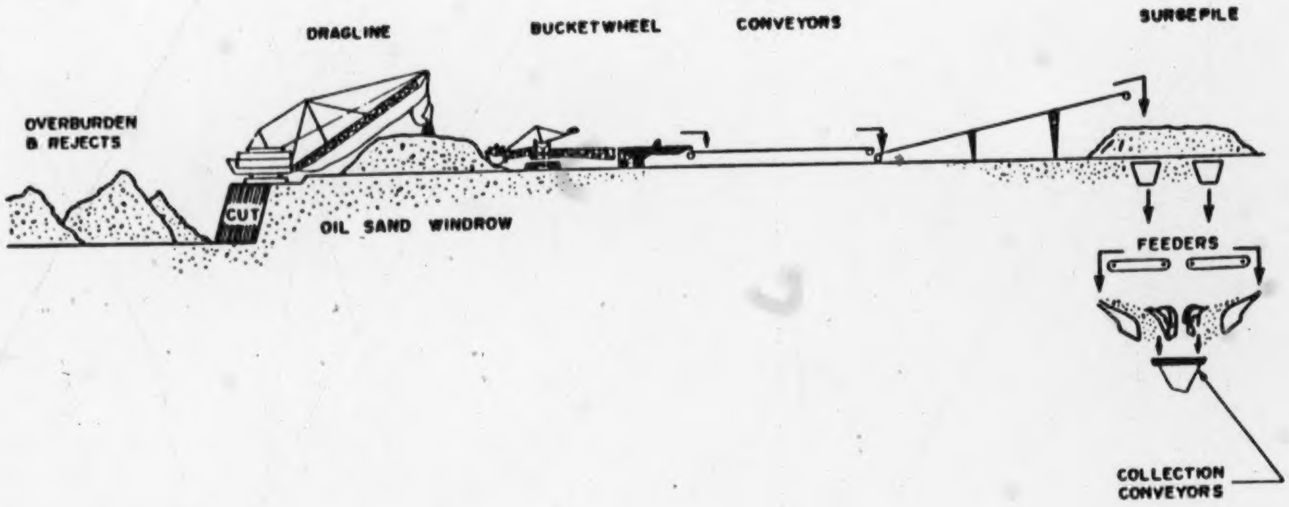
OVERBURDEN
& REJECTS
DRAGLINE
CUT
OIL SAND WINDROW
BUCKETWHEEL
CONVEYORS
SURGEPILE
FEEDERS
COLLECTION
CONVEYORS

Figure 2.3: Diagram showing the oil sands operation at the Syncrdue mine site (Shaw *et al.*, 1996)

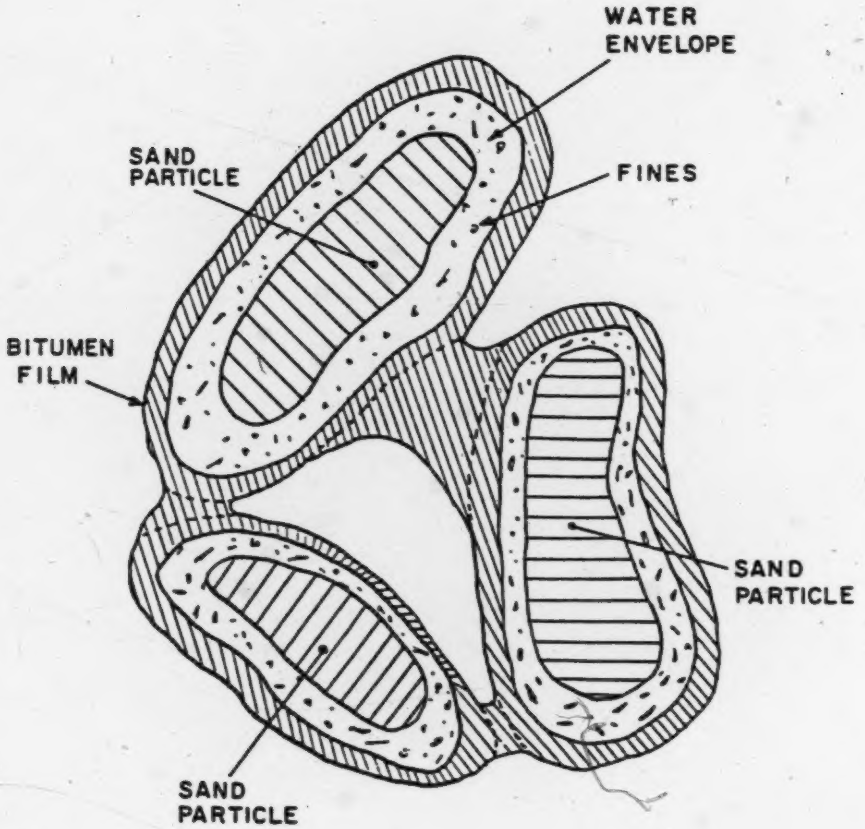
WATER
ENVELOPE
SAND
PARTICLE
FINES
BITUMEN
FILM
SAND
PARTICLE
SAND
PARTICLE

Figure 2.4: A model of the Athabasca oil sands (Shaw *et al.*, 1996)

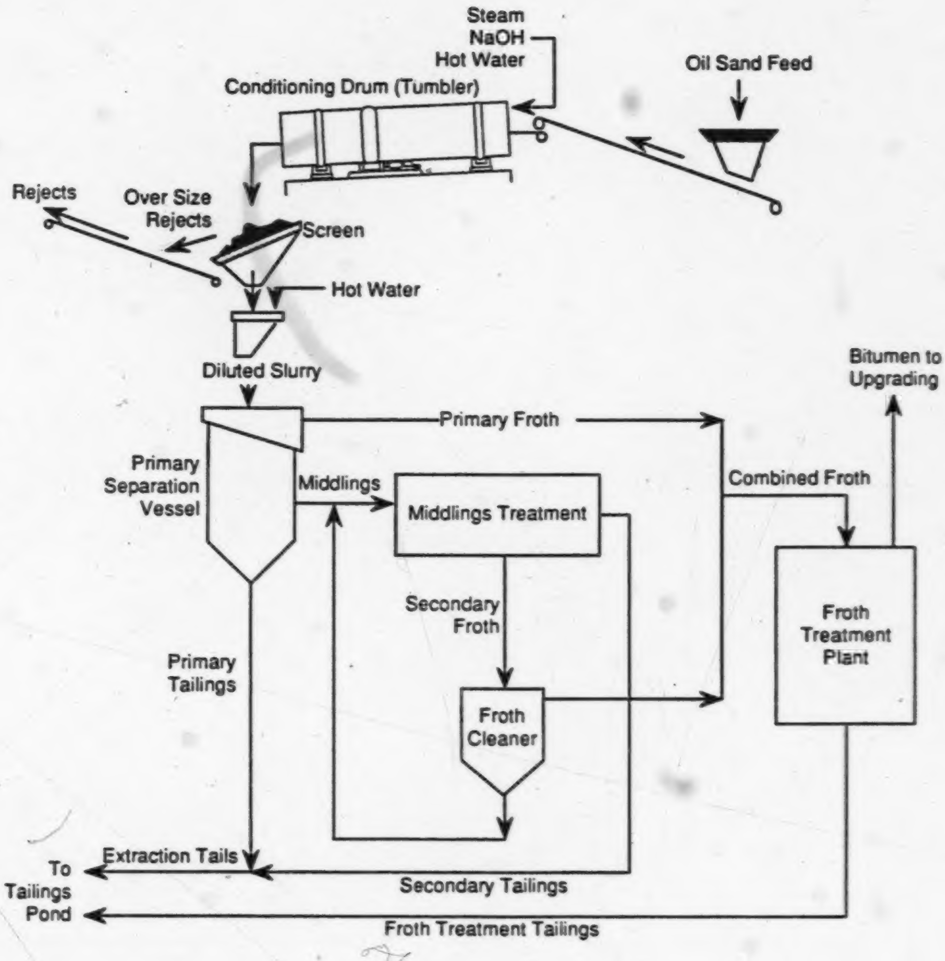
Steam
NaOH
Hot Water
Oil Sand Feed
Conditioning Drum (Tumbler)
Rejects
Over Size Rejects
Screen
Hot Water
Diluted Slurry
Bitumen to Upgrading
Primary Froth
Primary Separation Vessel
Middlings
Middlings Treatment
Combined Froth
Froth Treatment Plant
Secondary Froth
Primary Tailings
Froth Cleaner
Extraction Tails
To Tailings Pond
Secondary Tailings
Froth Treatment Tailings

Figure 2.5: Schematic of the oils sands extraction process (Mikula *et al.*, 1996*a*)

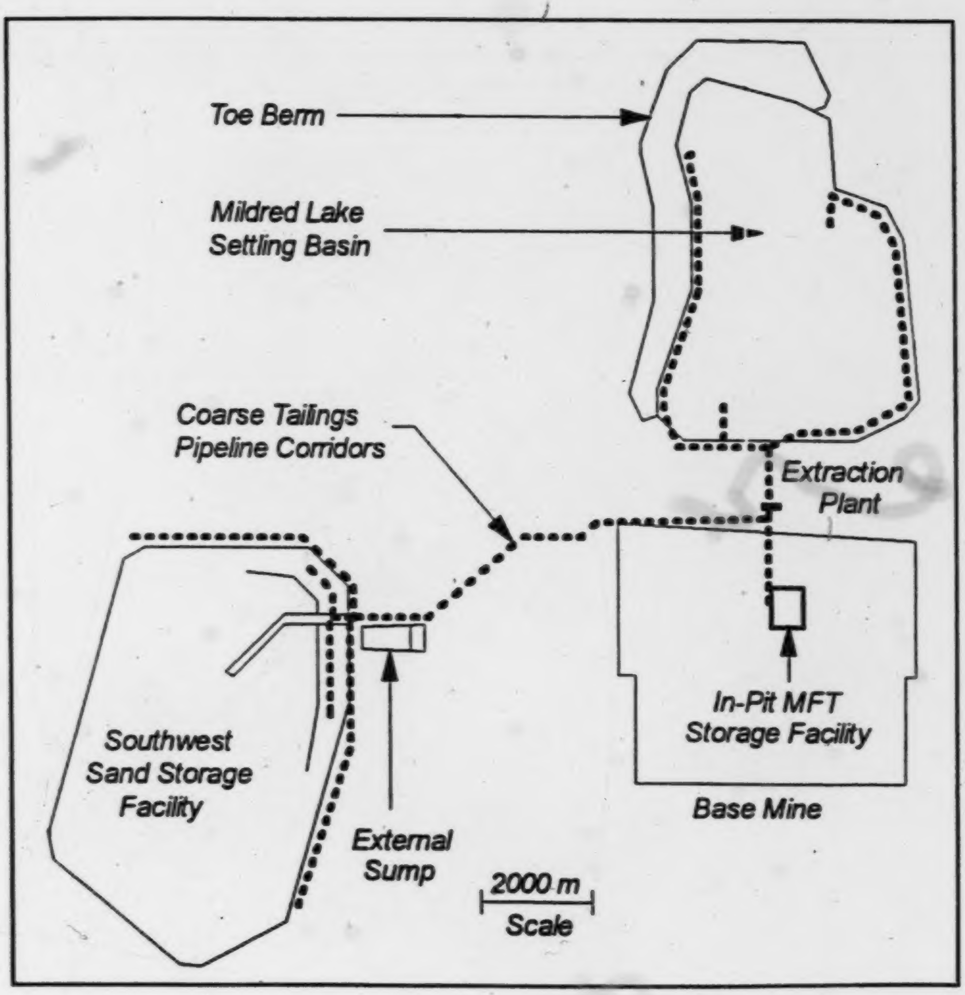
Toe Berm
Mildred Lake
Settling Basin
Coarse Tailings
Pipeline Corridors
Extraction
Plant
In-Pit MFT
Storage Facility
Base Mine
Southwest
Sand Storage
Facility
External
Sump
2000 m
Scale

Figure 2.6: Plan view of Syncrude site (List and Lord, 1997)

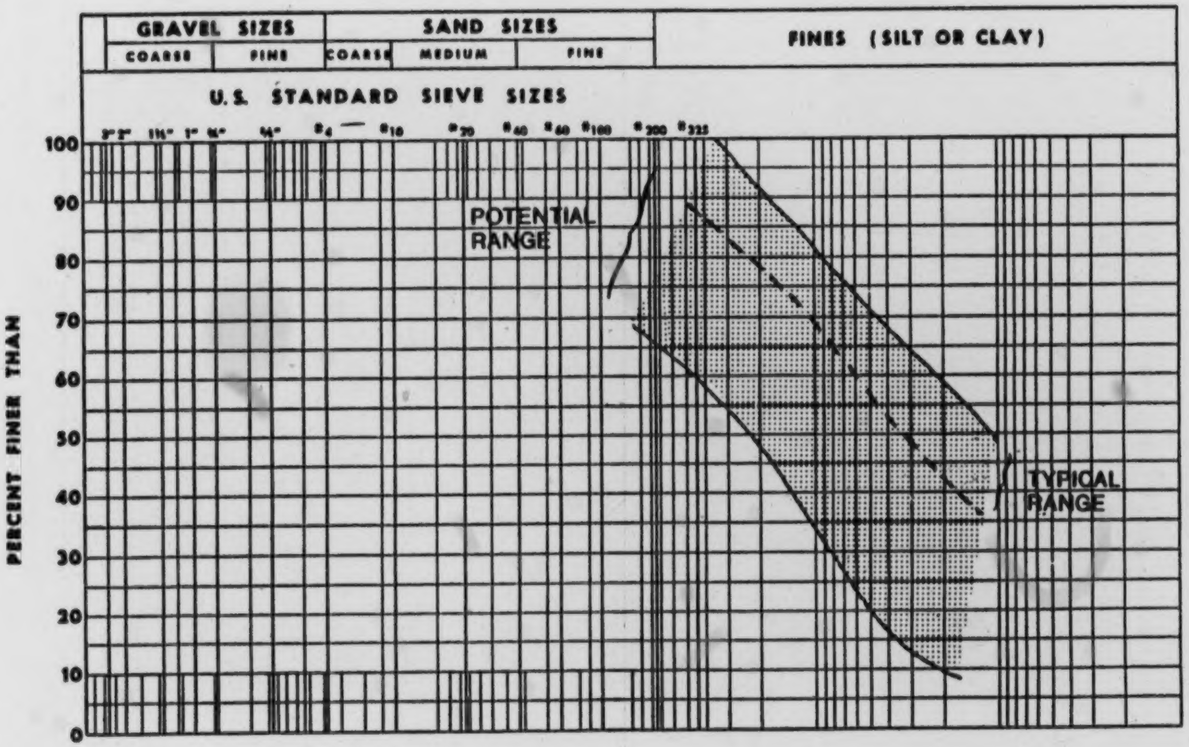

Figure 2.7: A typical size distribution of oil sands fine tailings (FTFC, 1995*a*)

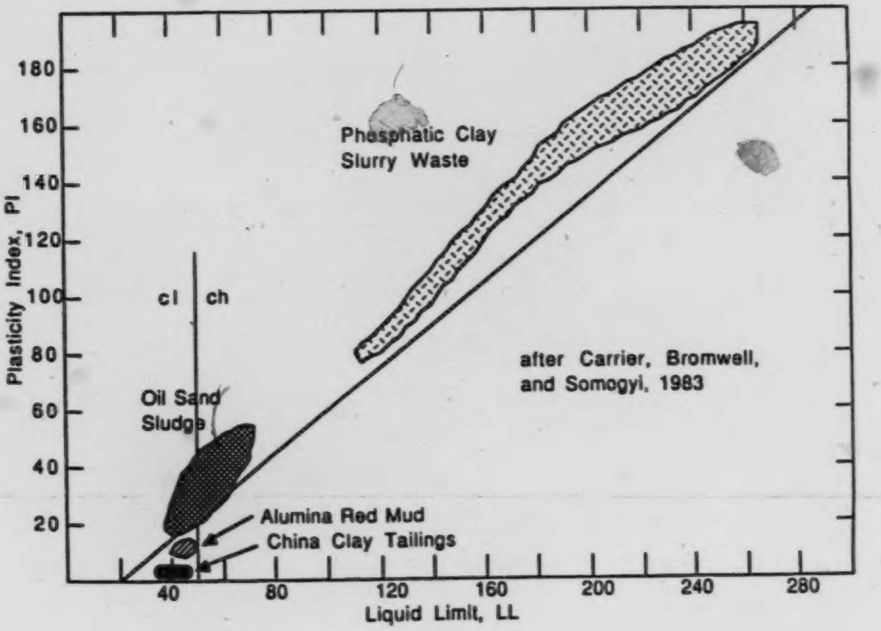

Figure 2.8: Plasticity of various mine waste sludges (FTFC, 1995*a*)

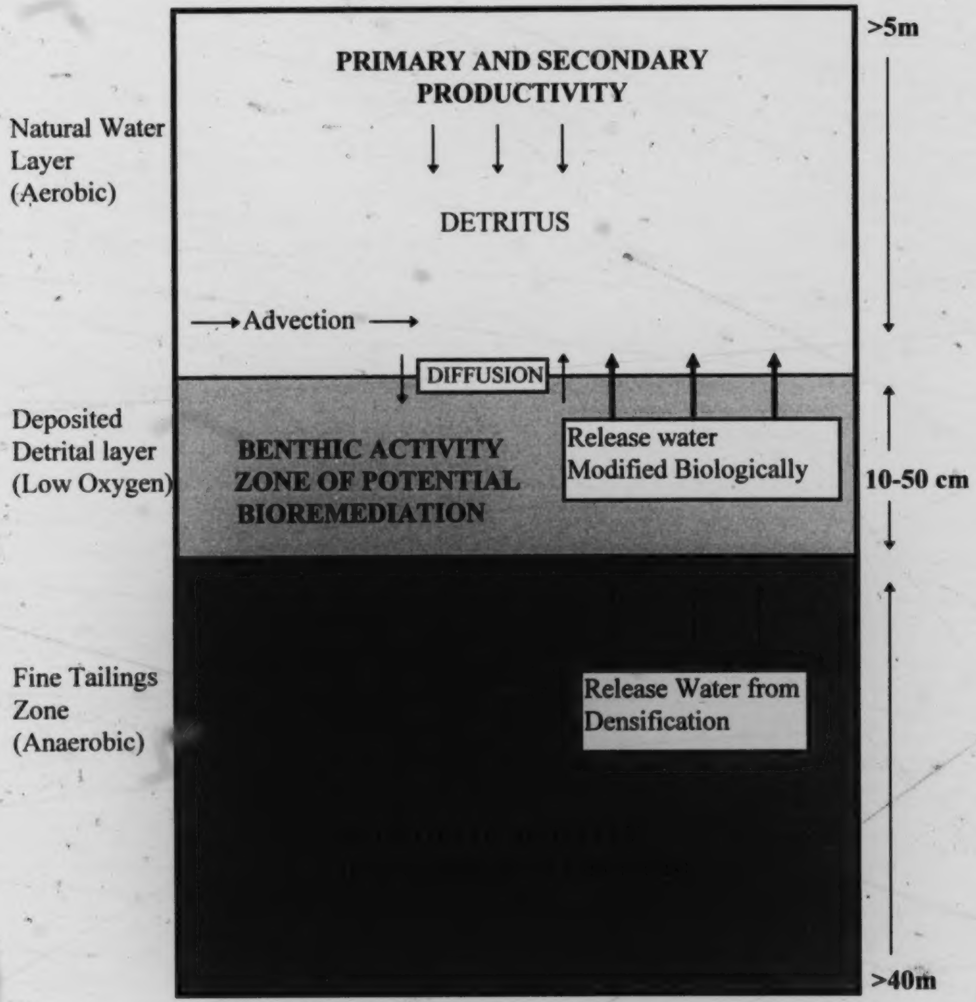
Natural Water Layer (Aerobic)
Deposited Detrital layer (Low Oxygen)
Fine Tailings Zone (Anaerobic)
PRIMARY AND SECONDARY PRODUCTIVITY
DETRITUS
Advection
DIFFUSION
BENTHIC ACTIVITY ZONE OF POTENTIAL BIOREMEDIATION
Release water Modified Biologically
Release Water from Densification
>5m
10-50 cm
>40m

Figure 2.9: Cross section of the interface of the fine tailings zone and the water capping layer. The detrital zone of high benthic and microbial activity at the interface is shown. (Gulley and MacKinnon, 1993)

3.0 EXAMINATION OF MFT MICROSTRUCTURE USING SCANNING ELECTRON MICROSCOPE

This is an introductory study which examines the fundamental colloidal behaviour of MFT. The purpose of this study is to better comprehend how the MFT structure is formed, and what chemicals are responsible for the MFT structure formation. In a nonsegregating mixture, the MFT structure is strengthened by chemical addition such as gypsum or lime. Hence the study of the MFT colloidal behaviour would assist in the understanding of the clay-water chemistry interactions in CT that can affect its segregation and initial consolidation behaviour.

3.1 Literature Review

3.1.1 Flocculation and Dispersion of Clays in Colloidal Solution

In soil chemistry, a colloidal system is a mixture of small clay particles, water and electrolytes in which the clay particles settle slowly. Clay particles have large surface areas which are influenced by the force fields interacting between the minerals, and between the minerals and the electrolytes. The combined effects of the surface force interactions and the small particle size create a variety of interparticle attractive and repulsive forces. Consequently, the flocculation and dispersion characteristics, volume change, and the strength properties of the clays in suspension are influenced by these interparticle forces.

In a colloidal solution, a clay will adsorb a specific type and amount of cations to balance the charge deficiency of the solid particles. The amount of cations which may be exchanged on a clay is called the cation exchange capacity (CEC) and is usually expressed as meq/100g or cmol(+)/Kgm of dry soil. The processes which determine the CEC of clay are: isomorphous substitution, broken bonds, and replacement (Mitchell, 1993). Isomorphous substitution is defined as the process in which cations in the clay lattice are replaced with cations of lower valences during mineral formation resulting in a net negative charge on the clay particle. Common examples of cation replacements are Al^{3+} for Si^{4+} in the silica tetrahedral sheets, and Mg^{2+} for Al^{3+} in the octahedral sheet. The type of clay which is not significantly affected by isomorphous substitution is kaolinite. In kaolinite, broken bonds are the major source of the exchange capacity (Mitchell, 1993) as exchange sites are present along particles edges and on non-cleavage surfaces. Cation exchange by replacement involves the hydrogen of an exposed hydroxyl to be replaced by another type of cation.

There are two major classes of hydrous colloidal systems, the hydrophobic and hydrophilic colloids (van Olphen, 1977). These terms are commonly used when describing the wetting surface properties of the clay particles. A hydrophobic colloid has a surface that is preferentially wetted by oil in competition with water even though the colloid can be wetted by water. A hydrophilic colloid behaves contrary to a hydrophobic colloid. The hydrophobic and hydrophilic colloids are distinguished by their sensitivity to the addition of salts. A hydrophobic colloid is more sensitive to salts and will flocculate in their presence.

The flocculation and dispersion of a colloid solution can be explained using the diffuse double layer theory. In an electrolyte solution, the cations are attracted to the negatively charged clay surface resulting in a higher concentration of cations near the clay surface. However, the cations try to diffuse away from the clay surface in order to equalise the concentration in the solution. The charged surface and the distributed cations in the adjacent phase are together termed the diffuse double layer. Based on this model, the theory states that the thicker the diffuse layer, the less tendency for the clay particles in suspension to flocculate. The thickness can be affected by the cation valence, dielectric constants of the pore fluids, temperature, and the ionic strength of the solution. In a flocculated colloidal system, its diffuse layer is suppressed by multivalent exchangeable cations, increased dielectric constant of the pore fluid, decreased temperature, and/or increased ionic strength of the solution.

The pH of the colloidal solution can also determine whether the clay particles are in a dispersed or a flocculated state. In an alkaline solution, a stable suspension or dispersion of clay particles is caused by:

1) the dissociation of hydroxyl ions in clay particles causing the particles to be more negatively charged;
2) the amphoteric clay particles being ionised negatively.

The exchangeable sodium ratio (ESR) is another method commonly used to evaluate the state of a colloidal system. ESR is calculated based on the Gapon Equation (a cation exchange equation) that relates the cation composition of the solution phase to the composition of the adsorbed phase (Dudas, 1996). The concept of the Gapon Equation is illustrated as follows:

$$(Ca_{\frac{1}{2}} - X) + Na^{+} = (Na - X) + \frac{1}{2}Ca^{2+} \tag{3.1}$$

X in the equation represents the clay particles and the symbol, " – ", indicates the adsorption of the Na^{+} or the Ca^{2+} ion to the clay particles. The free ions, Na^{+} and Ca^{2+}, represent the ions in the solution phase. In applying the Gapon Equation, the relative amount of exchangeable Na^{+} adsorbed to the clay particles is empirically related to the concentration of the cations in the solution by the Gapon exchange coefficient, K_G. This equation is written as follows:

$$\frac{[Na - X]}{[(Ca - X) + (Mg - X)]} = K_G \frac{[Na]}{\sqrt{[Ca^{2+} + Mg^{2+}]}} \tag{3.2}$$

where the "[]" brackets represents the concentration of the ions within the solution. The concentration of the adsorbed cations is expressed in meq/100g or mmol/L. Hence the relationship between the ESR and the sodium adsorption ratio (SAR) for the associated liquid phase is written as:

$$\text{ESR} = K_G\,(\text{SAR}) \tag{3.3}$$

$$\text{and, SAR} = \frac{[Na^{+}]}{\sqrt{\frac{[Ca^{2+}] + [Mg^{2+}]}{2}}} \tag{3.4}$$

The value of K_G which is determined through laboratory tests is approximately 0.015 (mmol/L)$^{-1/2}$ for Western Canadian clays with a SAR less than 30 and decreases as SAR increases above 30 (Dudas, 1996).

If a colloidal solution has an ESR greater than 0.1, it is identified as a potentially dispersed system if the ionic strength is low. Under this condition, the diffuse double layer thickness is increased. If the ESR is less than 0.1, the colloidal solution is considered as flocculated system with a compressed diffuse double layer thickness. In a clay system that has compressed diffuse double layer thickness, the clay particles have higher attraction forces than repulsion forces. As a result, this causes the clay particles to coagulate forming an aggregated or a flocculated clay system.

3.1.2 Theories Developed to Explain the Structure of MFT

The structure of MFT is a highly dispersed system (Babchin *et al.*, 1991) with a *card-house* like structure (Mikula *et al.*, 1991). van Olphen (1977) described a *card-house* structure as a three-dimensional formation with clay particles aligned in a *edge-to-face* and *edge-to-edge* pattern. The particles in the colloidal system remain dispersed due to the balanced internal charges in the system. It is balanced because the forces of attraction and repulsion that exist between the particles are in an equilibrium state. The high water holding capacity of MFT may be explained by this *card-house* structure. This type of clay particle arrangement exposes more mineral surfaces resulting in a higher degree of water to mineral bonding (FTFC, 1995*f*).

The *card-house* structure is also referred to as a gel structure. van Olphen (1977) explained that a gel is a homogeneous system displaying some rigidity and elasticity which occurs in certain clay soils, and that plate-like particles such as kaolinite may associate as a rigid *card-house* structure. He also explained that the rigidity of gel will depend on the number and the strength of the particle links within the continuous structure.

Preliminary studies by Mikula *et al.* (1991) suggested that the MFT structure was based loosely on the *card-house* type structure. Babchin *et al.* (1991) conducted an experiment to study the structural units that are responsible for the dispersed state of fine tailings, and they proposed that the *card-house/chain-like* structure is caused by the combination of internal dipole-quadrupole nature of the kaolinite particles illustrated on Figure 3.1.

The structure of MFT has found to be dependent on the pH of the pore water. Mikula *et al.* (1993) measured the rheological parameters of MFT at a pH less than 7 and at a pH greater than 10. Their results show that at these pH values, the MFT has a highly flocculated structure. At the intermediate pH values, the MFT structure has a *card-house* like dispersed structure. They also found that the elastic modulus, G', of the MFT was the lowest at pH values ranging from 8 to 10, which indicate a dispersed clay system. This pH dependence indicates that the dispersed state of MFT at a pH of about 8.5 corresponds to the pH where the concentration of bicarbonate (HCO_3^-) is at a maximum.

Mitchell (1993) explained that a clay-water system with an ESR greater than 0.1 will generally exhibit a dispersed clay structure. Since the ESR of MFT ranges between 0.6 to 0.7 calculated using the Equations (3.3) and (3.4) with the concentrations of Na^+, Ca^{2+}, Mg^{2+} listed on Table 2.1, the MFT clay structure can also be described as a highly dispersed structure.

The MFT structure has also found to be dependent on the organic matter found in the tailings. Majid *et al.* (1990) postulated that the insoluble organic matter or the *strongly bound* organic matter found in the MFT imposed a hydrophobic character on the clay surfaces allowing interparticle bridging of residual bitumen to set up a weak gel structure. Kotlyar and Sparks (1990) confirmed that this organic matter acted as a surface active agent (surfactant) which modified the hydrophilic character of the clay surfaces rendering them hydrophobic. This hydrophobic nature allowed the bitumen to adsorb onto the clay surfaces resulting in a gel formation and a reduced bitumen recovery.

Another class of organic matter found in the oil sands tailings are the natural surfactants, naphthenates and sulfonates, which are produced during the Clark extraction process. These surfactants also have a strong affinity for clay particles. The adsorption of natural surfactants on to the clay particles produces a higher negative charge on the clay surfaces and the particles are *bulky* or *fuzzy* (FTFC, 1995*c*). Highly negative charged particles produce stable suspensions or dispersion of clay particles (Mitchell, 1993).

3.1.3 The Functions of a Scanning Electron Microscope (SEM)

SEMs have been used extensively in examining biological specimens such as cells, muscle tissues, insects, and microbial organisms. Other types of material such as soil, rock, metals, and fibre have also been examined using the SEM. Its popularity is mainly due to the fact that the SEM can produce clear, three-dimensional images at high magnifications. A light microscope or a transmission electron microscope can only produce two dimensional images because these instruments have very limited depths of field. Moreover, ranges of magnification are limited for light microscopes.

There are four principal parts of a SEM: an electron-optical that produces the scanning electron probe, a sample or specimen to be observed, a detection system, and the display system. Figure 3.2 illustrates a schematic description of the SEM column. The electron beam originates from a high negatively charged tungsten cathode heated by a controlled current in the electron-optical compartment (illustrated on the top left corner of the Figure 3.2). The emitted electrons are accelerated from the cathode through a grid and then through an anode that is at ground potential. A system of magnetic lenses demagnify the electron beam. The demagnified electron beam is then passed through a deflection yoke to move the beam across the sample in a raster pattern. As the primary electron beam strikes the sample, secondary electrons are emitted from the sample as a result of its bombardment by the fast primary electrons. The bombardment of the primary electrons also emits backscattered electrons and photons. The primary electrons, secondary electrons, backscattered electrons and the photons are then collected by a detector to produce images shown at the bottom left side of Figure 3.2. This is why a SEM can provide three dimensional images. It records both the primary electrons passing through the specimen and the secondary electrons along with the backscattered electrons and photons. The images are then displayed through a cathode ray tube shown on the right side of Figure 3.2. The envelope of the impinging beam is like a sharp needle and therefore the instrument can achieve greater depth of field than the conventional light microscopes. The electron beam can penetrate the sample up to 50 angstroms (Everhart and Hayes, 1972).

The resulting image from the scanning is formed by a time sequencing technique similar to the one used in commercial television. However, there are two major differences. The picture produced on a television is composed of 525 lines, and a SEM image varies from 100 to more than 1000 lines. Secondly, the rate of scan in a SEM is much lower than the scanning rate used in a television because it is more difficult to focus the electron beam onto an area that is only 100 angstroms in diameter. Hence, the beam must dwell on the area for a longer time to build up a secondary electron signal that is strong enough to create an image.

3.1.4 Issues on Artefact Observed in Cryogenically Treated Slurry Samples

The SEM sample preparation technique commonly used for slurries is the freeze-fracturing method. The samples are required to be frozen because of the high vacuum applied in the SEM column during the time of observation (Braybrook, 1997). The slurry samples are frozen rapidly in a matter of seconds at an extremely low temperature. An example of the agent used for freezing samples is liquid nitrogen. The sample is then fractured to expose the internal structure of the sample before being observed.

The observed structure of any clay slurry sample is only valid if the structure in the solid frozen state is a replica of the structure in the semi fluid-solid state. Artefacts are features which are not naturally present in the original sample but occur due to the ice crystal formation. Ice crystals can form during the freezing and/or the sublimation processes. At a slow freezing rate, the ice crystal formation tends to push the clay particles and solutes into eutectic phases (Mikula *et al.*, 1991). They are frozen later to produce features which are not part of the original sample structure. If the sublimation process proceeds at a temperature warmer than -40°C, artefacts can be produced due to recrystallization of the pore water (Braybrook, 1997). Ice crystals will form regardless of the freezing rate, however, the faster the freezing rate, the smaller the ice crystals, thus the less influence of the ice crystals on the clay structure.

Erol *et al*. (1976) examined the influence of different freezing rates on the structure of sodium montmorillonite clay-distilled water system using a SEM. They compared the structures that were frozen at three different rates. The first process involved freezing a sample at -160°C in 15 to 20 seconds. In the second process, a sample was frozen within 3 to 4 minutes at a temperature of -129°C. The third sample was placed in a freezer at -17°C for 24 hours. The sample that was frozen at the coldest temperature exhibited the smallest pore spaces and the clay particles were more uniformly distributed. The structure of the third sample had the largest pore spaces with thicker stacks of tightly packed clay particles. This experiment shows that at a warmer temperature, the ice crystals are allowed to grow to a larger size. The formation of larger ice crystals pushes the clay particles together resulting in larger voids. At a lower temperature, the ice crystals were formed more quickly and they were not large enough to push the clay particles together, therefore a finer clay structure was produced.

In this study, a similar exercise was conducted with a kaolinite clay-water system. The results are presented and discussed in Section *3.3.2* to show that the observed structure in the MFT is not an artefact of freezing. Only then will the effect of pore water and clay mineralogy on the MFT structure be addressed.

3.2 Experimental Procedures and Sample Preparation

3.2.1 Index Tests

The materials tested in this study were MFT, kaolinite clay, and finely ground Ottawa sand (silica flour). The MFT was collected from the Mildred Lake Settling Basin at SCL in 1994. The barrel of MFT was identified as SY-22.

The hydrometer test for the MFT was done according to ASTM D422-63 except for a slight modification. Only 2.5g of dispersing agent, Calgon, was used with the MFT sample because a dispersing agent, NaOH, has been added to the oil sands during the extraction process. Hence, the MFT would not require the same amount of dispersing agent as stated in the ASTM. Previous hydrometer tests performed on MFT found that only 2.5g of Calgon (based on 50g of dry MFT solids) was adequate and the results are reproducible (Hereygers, 1997). Note that each of the hydrometer tests were conducted with wet MFT solids. The wet mass of the sample was initially calculated using its solids content and was equivalent to 50g of dry MFT solids. This calculation is shown in Appendix 1.

The hydrometer test for the kaolinite clay and the silica flour were carried out according to the ASTM D422-63. The amount of dry solids used was also 50g. All of the hydrometer tests were run for 48 hours which were sufficient to measure the particle size distribution of interest in this study.

The Atterberg limits tests were performed according to ASTM D4318-84. The Atterberg limits of an air-dried MFT sample were compared to that of a centrifuged MFT sample. The purpose of this exercise was to determine if the Atterberg limits of the MFT would be affected by the increased concentration of electrolytes in the air-dried MFT soil mass.

For the air-dried MFT sample, approximately 1 litre of MFT was placed in a ventilated oven for two days during which the sample was stirred occasionally to prevent a top crust of dry material from forming. The temperature of the oven was set at approximately 26°C. Once the desired water content was achieved, the sample was then divided into two portions for the liquid and plastic limit tests. Another sample of MFT was centrifuged at 7000 rpm for about 7 hours at 22°C. The centrifuge machine was a Sorvall RC-5B model manufactured by Dupont Instrument. Only the liquid limit test could be done on the centrifuged MFT because the sample did not achieve a low enough water content for the plastic limit test. This centrifuged MFT soil sample was then left to evaporate the excess pore fluid from the soil surface.

The Atterberg limits tests were performed on kaolinite clay with two different types of pore water, distilled water and saline water with 0.6M of NaCl which was chosen arbitrarily. This was to examine the effects of different pore fluid chemistry on the Atterberg limits of kaolinite clay. Since the kaolinite clay was dry initially, fluid was added to the kaolinite clay until the desired consistency was achieved. The Atterberg limits tests then proceeded according to ASTM D4318-84.

The bitumen content of MFT was measured using the Soxhlet extraction process in which the bitumen was extracted by toluene. Approximately 500g of a wet sample was weighed and dried to obtain its total dry mass. The oven was set at 110°C and the sample was left for 16 hours. The dried sample was then transferred into a pre-weighed timble, and the total mass was obtained. In the Soxhlet apparatus, the solvent was condensed and the distilled water was continuously separated in a trap where the water was being retained in the graduated section. The solvent was then recycled through the apparatus to dissolve the bitumen contained in the MFT sample. The final mineral mass was dried, weighed, and the mass of bitumen was calculated by the difference from the mass of the dry MFT sample at the start of the test. Equation (2.1) was then used to calculate the bitumen content.

For the solids content determination, the wet sample of MFT was first weighed and then dried in the oven for 16 hours at 110°C before determining the mass of the dry sample. The solid content was then calculated using Equation (2.2).

The specific gravity test procedure outlined in ASTM D854-83 was slightly modified to determine the specific gravity of MFT due to the contained bitumen. Instead of applying a vacuum to the sample, the MFT sample in an Erlenmeyer flask was boiled for approximately for 1.5 hours to release the trapped bitumen. The sample was then cooled to room temperature. The mass of the MFT and the flask were recorded. The flask was then emptied and washed clean with distilled water into a pre-weighed aluminium tray to dry in an oven. The formula used to calculate the specific gravity of this test was:

$$G_{fb} = \frac{W_s}{W_s + W_{b+w} - W_{b+w+s}} \,, \tag{3.5}$$

W_s is the mass of dry soil of MFT, W_{b+w} is the mass of flask and water at the temperature of the soil, and W_{b+w+s} is the mass of the flask, water and sample. Both equation (2.4) and (3.5) should give similar results.

X-ray diffraction test was performed by the AGAT Laboratories in Calgary, Alberta to determine the mineralogy of the MFT. Norwest Laboratories in Edmonton, Alberta carried out the CEC test and the water chemistry analysis. The ESR of MFT was calculated using the Gapon Equation (shown in Appendix 1) given the concentrations of Na^+, Ca^{2+} and Mg^{2+} ions of MFT pore water in Table 3.4.

3.2.2 Cavity Expansion Test

Suthaker (1995) found that the cavity expansion test was successful in estimating the thixotropic strength of fine tailings. The cavity expansion test was then used in this study to measure the thixotropic strengths of a MFT sample and a MFT sample treated with laboratory grade gypsum (LGG).

Clear plastic containers of about 1.5L and 150mm high were used to store the MFT samples. The MFT with LGG sample was prepared by initially stirring the MFT with a hand-held cake mixer for 5 minutes. Prior to the mixing of LGG, the powder was weighed and wetted with 2 to 3mL of distilled water before being added to the MFT. The sample was then stirred for another 5 minutes to thoroughly mix the LGG into the MFT.

These samples were left for 48 hours before being tested for their strength. This was to allow the samples to gain their thixotropic strength so that the *short term* thixotropic strength of the chemically treated and untreated MFT samples could be compared. A suitable time frame was chosen based on the rate at which the thixotropic strength of the MFT increased. Suthaker (1995) showed that the thixotropic strength of the MFT with 233% water content gained only 20Pa between the second and twentieth day. The sample with 300% water content gained only about 10Pa. The water content of the MFT used in this study was 268%, hence the strength gain would not be expected to be significant after adding the LGG. Thus, the 48 hours waiting period was chosen for these samples.

The following is a brief description of the cavity expansion test procedure. A detailed description of the theory, equipment set-up and the test procedures have been described in detail by Suthaker (1995). Figure 3.3 shows the set-up of the cavity expansion apparatus. A transducer was connected to the signal conditioning board which was connected from the computer to its data acquisition board. A steady flow of distilled water travelled in the nylon tubing which joins the cavity expansion needle to the valve located at the top of the syringe pump. The pump was set to deliver distilled water at 4mL/hour during the test. The transducer was then saturated with distilled water by turning the pump on to allow the water to run through the transducer. This procedure was repeated a few times during the test to ensure the bubbles in the transducer were removed.

The samples were poured in the plastic containers 48 hours prior to the cavity expansion test to a height of 75mm. This was done because the apparatus was set such that the tip of the needle would penetrate to 25mm below the surface of the sample when it was lowered into the samples. After the needle was inserted into the MFT sample, the pump was turned on to expand the cavity (water bubble) from the tip of the needle at a constant rate until the MFT yielded. The test was repeated in different areas of the sample to obtain an average shear strength of the MFT. The computer recorded the time and the pressure as the bubble expanded in the sample.

3.2.3 Slurry Samples Preparation Procedures for a Scanning Electron Microscope

A total of twelve samples were prepared for the SEM, and three of these samples were used to address the issues of artefacts. All samples were approximately 150mL to 200mL. The void ratios, pH, and the contents of the samples are listed on Table 3.1. To obtain a clay medium similar to the MFT, the kaolinite clay slurries were prepared to approximately the same void ratios as the MFT. The void ratios of each sample were calculated based on the measured solids contents. The solids contents of the MFT in this study was 27.3%, therefore the slurry samples were prepared accordingly. Appendix 1 shows a sample calculation.

Samples 1, 2, and 3 were MFT, kaolinite clay mixed with deionized water, and kaolinite clay mixed with MFT pond water respectively. The MFT pore water was obtained by centrifuging a MFT sample for 6 hours. Samples 4, 5, 6 and 7 were chemically treated with $NaHCO_3$, NaOH, sodium naphthenates and LGG respectively. Both $NaHCO_3$, and NaOH were laboratory grades purchased from Chemistry Store at the University of Alberta. Syncrude Research Centre provided the sodium naphthenates solution which had been extracted from MFT pond water.

Sample 8 was prepared by removing the pore water of the MFT and replacing it with deionized water. Approximately 400mL of MFT sample was centrifuged at 8000 rpm for 7 hours at room temperature. The same centrifuge machine was used as described in the Atterberg limits tests. The supernatant was decanted and the pore water was replaced with deionized water which was then mixed with the centrifuged MFT soil to obtain a void ratio of 6.6. This process was repeated again to further dilute the MFT pore water. The final supernatant was analysed to ensure that the MFT pore water was sufficiently diluted. The water chemistry results are presented in Section 3.3.

Sample 9, a slurry of kaolinite clay and MFT pond water, was heated to the same processing temperature as used in the Clark Hot Water Extraction process. The sample was heated on an electric hot plate to a measured temperature of 80°C. Once the temperature was reached, the sample was removed and cooled to room temperature (22°C).

Sample 10 and 11 were prepared with the same chemicals and concentrations, 5000ppm of NaOH and 106ppm of LGG. These concentrations were obtained using the Gapon equation. This equation was used as a guideline to predict the approximate amount of NaOH and LGG that would result in a dispersed clay structure. The calculation and assumptions made are found in Appendix 1.

Sample 12 was a MFT sample that was frozen at a slower freezing rate during the SEM preparation process. The clay structure of this sample was compared to the structure of a similar sample that was prepared at a rapid freezing rate. The preparation processes are described in Section 3.2.3.1.

All the aforementioned samples, except for Sample 7, were stirred or shaken for 5 minutes and left undisturbed for 24 hours before being observed under the SEM. Sample 7 was prepared according to the procedure as described in the cavity expansion test. The pH of all the samples were measured immediately after agitation. The pH meter was an Accumet pH meter 50 model. It was calibrated before any readings were recorded.

3.2.3.1 Freeze-drying Method

The freeze-drying method was used to prepare the slurry samples for the SEM. The SEM was a JEOL model, JSM.6301FXV located in the Earth Science Building at the University of Alberta.

Before freezing, each sample was shaken or stirred to resuspend the particles. The prepared samples were then left for at least 5 minutes before a sub-sample was obtained. A square tube (5mm inside width) or a drinking straw (3mm I.D.) was inserted into the container to collect the sub-samples. The tube or straw was then inserted directly into a cup of liquid nitrogen slush which had been cooled to its freezing point of -208°C in a cryosystem model, Emitech K1200. The time to freeze the samples was approximately 1 to 2 seconds.

A 20mm long rectangular copper box was used to hold the frozen slurry samples. The frozen samples were quickly placed vertically in the box filled with glue. The samples were then frozen in place by submerging the copper box and the glued samples into the liquid nitrogen. The frozen samples were fractured while in the liquid nitrogen to expose their internal structure; this process is known as a freeze-fracturing.

These samples underwent a sublimation process in the SEM optical vacuum chamber to remove the ice from the surface of the samples. The surrounding temperature of the chamber was maintained below -40°C to prevent ice recrystallization on the sample surface (Braybrook, 1997). The final stage involved "sputter" coating the samples with gold. The gold coating can penetrate up to a depth of 100 angstroms into the samples.

During observation, the samples were placed in the SEM column on the observation stage with a chamber vacuum set at 6×10^{-7} torr and a temperature at -157°C.

In the slow freezing process, a sample of MFT was collected in a drinking straw. A small cork was used to plug one end of the drinking straw and the sample was left in a freezer for 30 minutes at a temperature of approximately -15°C. The sample was then inserted in a cup of liquid nitrogen slush to preserve the clay structure developed at the ambient temperature of -15°C. The next step was to fracture the sample while in the liquid nitrogen, and the remaining preparation procedures proceeded as described above.

3.3 Results and Discussion

The intent of this study was to develop an understanding of the colloidal behaviour of MFT. This was done by identifying the aforesaid chemical constituents in the pore water of MFT that are responsible for forming the *card-house* structure, and to examine the effects of gypsum addition, and elevated temperature on the MFT structure.

The MFT, kaolinite clay, and Ottawa Sand (silica flour) were used in this study. The purpose of using the kaolinite clay-water slurry was to examine the influence of MFT pore water chemicals individually or in combination on its clay structure. The results infer the effects of these chemicals on the MFT structure. Kaolinite clay was chosen because it is the most abundant clay mineral found in MFT, however the kaolinite clay-water system was not designed to recreate a MFT.

Silica flour slurries were prepared to determine if pore water chemistry would cause the formation of the same card-house structure as seen in the MFT during the SEM sample preparation process. This would determine if the structure was an artefact of the preparation process. The results of this experiment are reported in Section *3.3.2*.

Three-dimensional images of the clay structure produced by the SEM are presented. The following sections will discuss the soil material properties, the issues related to artefacts, and the effects of pore water chemistry on the MFT and kaolinite clay-water structure.

3.3.1 Material Properties

The X-ray diffraction test showed that approximately 32% of clay minerals contained in the MFT sludge are kaolinite, 17% are chlorite, 26% are illite, and 4% are mixed-layers clays. This sample has less amount of kaolinite clays then expected as it has been reported in literature (FTFC, 1995*a*) that 80% of the clay minerals in MFT are kaolinite clays. This may be due to experimental errors in the X-ray diffraction test and more samples are required for testing to verify the accuracy of the above obtained data.

The grain size distribution of the MFT, kaolinite clay, and silica flour (also referred to as Ottawa Sand) are illustrated on Figure 3.4. It shows that 95% of the MFT passed through the #325 sieve (45 μm), and approximately 55% of the material was clay size (<2 μm). The grain size analysis of kaolinite clay indicates that the clay had 100% fines content (<45μm) and 60% of the mineral were clay size. The figure also shows that the sand has 100% fines content and only 15% of the mineral was clay size.

The liquid limits of the air-dried MFT sample and the centrifuged MFT sample were 47.6% and 48.7% respectively. The plastic limit of the air-dried sample was 21.4%.

Since the sample could not reach a low enough water content by centrifuging, the sample was air-dried for the plastic limit determination. The plastic limit was found to be 22.8%. It was concluded that the two dewatering processes had little effect on the measured Atterberg limits. The results of the Atterberg limits are also listed in Table 3.2.

Although the X-ray diffraction test showed that the MFT clay minerals consisted of only 32% kaolinite clay, other evident contradicted this finding. The Activity of this particular MFT was calculated to be 0.47. This indicated that the minerals of MFT were mainly kaolinite clays. The cation exchange capacity (CEC) of kaolinte clay ranges between 5 and 15 meq/L (Mitchell, 1993). The measured CEC of the MFT was found to be 11.5 meq/L, and this result suggested that the clay minerals in MFT are predominantly kaolinite clay.

An Atterberg limits test was also performed on kaolinite clay with two different types of pore water, distilled water and saline water. The purpose of this test was to examine the effects of different pore fluid chemistry on the Atterberg limits, and to verify if the limits were affected by the different chemicals which were added to the kaolinite clay slurry for the SEM. The results are listed in Table 3.2. The test results showed that the Atterberg limits of the kaolinite clay were not affected by different pore water chemistry. Since kaolinite clays have little isomorphous substitution and the permanent charge is very small, the clays do not respond actively to the change in the pore fluid chemistry. Hence, it is also expected that the Atterberg limits of the chemically treated kaolinite clay slurry for the SEM examination would be similar to the Atterberg limits found in the above test results.

The measured solids content, bitumen content, water content, specific gravity, and the pH of the MFT are tabulated in Table 3.3. These results were found to be in the expected range that was typically reported in the literature.

Table 3.4 lists the results of MFT pore water chemistry analysis. For comparison purposes, the water chemistry analysis was only done on the ions which are considered as "major ions" according to FTFC (1995*b*). Hence, an equivalence balance between the anions and the cations were not calculated. The analysis showed that the pH of the MFT is 8.6 and the most abundant cation and anion are the Na^+ and the HCO_3^- respectively. Compared to the concentrations given in Table 2.1, the water analysis of the MFT in this study gave reasonable results. The difference in the results may be due to the variation of water chemistry in different MFT samples.

Given the concentrations of Na^+, Ca^{2+}, and Mg^{2+} ions, the ESR calculated based on the Gapon Equation was 1.1 which suggested that the MFT has a highly dispersed structure. However, this ESR is overestimated because the SAR of the MFT is 73 and the ESR was calculated using K_G of 0.015 $(mmol/L)^{-1/2}$. Recall that this coefficient is used for soil that has a SAR less than 30 and K_G decreases as the SAR exceeds 30. Since this study does not require the exact ESR of the MFT, the aforementioned ESR gives an sufficient indication that the MFT has a dispersed structure. The dispersed structure of MFT is evident in the SEM micro-graph discussed in Section *3.3.3*.

In order to obtain an accurate ESR of MFT, it is necessary to determine K_G through laboratory testing. This testing is beyond the scope of the thesis and therefore the experimental program for future work is briefly described in the Recommendations, Section **5.3**.

3.3.2 Is the Observed Clay Structure an Artefact of the SEM Preparation Procedure?

Prior to the examination of MFT structure, it was imperative to verify whether or not the observed slurry clay structures shown on the micro-graphs truly represented its unfrozen structure. The authenticity of the structure is dependent on the freezing rate which depends on the freezing methodology, and the size of the sample which affects the freezing rate.

Figure 3.5a and b illustrate the MFT structure prepared by fast freezing and slow freezing respectively. Fast freezing involved freezing of sample in cooled liquid nitrogen (-208°C), and slow freezing referred to the process in which the sample was frozen at -15°C. Figure 3.5b shows that the clay particles were pushed together by the large ice crystals seen in the spacing between each stack of clay particles. This experiment showed that the faster the freezing rate, the smaller the ice crystals which formed within the sample. Thus, the liquid nitrogen slush at -208°C and a small diameter sample tube were used for SEM preparation process.

The main concerns suggesting that an observed structure of a slurry sample was an artefact of freezing are as follows:

1. The spacing between rows of clay particles are much larger than can be accounted for based on the double layer theory. The theory states that the electric double layer thickness of kaolinite rich clays is about 10 angstroms. Figure 3.6 shows the typical structure of MFT where the spacing is observed to be 50,000-90,000 angstroms (5-9 μm).

2. Electrolytes in the pore water of the MFT or kaolinite clay-water system may cause the ice crystals to form in a certain pattern that forces the clay particles to align in the same direction.

The first concern stated that the spacing between aligned clay layers was too large according to the electric double layer theory. The author agrees with this statement and adds that the spacings observed on the micro-graphs are not representative of the electric double layer thickness. The theory proposed by Babchin *et al.* (1991) described the formation of the *card-house* structure as being due to the internal dipole-quadrupole interactions of kaolinite clay. Further investigation of the internal dipole-quadrupole theory requires the expertise of a clay mineralogist which is beyond the scope of the thesis. Note however, that many of the cross-links between the clay layers were unintentionally removed during the fracturing and sublimation processes. When the frozen sample was fractured, some of the weakly bonded cross-linking clay particles may have been plucked off. Similarly, these clay particles could also have been removed by the applied vacuum in the SEM chamber. As a result, the clay particles may appeared to aligned mainly in a *face-to-face* chain-like pattern and less in a edge-to-face pattern. There are examples, however of these cross-linking particles throughout the image which inferred the *card-house* structure as suggested by Babchin *et al.* (1991) and Mikula *et al.* (1991).

The second issue was resolved by comparing the structure of a kaolinite clay slurry (Sample 10) to a silica flour slurry (Sample 11) which were prepared with similar chemicals and concentrations. The preparation procedures have been described in

Section *3.2.3*, and the assumptions made in the calculation to obtain the chemical concentrations are presented in Appendix 1.

Figure 3.7a and b compare the structures between the kaolinite clay and the silica flour slurries. If the observed particle alignment was due to the influence of water electrolyte on the ice crystals growth pattern, it should be reflected in both kaolinite and silica flour samples with similar pore fluids chemistry. Comparing the structure of kaolinite clay slurry to that of silica flour slurry, the kaolinite clay slurry exhibited a dispersed structure that is similar to that of MFT. The structure of the silica flour slurry with the same water chemistry remained unchanged. This experiment indicates that the electrolytes in the pore water did not cause ice crystals to distort the structure of the slurries during the freezing process, otherwise, both of these silica flour and kaolinite clay slurries would have had the same structure.

Other evidence which suggested that the cryogenic electron microscopy is useful for probing the MFT structure were presented by Mikula *et al.* (1996*a*). They used a confocal microscope to examine the structure of an unfrozen MFT sample. Figure 3.8 shows that the orientation or structuring of the clay component was similar to that observed in the cryogenic sample prepared for SEM. This suggests that the structure of the slurry sample was not affected by the freezing process since a similar structure has been observed in a unfrozen sample.

In another test conducted by Mikula *et al.* (1996*a*), two samples of MFT were sheared in a blender to destroy the floc structure. The first sample was allowed to sit for a short time before it was frozen rapidly, and the other sample was frozen immediately after the disturbance. The specific time periods were not reported for the tests. The method of preparation involved freezing the sample in a liquid nitrogen slush and then freeze fracturing them to expose the internal structure. The details of the preparation method are described in Mikula, *et al.* (1991). The structure in the first sample showed a slightly disoriented *card-house* structure, while the structure of the latter sample was completely disoriented. By leaving the first sample undisturbed for a short time, the clay particles in the MFT were allowed to move towards an equilibrium between the attraction and repulsion forces thus forming the *card-house* structure. However, this sample was frozen before an equilibrium was fully achieved, thus achieving the semi-oriented structure presented in Figure 3.9. In the second sample, the clay particles did not have the time to equilibrate and reorient themselves, therefore the particles appeared to be scattered (Figure 3.10). This showed that the clay structures in the liquid state was preserved in the solid state. Furthermore, if the freezing process creates artefacts, both samples would have had the same clay structure when observed in the SEM.

3.3.3 Effects of Various Pore Water Chemicals on the MFT Structure

Section *3.1.2* reviews the theories developed by several researchers explaining the formation of MFT structure. The formation of MFT structure involved the interactions between the clay particles and the chemicals associated with the MFT. The suggested inorganic chemical that is responsible for the formation of the MFT structure is HCO_3^-, and the organic chemicals are the bitumen, *strongly bound* organic matter and the surfactants. The structures were examined directly using a SEM to better understand how these chemicals are responsible for the MFT structure. Following the discussion of the effects of the pore fluid chemistry on the slurry structure, the observed particles settling behaviour of these slurries are described.

Initially in this study, a sample of MFT, kaolinite clay with deionized water, and kaolinite clay with MFT pond water were prepared. The structures of these three samples were then observed using SEM and then compared. In Figure 3.6, the typically observed *card-house* structure of MFT is evident. van Olphen (1977) stated that a *card-house* structure is a three-dimensional formation with clay particles aligned in a *edge-to-face* and *edge-to-edge* pattern. Although the described patterns are evident in the MFT structure, the clay particles were also oriented in a *face-to-face* fashion forming parallel alignment of the clay particles. This structure is classified as highly dispersed. Figure 3.11 shows the kaolinite clay mixed with deionized water and Figure 3.12 shows the structure of kaolinite clay mixed with MFT pond water. A typical flocculated structure can be seen in kaolinite clay slurry mixed with deionized pore water. When mixed with MFT pond water, a *card-house* structure was observed; it has a similar but more aggregated structure than that of the MFT shown in Figure 3.6. These results indicates that the pore water chemistry likely plays a major role in the formation of the *card-house* structure in MFT, thus further investigation of the chemicals affecting the formation of the structure observed in the MFT was essential.

The effects of these chemicals on the MFT structure can be inferred using the kaolinite clay-water system. Kaolinite clay was chosen because according to past literature, it is the dominant clay mineral in MFT. The experiment was therefore carried out by examining the kaolinite clay slurries structure with the addition of inorganic chemicals such as NaOH and HCO_3^-. The effects of sodium naphthenates on the kaolinite slurry structure was also examined. In another test, the pore water in MFT was replaced by deionized water to observe if the remaining organic chemicals, bitumen and *strongly bound* organic matter, is also responsible for the *card-house* structure observed in the MFT.

The effects of HCO_3^- on the structure of kaolinite clay is shown in Figure 3.13. This structure is similar to the MFT structure shown on Figure 3.6. It is evident that the addition of HCO_3^- produces wider spacing between aligned clay particles in the kaolinite slurry than with the addition of MFT pond water (Figure 3.12). This suggests that:

1) presence of HCO_3^- in the MFT pond water may contribute to the formation of the MFT *card-house* structure;
2) the structure of MFT may be due to the pH level of the MFT colloidal system (typically 8.5) at which the formation of the *card-house* structure occurs;
3) The *card-house* structure may be affected by Na^+ dissociated from the added $NaHCO_3$.

It appeared that the presence of HCO_3^- may contribute to the formation of the MFT *card-house* structure. Mikula *et al.* (1993) reported that the high degree of dispersion of MFT was related to the HCO_3^- content of the pore fluid. HCO_3^- in a water system exists only between a pH of 8.3 to 10.8 (Sawyer *et al.*, 1994), and the least desirable properties of MFT are usually around 8.5 which is also the pH commonly measured in MFT. The least desirable properties of MFT include the poor consolidation behaviour and the MFT *card-house* structure. However, their findings could also explain that the pH in relation to the existence of HCO_3^- may have an influence on the clay structure instead of the chemical constituent, HCO_3^-. The first two issues require further research which is discussed in Section *5.3.2*.

Thirdly, the *card-house* structure may be caused by the Na^+ ion dissociated from $NaHCO_3$. Mikula *et al.* (1991) created a model slurry system, which consisted of koalinite clays in a 455ppm of Na^+ and 165ppm of Cl^- solution, to simulate the actual fine tailings. The observed clay structure exhibited randomly distributed clay particles which indicated that neither the Na^+ nor the Cl^- were responsible for the *card-house* structure formation.

The Clark extraction process uses NaOH and hot water to improve the separation of bitumen from the oil sands. NaOH is a dispersing agent and may also have an effect on the clay structure of MFT. The influence of NaOH on the MFT can therefore be better understood by examining the type of structure formed in a kaolinite clay-water system after the addition of NaOH. In this experiment, 140ppm of NaOH was added to the kaolinite clay-deionized water slurry; the observed structure is presented in Figure 3.14. Compared to a mixture with only deionized water (Figure 3.11), a slight parallel pattern of clay particles was observed but not nearly to the extent when HCO_3^- was added. The NaOH made the pore fluid highly alkaline ($pH = 12.3$) producing more negatively charged clay particles. This combination of an alkaline solution and negatively charged clay particles resulted in a stable suspension with a slightly dispersed structure. Thus NaOH appeared to cause a slightly dispersed structure in kaolinite clay slurry. This result infers that NaOH added during the bitumen extraction process increases the pH of the processing water which may contribute to the formation of the MFT *card-house* structure.

The natural surfactants, naphthenates and sulfonates, produced during the Clark process also have a strong affinity for clay particles and can cause higher negatively charged clay particles (FTFC, 1995*d*). Sodium naphthenates, provided by Syncrude, were extracted from the MFT pond water which has about 100ppm naturally. The chemicals was then mixed with kaolinite clay to examine if they would cause the kaolinite clay particles to form a *card-house* structure. The SEM micro-graph shown in Figure 3.15 indicates that this surfactant had little effect on the arrangement of the clay particles since a random flocculated system can be seen. This suggests that sodium naphthenates, by themselves, may not be responsible for the formation of the *card-house* structure observed in the MFT.

A test was performed to examine the effects of the bitumen and the *strongly bound* organic matter on the structure of MFT. A sample of MFT was centrifuged to separate the pore water from the solids, and the pore water of the sample was replaced with deionzied water. This process was repeated once more to ensure that the MFT pore water was diluted. The water chemistry analyses of the original MFT pore water and the diluted MFT pore water are listed on Tables 3.4 and 3.5 respectively. The pH and especially the concentration of Na^+, SO_4^{2-}, Cl^- and HCO_3^- ions were considerably reduced, and the concentration of Ca^{2+}, Mg^{2+} and K^+ ions increased slightly. The ESR of this sample calculated based on the Gapon Equation was 0.05. According to Mitchell (1993), an ESR of 0.05 will produce a flocculated clay-water system. However a *card-house* system was observed as shown in Figure 3.16. This suggests that the bitumen and the strongly bound organic matter appeared to be also responsible for forming the *card-house* structure of MFT. This observed structure can be explained by the theory proposed by Majid, *et al.* (1990) that the *strongly bound* organic matter imposed a hydrophobic character on clay surfaces allowing interparticle bridging by residual bitumen to set up a weak gel structure. However, it is also possible that the low concentrations of HCO_3^-

(83mg/L) that remained in the pore water was sufficient to form the structure or the pH of this sample may have created the structure. Further investigation of this issue is discussed in Section *5.3.2*.

The structure of MFT after the addition of LGG is shown on Figure 3.17. Both Figures 3.6 and 3.17 exhibit a *card-house* structure, however the latter figure shows a more crowded, less organised and agglomerated network of clay particles. This may be explained by the replacement of Na^+ ions by the Ca^{2+} ions which reduced the diffuse double layer thickness of clay particles moving the system to a less dispersed state. The measured thixotropic strengths of the two day old MFT with and without gypsum were 420Pa and 165Pa respectively. The output data of the cavity expansion test is shown on Figure A-1 and A-2 in Appendix 1 with a sample calculation. Thus the addition of gypsum produced a finer and stronger clay structure in the MFT.

The structure of a kaolinite mixed with MFT pond water at 80°C is shown in Figure 3.18. In comparison to the *card-house* structure of unheated MFT pore water (Figure 3.12), the heated structure has a larger spacing between aligned clay particles. Heating the sample caused the spacings to approximately increase from approximately 5μm to about 10μm. Mitchell (1993) explained that in a clay-water system, an increase of temperature in the system will increase the diffuse double layer thickness as illustrated in the following equation:

$$\frac{1}{K} = \left(\frac{\varepsilon_0 DkT}{2n_o e^2 v^2}\right)^{\frac{1}{2}} \tag{3.7}$$

In this equation, $\frac{1}{K}$ is related to the thickness of the double layer and is shown to be a function of the dielectric constant of the solvent (D), temperature (T), electrolyte concentration (n_o) and the cation valence (ν). ε_o, e and k are the permittivity of the medium, electronic charge (1.602 X 10^{-19} coulomb), and the Boltzmann constant (1.38 X 10^{-23} J°K^{-1}) respectively. Provided that all the other parameters remain constant, an increase in temperature of the medium will increase the double layer thickness causing the clay-water system to have a less tendency to flocculate. This action was probably the cause for the change in the observed structure although the increased spacing between the clay alignments displayed in Figure 3.18 should not be interpreted as the double layer thickness. This experiment suggests that the hot water used in the extraction process of the oil sands combined with the aforementioned chemicals enhances the structure of tailings creating a highly dispersed MFT structure as seen on Figure 3.6.

3.3.4 Settling of Clay Particles Observed on the SEM Samples

Standpipe tests were not performed on the aforementioned kaolinite clay or MFT slurries to examine the effects of pore water chemistry on the initial consolidation characteristics of MFT because the topic is beyond the scope of the thesis. However, during the sample preparation for the SEM, observation of the settling particles were made.

It was observed that the clay particles in kaolinite slurries mixed with deionized water, MFT pond water, or HCO_3^- settled within the first 2 to 3 hours after mixing leaving a clear layer of water atop the settled clay particles. Similar behaviour was also observed in the heated kaolinite sample mixed with MFT pond water. The kaolinite clay mixed with NaOH and deionized water did not settle as quickly; 3 hours after mixing, most of the clay particles appeared to have settled but the water remained cloudy. This behaviour was also observed in the kaolinite clay mixed with the sodium naphthenates solution.

In the MFT sample, identified as Sample 8 in Table 3.1, most of the clay particles settled within 10 minutes after stirring but the water remained muddy. In a LGG treated MFT sample, only a thin layer of clear water was observed 48 hours after stirring.

From the above observation, it is concluded that the *card-house* structure of MFT is not solely responsible slow long-term consolidation rate of MFT. Although the card-house structure was most evident in the kaolinite slurry mixed with HCO_3^- or MFT pond water, their particle settling behaviour were unaffected by these chemicals compared to MFT. The NaOH and sodium naphthenaes in the kaolinite clay-deionized water system acted as dispersing agents causing the particles to repel each other and prevented them from settling. This infers that the these chemicals would also have a similar effect on the MFT.

Recommendation for future study of the effects of the above pore water chemicals on the consolidation characteristics of MFT is discussed in Section *5.3.2*.

3.3.5 Engineering Applications

The overall consolidation rate of MFT may be accelerated if the dispersed MFT *card-house* structure is destroyed. MFT with a flocculated structure would be expected to consolidate much quicker than MFT with the dispersed *card-house* structure because a flocculated structure opens up more flow paths for the pore water to escape to the surface. Furthermore, the *card-house* structure of MFT exposes more mineral surfaces resulting in a higher degree of water to mineral bonding (FTFC, 1995*f*). In understanding what chemicals are responsible for the formation of the MFT structure, the water chemistry of the MFT pore water may be altered to destroy the dispersed *card-house* structure. The application of this study in aid of increasing the overall consolidation rate of MFT are listed in the following:

1. In the discussion, it was suggested that HCO_3^- may contribute to the formation of the MFT *card-house* structure. It was also suggested that the pH value of 8.5 may cause the formation of the structure instead of the HCO_3^-. If the HCO_3^- is responsible for the formation of the *card-house* structure, it is possible to destroy the MFT *card-house* by increasing the pH of MFT above 10.8 or decreasing the pH below 8.3 to convert the HCO_3^- to CO_3^{2-} or H_2CO_3 respectively. If the pH of MFT system is responsible for the formation of the structure, the structure may be destroy with the modification of the pH levels as suggested above.
2. The addition of NaOH accelerates the release of naphthenic acids (natural surfactants) into the process water. Previous studies by other researchers hypothesised that the natural surfactants are responsible for the slow settling behaviour and toxicity of MFT (FTFC, 1995*c*). Hence, if the use of NaOH is reduced or excluded, the above effects on the MFT may be lessened.
3. It was found that the MFT structure might be formed in the presence of bitumen and the strongly-bound organic matter. Re-extracting the bitumen from the MFT may

prevent the formation of the *card-house* structure as observed in the SEM micrograph.

4. The micro-graph of the heated kaolinite clay-water system displayed larger spacing between rows of aligned clay particles causing the system to be even more dispersed. This indicated that the high processing temperature used in the bitumen extraction process increased the spacing between each clay alignment in MFT structure. It is suspected that by lowering the temperature of the processing water, the observed spacing in MFT structure may be smaller, thus generating a less dispersed structure.
5. The use of LGG in MFT is advantageous because the chemical strengthens and produces a more aggregated structure so that it can hold the sand grains forming a nonsegregating mixture. The sand grains act as an internal surcharge resulting in a rapid initial consolidation of MFT.

3.4 Summary

A Scanning Electron Microscope was used to examine the effects of HCO_3^-, NaOH, organic matter, sodium naphthenates, laboratory grade gypsum, and the processing temperature on the structure of MFT. A simplified clay-water model of MFT using kaolinite clay slurry was created for the purpose of studying the behaviour of the clay particles under the influence of various chemicals. It was not designed to recreate MFT although a remarkably similar *card-house* structure was formed using kaolinite clay.

The possibility of the observed structure being an artefact of the cryogenically treated slurry sample was examined. Experiments performed in this study showed that the freezing temperature and the agents used in the freezing process produced a fast enough freezing rate to inhibit large ice crystal growth. It was found that large crystals formation can distort the original clay structure when the sample is frozen slowly.

In another experiment, the structure of kaolinite clay slurry was compared to that of silica flour slurry. The purpose of this test was to determine if the water chemistry in the slurry pore water can cause the formation of artefacts. Both of these slurries were prepared with the same chemicals and concentrations. It was found that the kaolinite clay slurry structure exhibited a *card-house* structure similar to that of MFT. The silica flour structure displayed randomly distributed particles. If the pore fluid electrolytes cause the ice to form in a certain pattern that forces the particles into a *card-house* formation, one would expect the silica flour to display a similar structure as the kaolinite clay slurry.

Thus it was concluded that the observed structures in the clay-water slurry and MFT were not artefacts of freezing. These results were supported in the studies by Mikula *et al.* (1996) where confocal microscopy observed similar MFT structure and redevelopment of the structure with time after disturbance was not evident.

The effects of inorganic compounds on the structure of MFT were analysed. The result suggests that HCO_3^- in the MFT pore water may contribute to the formation of the MFT structure. The HCO_3^- mainly comes from the connate water in the oil sands and from the adsorption of CO_2 during the aeration process in the plant. HCO_3^- exits at a pH level between 8.3 and 10.8. However, it is possible that the pH of the MFT (typically 8.5) may have caused the formation of the *card-house* structure.

The NaOH (added during the Clark extraction process) had a lesser effect on kaolinite clay-water system than the HCO_3^-. The addition of NaOH increases the pH of the processing water which may enhance to the formation of the observed MFT structure.

The organic compounds that were examined are the sodium naphthenates, bitumen and the *strongly bound* organic matter. The addition of sodium naphthenates did not affect the structure of the kaolinite clay-water system. The kaolinite clay-water system retained a flocculated structure. It appears that this surfactant is not responsible for the dispersed structure of MFT. It was observed that both the bitumen and the *strongly bound* organic matter in MFT also have an effect on the dispersed *card-house* structure even though the ESR calculated for the sample indicated that a flocculated system should be present. This inferred that the bitumen and the organic matter may also be responsible for the formation of the MFT *card-house* structure with little influence of the water chemistry.

The effects of laboratory grade gypsum, and the processing temperature on the structure of MFT were also examined. The addition of gypsum to MFT did not change the structure but made it finer and much stronger.

The processing temperature used in the Clark Hot Water Extraction process is 80°C. The high temperature used in the extraction process combined with the organic and inorganic chemicals enhanced the *card-house* structure of MFT. The width of the spacing between the aligned clay particles of a preheated kaolinite-HCO_3^- slurry sample doubled compared to an unheated one. Hence, if the temperature of the processing water is lowered during the extraction of bitumen from the oil sands, the spacing between the clay alignment of the MFT would expect to be smaller.

The Gapon Equation was used to calculate the ESR of MFT. Although the ESR (1.1) was overestimated, for this study, it gave sufficient indication that the MFT is a highly dispersed structure. This structure was observed in the SEM micro-graphs. In order to obtain an accurate ESR, it is necessary to determine the Gapon exchange coefficient, K_G, through laboratory tests.

Standpipe tests were not performed on the kaolinite slurries or the MFT samples because it was beyond the scope of this thesis. However, the particles settling behaviour of these samples were observed. These observations inferred that the slow long-term consolidation rate of MFT is not controlled solely by its dispersed *card-house* structure. The kaolinite clay slurries composed of MFT pond water or HCO_3^- exhibited a *card-house* structure similar to the MFT structure, however the particles of these samples settled in 3 hours leaving a clear layer of water similar to the sample of kaolinite clay with only distilled water. Both the NaOH, and sodium naphthenates caused the clay particles in the kaolinite clay slurries to settle slowly. The water remained cloudy after most of the solids have settled to the bottom of the container. This indicates that these chemicals, along with other chemicals in the MFT, may cause the slow long-term consolidation of MFT.

The engineering application of these findings had been discussed. Several suggestions were made on altering the water chemistry of MFT to prevent the formation of the MFT dispersed *card-house*.

Table 3.1: Samples prepared for scanning electron microscopy.

Sample	Solids	Pore Fluid	Void Ratio	pH	Modification
1	MFT	MFT pore water	6.6	8.3	none
2	Kaolinite	deionized water	8.7	6.9	none
3	Kaolinite	MFT pore water	8.7	8.3	none
4	Kaolinite	deionized water	8.7	7.7	added bicarbonate (995ppm)
5	Kaolinite	deionized water	6.6	12.0	added NaOH (140ppm)
6	Kaolinite	sodium naphthenate solution	6.6	7.0	extracted from tailings water
7	MFT	MFT pore water	6.6	8.5	added $CaSO_4 \bullet 2H_2O$ (2500ppm)
8	MFT	deionized water	6.6	n/a	removed pore water by centrifuging
9	Kaolinite	MFT pore water	9.3	8.5	heated to 80°C
10	Kaolinite	deionized water	6.6	12.3	added NaOH (5000ppm), $CaSO4 \bullet 2H_2O$ (106ppm)
11	silica flour	deionized water	6.6	12.3	added NaOH (5000ppm), $CaSO4 \bullet 2H_2O$ (106ppm)
12	MFT	MFT pore water	6.6	8.3	slow freezing preparation

Table 3.2: The results of Atterberg limits of MFT samples and kaolinite samples.

	MFT		Kaolinite	
	Air-dried	Centrifuged	Distilled water	Saline Water
LL(%)	47.6	48.7	42.1	43.3
PL(%)	21.4	22.8[1]	25.1	22.5

[1] semi air-dried sample

Table 3.3: MFT properties.

Solids Content, *S* (%)	27.3
Bitumen Content, *b* (%)	3.26
Water Content, w (%)	263
Specific Gravity, G_{ss}	2.5
pH	8.6

Table 3.4: MFT water analysis.

Components	mg/L
Ca^{2+}	1.2
Mg^{2+}	1.1
Na^{+}	450
K^{+}	8.26
Cl^{-}	225
SO_4^{2-}	34.8
HCO_3^{-}	665

Table 3.5: MFT water analysis of diluted pore water.

Components	mg/L
Ca^{2+}	1.4
Mg^{2+}	4.6
Na^{+}	36.2
K^{+}	13.1
Cl^{-}	6.6
SO_4^{2-}	11.4
HCO_3^{-}	83

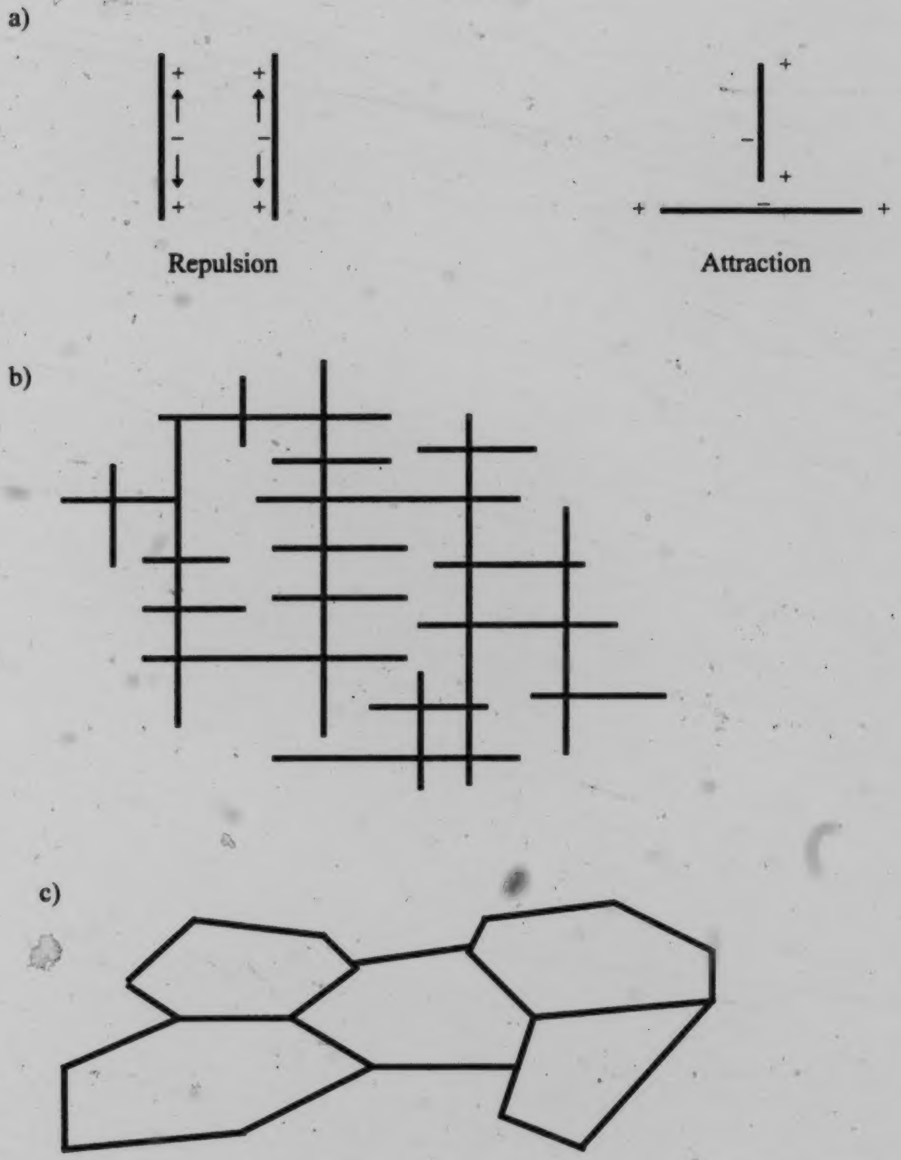
a)
+
−
+
+
−
+
Repulsion
+
−
+
+
−
+
Attraction
b)
c)

Figure 3.1: a) Repulsion and attraction forces between platelike clay particles represented as quadrupoles;
b) Cardhouse structure due to quadrupole interactions;
c) Chain spatial arrangement of dipole;
(Babchin *et al.*, 1991)

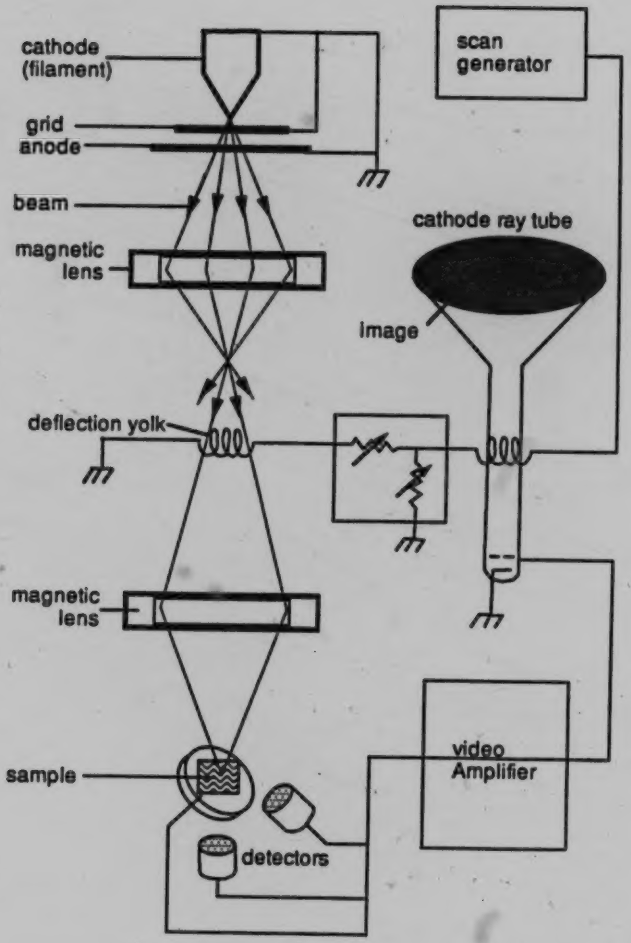
cathode
(filament)
grid
anode
beam
magnetic
lens
deflection yolk
magnetic
lens
sample
detectors
scan
generator
cathode ray tube
image
video
Amplifier

Figure 3.2 : A schematic of a scanning electron microscope column (Braybrook, 1997)

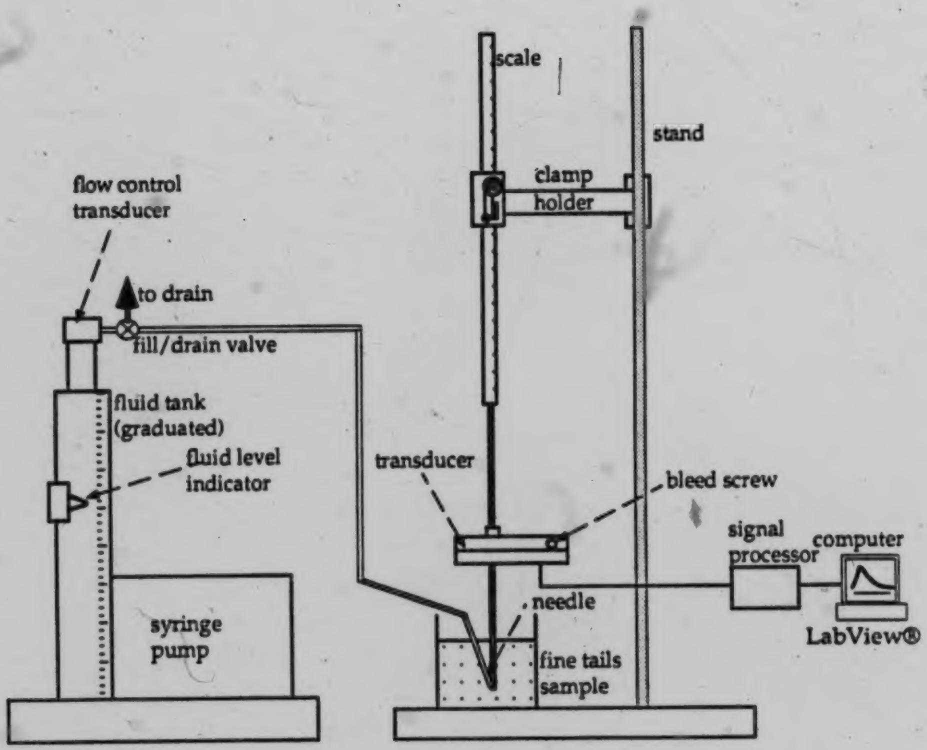
scale
stand
clamp
holder
flow control
transducer
to drain
fill/drain valve
fluid tank
(graduated)
fluid level
indicator
transducer
bleed screw
signal
processor
computer
needle
syringe
pump
fine tails
sample
LabView®

Figure 3.3: The experimental set-up for the cavity expansion test (Suthaker, 1995)

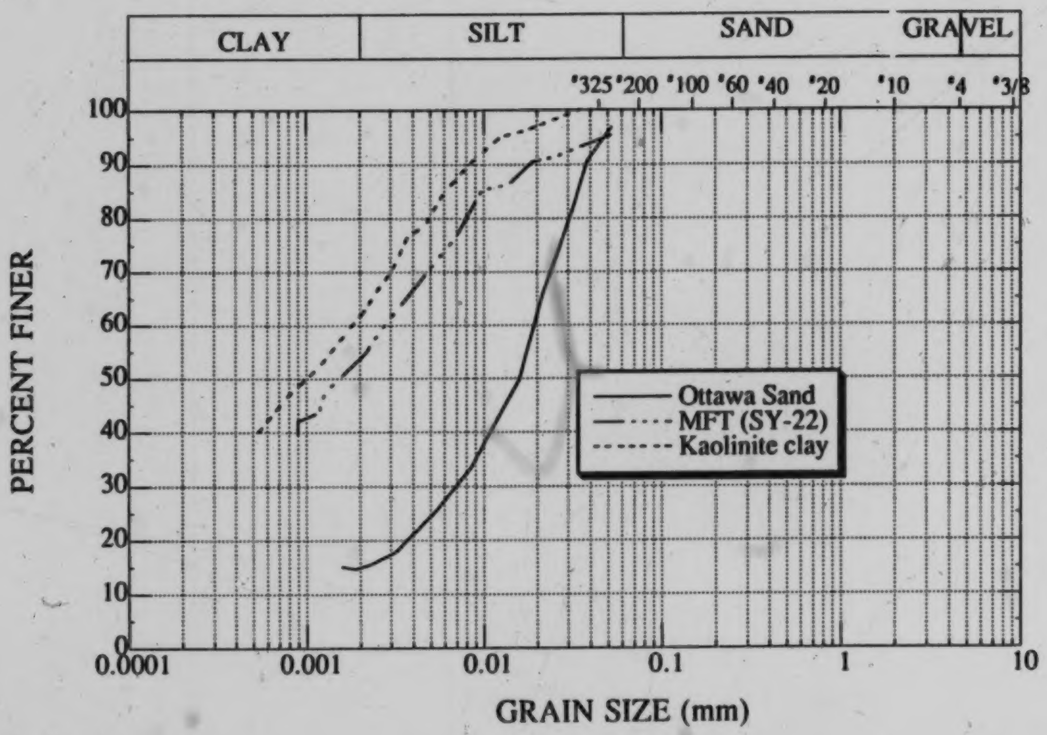

Figure 3.4: Grain size distribution for MFT (SY-22), kaolinite clay, and silica flour

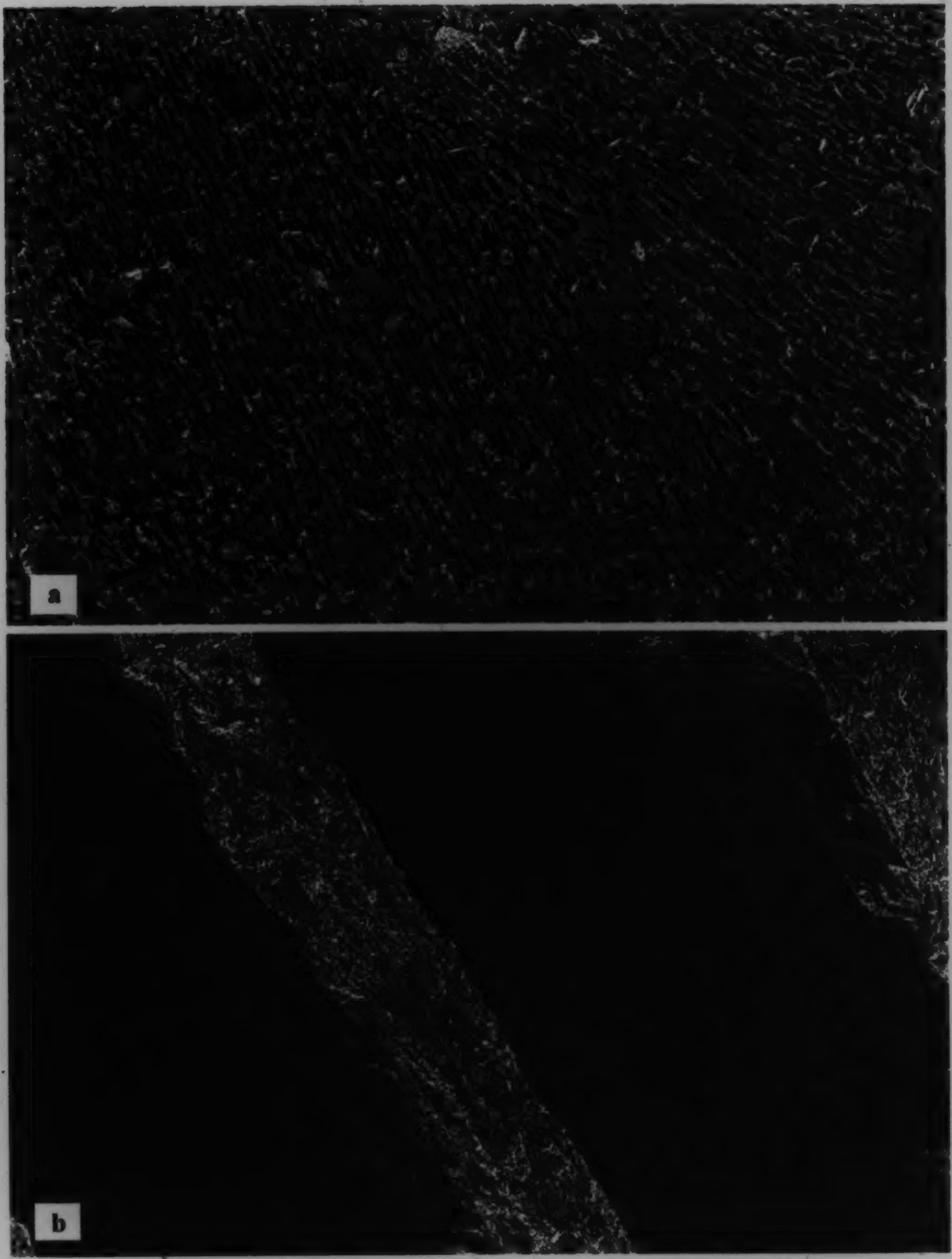

Figure 3.5: a) MFT exposed to fast freezing rate
b) MFT exposed to slow freezing rate

(Magnification at 200X: ▬ 10 microns)

Figure 3.6: MFT (SY-22)
(Magnification at 500X: ▬ 10 microns)

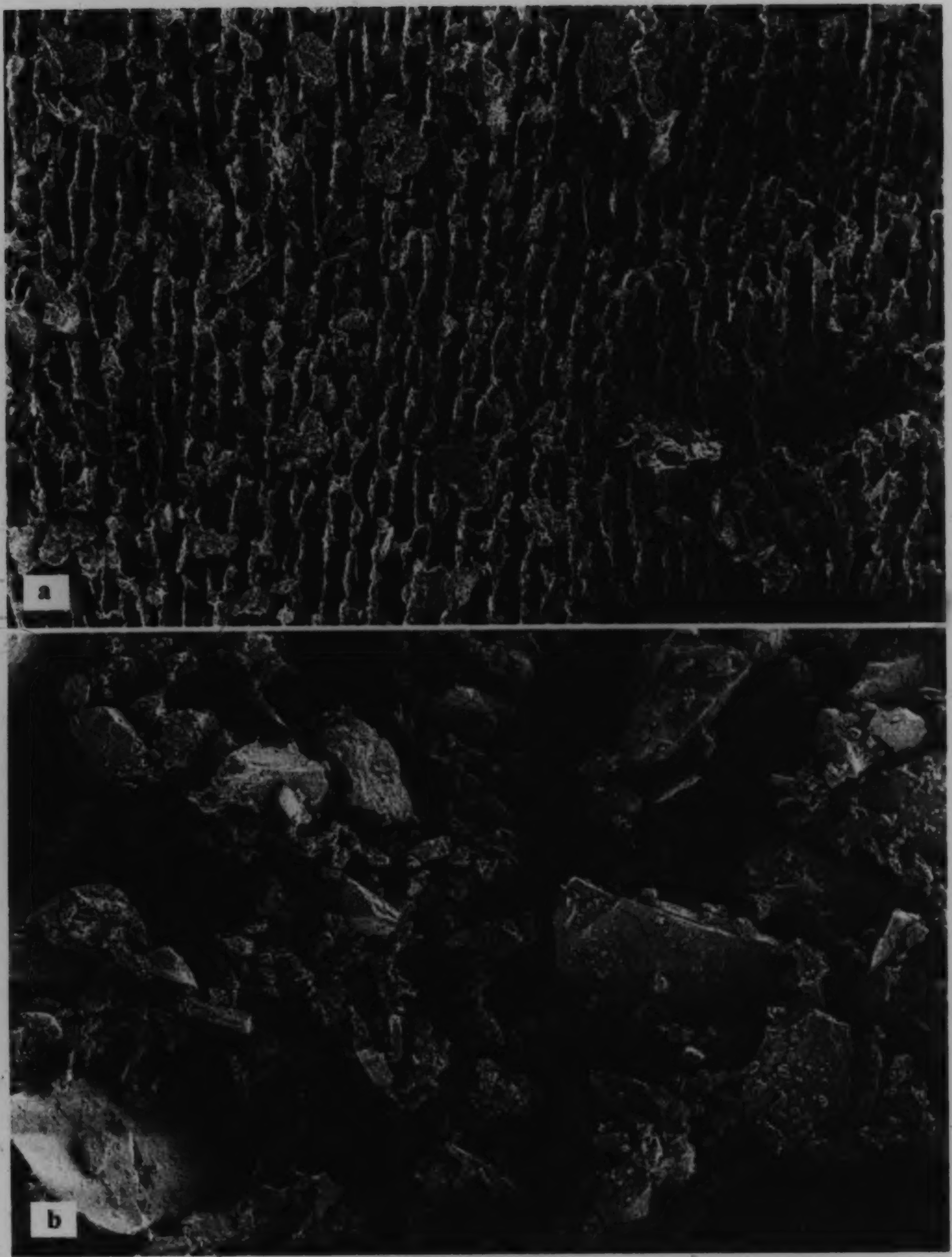

Figure 3.7: a) Kaolinite slurry with ESR near 2.0
b) Silica flour slurry with ESR near 2.0.
(Magnification at 500X: —— 10 microns)

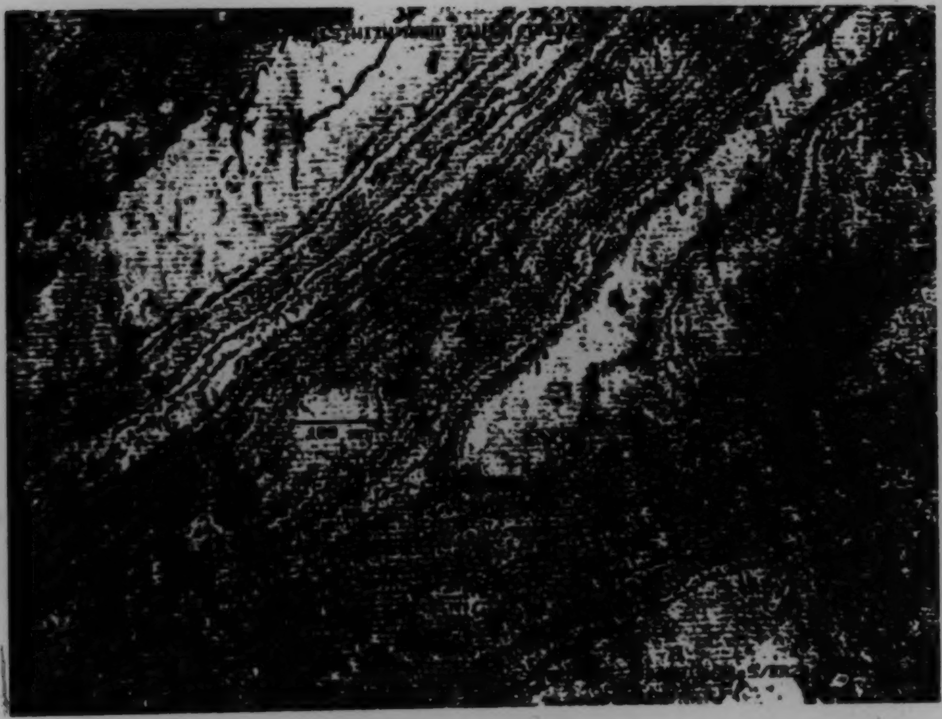

Figure 3.8: Confocal micrograph of a MFT sample that was unfrozen and observed using the confocal optical technique (Mikula *et al.*, 1996*a*)

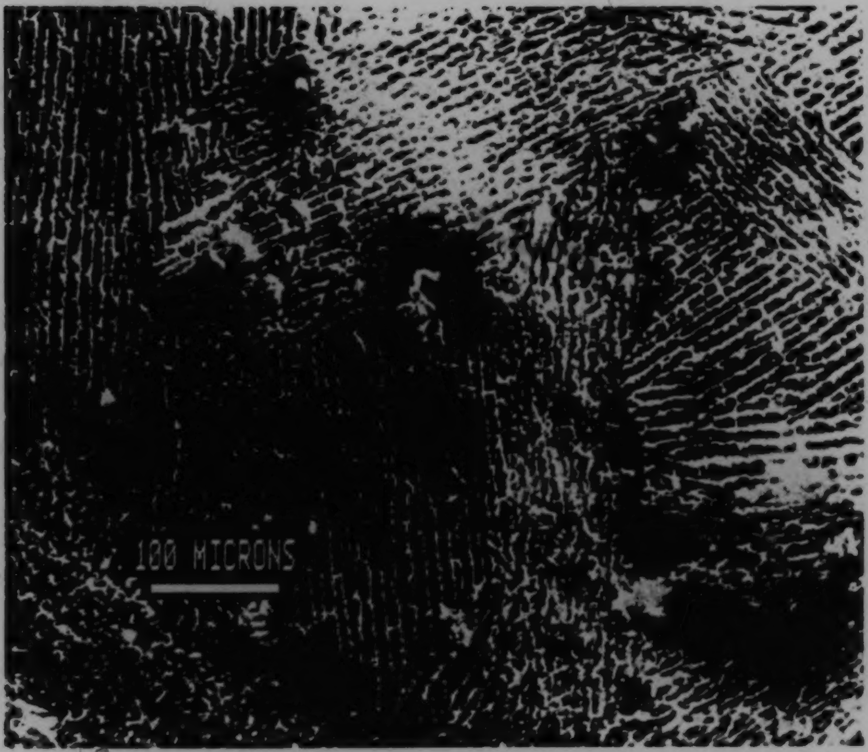

Figure 3.9: Electron micrograph of a MFT sample that was vibrated to destroy the floc structure and allowed to sit for only a short time before rapidly frozen (Mikula *et al.*, 1996a)

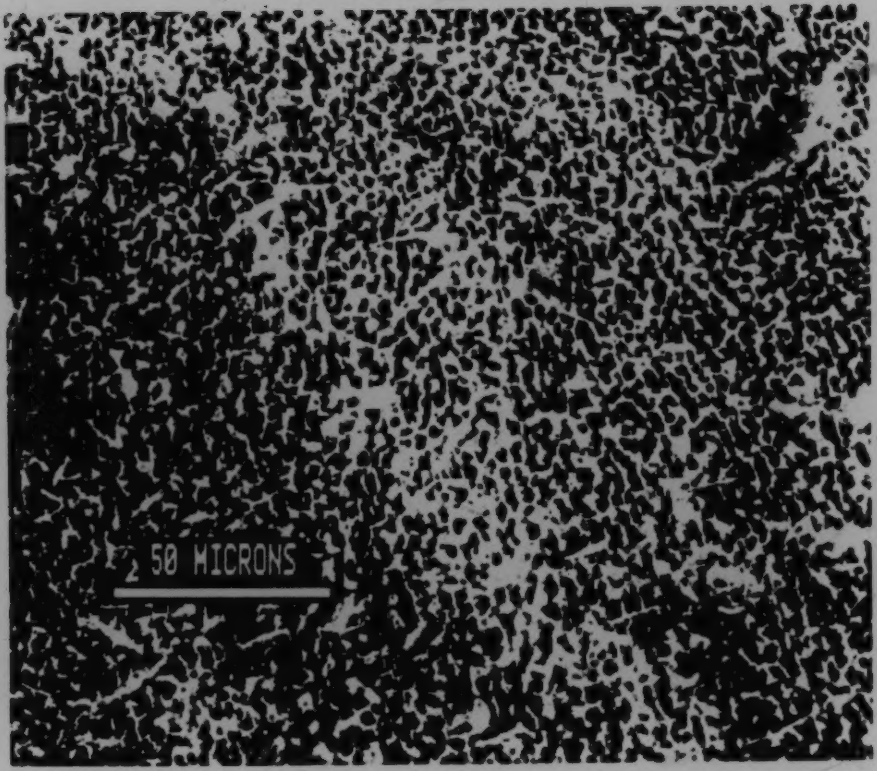

Figure 3.10: Electron micrograph of a MFT sample that was vibrated and then frozen immediately (Mikula *et al.*, 1996a)

Figure 3.11: Kaolinite clay mixed with deionized water.
(Magnification at 500X: —— 10 microns)

Figure 3.12: Kaolinite clay mixed with MFT pond water.
(Magnification at 500X: —— 10 microns)

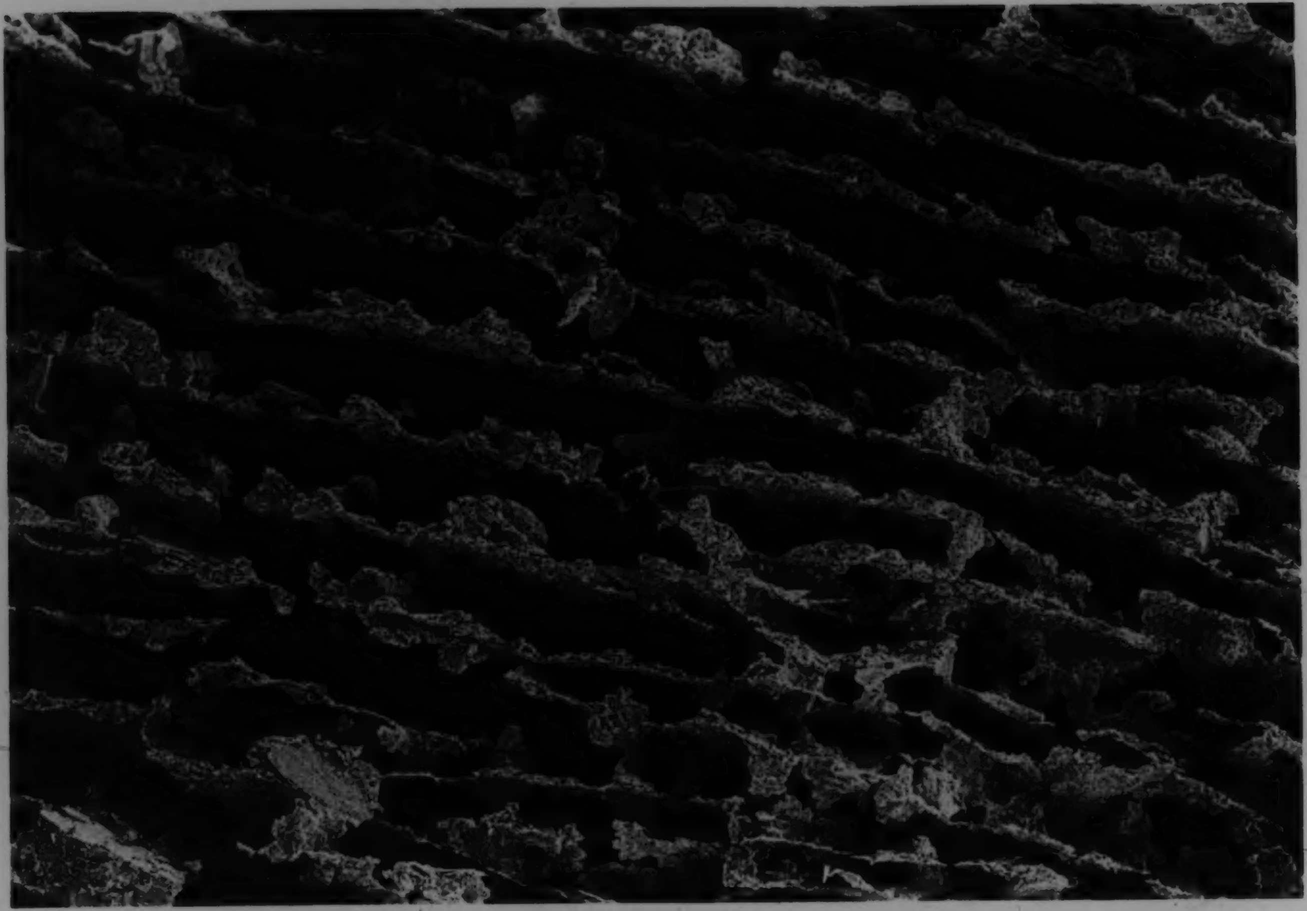

Figure 3.13: Kaolinite clay mixed with deionized water and bicarbonate.
(Magnification at 500X: —— 10 microns)

Figure 3.14: Kaolinite clay mixed with deionized water and NaOH. (Magnification at 500X: —— 10 microns)

Figure 3.15: Kaolinite clay mixed with sodium naphthenate solution.
(Magnification at 500X: ——10 microns)

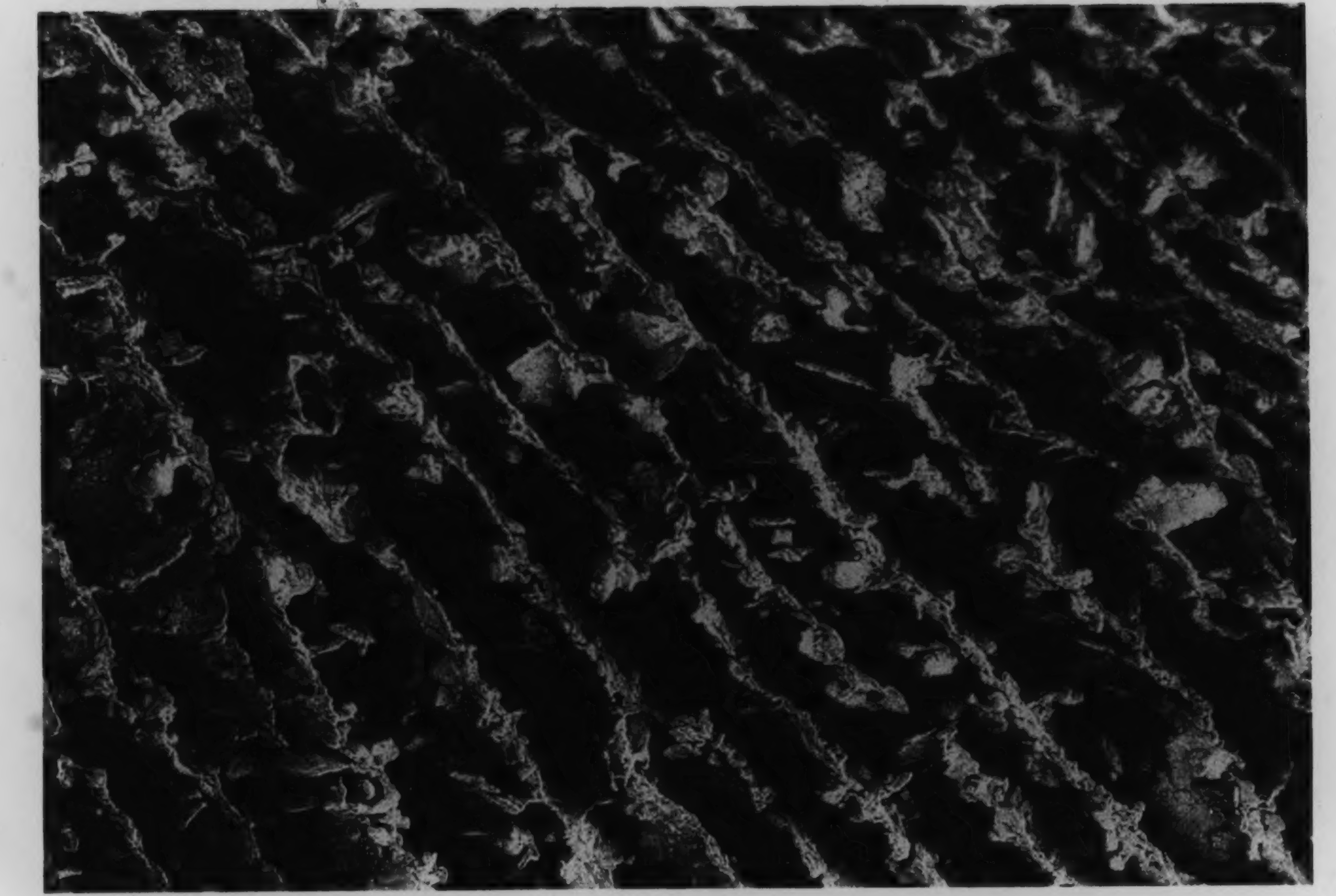

Figure 3.16: MFT was centrifuged twice and the pore water was replaced with deionized water. (Magnification at 500X: —— 10 microns)

Figure 3.17: MFT mixed with 2500 ppm of laboratory grade gypsum.
(Magnification at 500X: —— 10 microns)

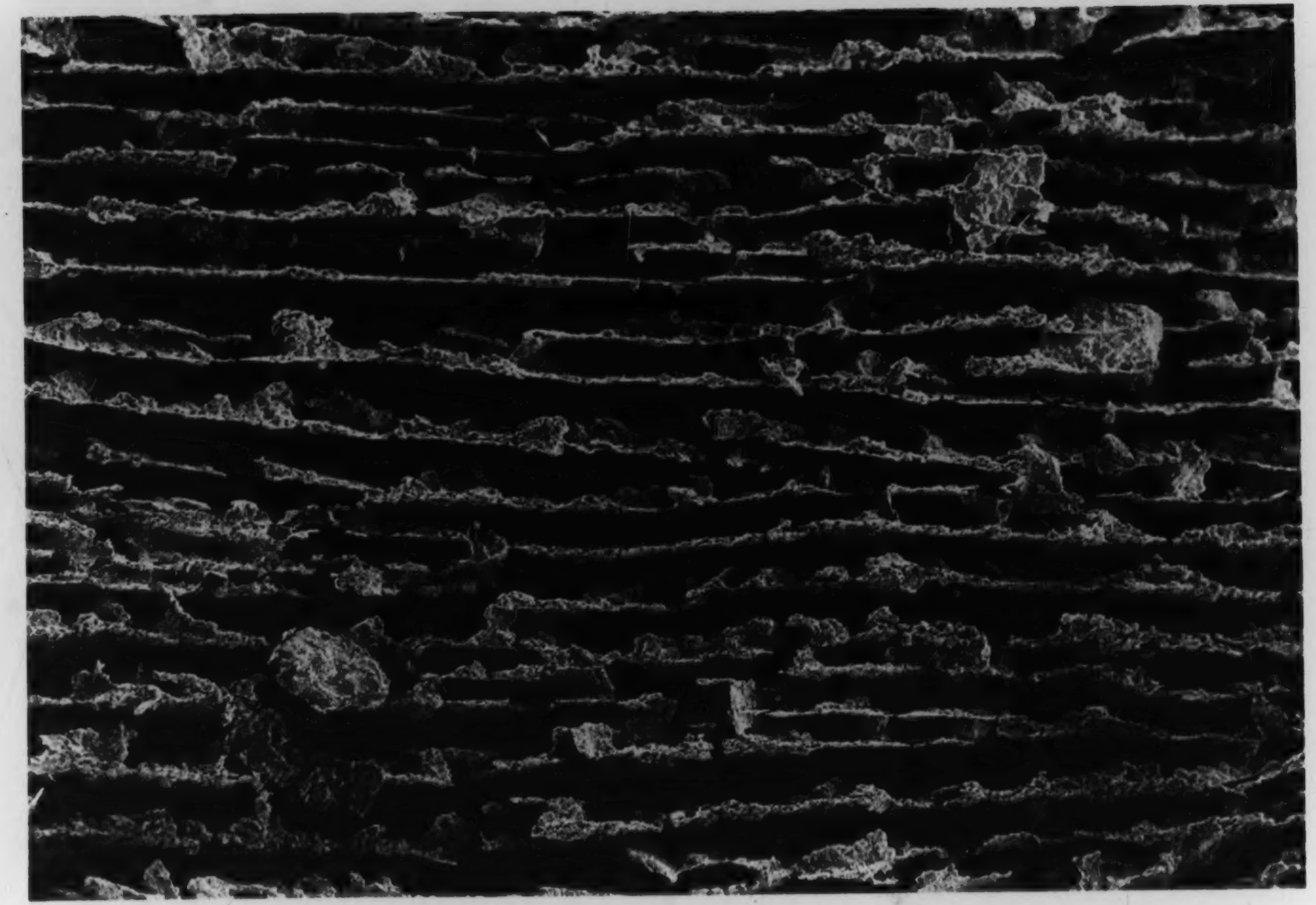

Figure 3.18: Kaolinite clay mixed with MFT pond water and heated to 80 degrees celcius. (Magnification at 500X: ——10 microns)

4.0 EFFECTS OF VARYING CLAY CONTENT ON COMPOSITE TAILINGS BEHAVIOUR

4.1 Literature Review

4.1.1 Fine Tailings Deposition Problem

The deposition behaviour of a hydraulically transported slurry can be classified as segregating or nonsegregating. Stahl (1996) defined segregation of a slurry as the tendency of the solid fraction in the slurry to settle and create a concentration gradient within its mass. On the contrary, a nonsegregating mixture maintains a uniform distribution of the solids (fines and sands) throughout its mass. Whether or not a slurry will segregate depends on the type of carrier fluid, the type and amount of chemicals added or which occur naturally, and the grain size distribution of the solids (Stahl, 1996). The deposition behaviour of Syncrude total tailings is classified as a segregating mix because its fine grained material separates from its coarse grained material when deposited into the containment basin. The segregating characteristics of the total tailings are due to its grain size distribution, high void ratio, and the high energy deposition environment.

The total tailings stream from the Syncrude processing plant has two distinct types of material: clay shale fines, and the oil sands. The combination of these soil materials in the parent oil sands ore results in a gap graded grain size distribution illustrated on Figure 4.1. This tailings stream consists of approximately 20% fines and 80% coarse grained material ranging from 0.5mm to 0.001mm in size. The fines usually refers to any solids in the tailings that is less than 44μm, however for practical purposes, the fines content in this study will define as any solids that pass through the #325 sieve (<45μm).

The SCL pipelines that transport the total tailings from the extraction plant flow at full capacity (Scott *et al*., 1993). Consequently, the fast flowing and mixing of the tailings cause a turbulent flow which entraps air as the tailings exits the pipelines into the settling basin. Air entrainment causes the fine material to segregate from the coarser material. This contributes to the segregation behaviour of the total tailings.

The amount of fine material captured or retained in the coarse material (tailings sands) depends on the soil composition of the tailings and the method of deposition. Due to the deposition method and the soil characteristics of total tailings stream described above, only one-third to one-half of the fine material is captured in the tailings sands (Scott *et.al*, 1993). Caughill (1992) explained that the fine tailings, after deposition, undergoes three zones of settling: a constant rate period, a first falling rate period, and a second falling rate zone. In the constant rate period, the freshly deposited fine material will settle by hindered settlement at a solid content of 8%. Hindered settling is defined as the mutual interaction among the particles where particles of different size and shape may agglomerate and settle at the same rate (Pane and Schiffman, 1997). Over time, effective stress begins to develop in the first falling rate period. In the second falling rate zone, the self-weight consolidation of the material dominates. The MFT (solids content in excess of 30%) would take more than several decades to fully consolidate under self weight consolidation due to its thixotropic strength and its low permeability (Scott *et.al*, 1993). Consequently, a large volume of MFT will accumulate over the production life of an oil sands operation. Since the MFT is toxic to the environment, it must be contained within the storage facility which will need to be reclaimed for lease-closure of the mining operation.

4.1.2 Slurry Property Diagram

The Slurry Property Diagram (SPD) shown on Figure 4.2 is a convenient tool for analysing and describing the numerous properties and characteristics of the fine and coarse material in the tailings. It is a ternary diagram that shows the relationship between the tailings solids content, the fines content (particles <45μm in size), and the ratio of fines content to fines content plus water content (F/(F+W)). The water content is obtained by subtracting the solids content from 100%. The solids content is plotted on the left axis, the fines content at the bottom axis, and the F/(F+W) ratio on the right axis.

A tailings with a specific amount of fluid, fines material, and coarse material (sands) will plot as a point on the diagram. As this tailings consolidates, it will follow a constant fines content path. The F/(F+W) describes the amount of fine particles and water between the pore spaces of sand particles. The increase of F/(F+W) ratio indicates a decrease in the hydraulic conductivity of the tailings.

The possible range of total tailings stream generated by SCL is plotted on Figure 4.2. The solids contents range from 35% to 62%, 9% to 35% for fines, and they lie between the 10% to 20% F/(F+W) path. The segregating/nonsegregating boundary (also referred to as the segregation boundary) divides the nonsegregating mixes from the segregating ones. Above this boundary, the coarse particles will settle from the fines producing segregated mixes. Below the boundary, no appreciable settling of coarse particles through the fines takes place (Caughill *et al.*, 1993). The boundary is fairly distinct as the slurry will change from a segregating mix to a nonsegregating mix with only a small change in solids content. Note that the total tailings stream plots above the segregation boundary which indicates that presently the tailings is a segregating mix. In order to prevent segregation in the tailings, it is necessary to increase its fines contents or solids contents.

The sedimentation/consolidation boundary (liquid limit) indicates the completion of the sedimentation stage followed by the self-weight consolidation stage of the tailings. The liquid/solid boundary defines the undrained shear strength required for the slurry to achieve a solid state. The sand matrix/fines matrix boundary defines the state at which the mix will change from a fines-water slurry containing sand grains to a sand matrix. In a sand matrix, the sand grains are in contact with one another and the fines-water slurry is contained in the voids between the sand grains.

4.1.3 Composite Tailings Background

Syncrude Canada Limited (SCL) has undertaken a research and development study to reduce the amount of fine tailings and MFT generated during future production. Their objective is to incorporate the fine material into the tailings sands to form a nonsegregating mixture which will accelerate the dewatering process resulting in a higher consolidation rate of fine tailings. In order to form a nonsegregating mixture, it is necessary to either increase the solids content, increase the fines content, or change the grain size of the fine tailings. This is described on the SPD as depicted in Figure 4.2. For example, spiking of the Syncrude tailings slurry with MFT was found to nearly double the amount of fine material captured in the tailings sand deposit (Morgenstern and Scott, 1994).

Previous researchers have experimented to determine the effect of adding chemicals such as hydrochloric acid, sulphur dioxide, polyacrylamides, $CaCl_2$, $MgSO_4$, and CaO on oil sands tailings. They found that some of these chemicals added to the fine tailings or MFT can also achieve a nonsegregating tailings stream. Their work has been summarized by Caughill (1992). Composite tailings (CT) is therefore used as a method to reduce the volume of fine tailings and MFT by chemically altering the colloidal behaviour of the tailings to form a nonsegregating tailings. The concept of CT is not to build a structure (e.g. a shallower beach), but to deposit the tailings in a containment area (Morgenstern and Scott, 1994). The addition of chemicals would accelerate the fine tailings consolidation process and form a reasonable thickness with time. When the consolidated tailings becomes a competent soil mass, it will be reclaimed as part of a dry landscape.

The success in producing CT depends on the solids and fines content of the tailings stream. At SCL, the three main types of tailings streams suitable for CT production are: the total plant tailings stream, a combination of the primary tailings and MFT, and a combination of MFT and the underflow of hydraulically cycloned plant tailings (FTFC, 1995*g*). Prior to the adding of sands, the chemicals are uniformly mixed with the fine tailings and MFT. When an adequate amount of chemical is added to form a nonsegregating mix, the clay matrix of the tailings is rendered stronger by the chemical admixture such that the sand particles can be held within the clay slurry. The sand particles act as an internal surcharge that aids in compressing the clay structure of the tailings. Due to the compression of the clay structure, the pore fluid is forced out of the dead end pores, and opens up larger flow paths for the free pore fluid to escape from within the sand matrix. Hence, the hydraulic conductivity of the fine tailings is increased resulting in a higher consolidation rate.

The University of Alberta conducted standpipe tests to evaluate the performance of CT with various chemicals. The standpipe tests were performed using 1L graduated cylinders. The purpose of these tests was to determine the segregation boundary of the tailings treated by the chosen chemicals, the optimum chemical dosage required to form CT, and to examine the consolidation behaviour of the CT. Hundreds of these standpipe tests were run and a procedure for adding chemicals to form CT was developed. The chemicals which have been proven most successful in preventing segregation are quicklime ($CaO \bullet H_2O$), sulphuric acid (H_2SO_4), and gypsum such as phosphogypsum and agriculture grade gypsum.

The efficiency of these chemical additives in forming CT varies when used with different types of tailings. The following lists some of the combinations of Syncrude tailings and the chemicals which have been tested and proven to be successful (FTFC, 1995*g*):

- quicklime with primary tailings
- quicklime with primary tailings spiked with MFT
- sulphuric acid with primary tailings
- gypsum with primary tailings and MFT
- sulphuric acid and quicklime with primary tailings

- sulphuric acid and gypsum with primary tailings

For CT to be implemented successfully in the field, it must first form a nonsegregating mixture and undergo a fairly rapid initial consolidation. The results of lime (CaO) will be briefly discussed to illustrate the influence of chemicals on the segregation boundary and the consolidation behaviour of CT. The segregation property of the CT is first discussed followed by the consolidation behaviour.

The difference between a segregating tailings and a nonsegregating tailings is distinguished by the amount of fines captured within the sand matrix of the CT. Morgenstern and Scott (1994) have defined a CT as a deposit in which 90% of the fines are retained in the sands of the CT. A segregating mix is defined as a deposit in which less than 50% of the fines are retained, and partially segregating mix lies in between 50% and 90% (Morgenstern and Scott, 1994). The optimum dosage of CaO required to produced a CT is 1250g/m^3 for all types of tailings (Scott, et al., 1993). This means that for 1 cubic meter of tailings, 1250g of dry quicklime was added. The segregation boundary of CaO is shown on Figure 4.3. A distinct boundary between the segregating mixes and the nonsegregating mixes is apparent. Compared to the segregation boundary of an untreated tailings, the new boundary was shifted upward from the untreated tailings boundary by the use of CaO addition as depicted on Figure 4.4. The addition of CaO to the fine tailings or MFT improved the segregation behaviour of the untreated tailings by increasing the range of solids contents at which a nonsegregating mix can be produced regardless of the fines contents.

Different amounts of chemical dosages can also affect the segregation boundary of CT. Standpipe tests performed on CT treated with phosphogypsum at the University of

Alberta showed that with a dosage of $600 g/m^3$, the CT plotted at a lower position on the SPD than that of a CT treated with $1000 g/m^3$ phosphogypsum as depicted on Figure 4.5. The experiment showed that with a lower chemical dosage, the CT has a weaker tailings clay structure than that with a higher dosage. Hence, at the same fines content, the CT with a lower chemical dosage will require a higher solids content to produce a nonsegregating mix. Similar findings would be expected for CT treated with CaO.

The solids contents of CT usually range from 40% to 60%. At such a high solids content, hindered settling theory cannot be used to explain the initial settling behaviour of the particles in CT. The two stages of consolidation are: initial consolidation, and long term self-weight consolidation (FTFC, 1995*g*). The initial consolidation of a CT would start almost immediately after deposition leaving a clear layer of water on the surface of the tailings. During this stage, the self-weight forces transfer from the sand grains to the clay particles of the fine tailings and the tailings undergoes a significant amount of volume reduction as the pore fluid is pushed out of the clay medium. The tailings-water interface usually drops significantly during the first 24 to 48 hours after deposition, and the initial consolidation completes within a period of several days to a few weeks (Liu *et al.*, 1996). The vertical effective stress at this stage is about 1 to 2 kPa. The long term self-weight consolidation then begins as the sand grains become in contact with one another and form a sand matrix. As the soil skeleton compresses and expels pore fluid, the effective stress of CT increases. Overtime, the CT becomes a competent soil which can be disposed of as a part of a dry landscape.

The rate and amount of initial consolidation depends on the amount and type of fines, and the amount and type of chemicals added to CT (Liu *et al.*, 1996). Figure 4.2

can also be used as a guidance in determining the possible combinations of solids and fines contents to form CT. As the fines content of a CT increases, the hydraulic conductivity and the initial void ratio of the CT decrease resulting in a slow initial consolidation. Experiments have shown that when the fines content of CT exceeds 25%, the rate of consolidation in the CT decreases considerably (FTFC, 1995g). As the void ratio of CT continues to decrease due to long term self-weight consolidation, this will further decrease the hydraulic conductivity hence reducing the rate of overall consolidation. The rate of the initial and long term self-weight consolidation of a CT is also dependent on the hydraulic conductivity of the fine tailings or MFT. Since the hydraulic conductivity of MFT is affected by the bitumen content, a MFT that has a higher bitumen content will result in a lower hydraulic conductivity and consequently a lower overall consolidation rate of CT.

The consolidation behaviour of CT is also affected by the different chemical dosages. Scott *et al.* (1993) carried out two standpipe tests with different dosages of CaO. Both of the tests produced nonsegregating mixes and were observed to have a fairly uniform solids and fines content throughout the standpipes. The test with a higher CaO dosage resulted in a rapid initial consolidation but exhibited little long term consolidation. The second standpipe test carried out using a lower dosage of CaO not only underwent a rapid initial consolidation but also resulted in greater long term self-weight consolidation (Scott *et al.*, 1993). Hence the optimum dosage must produce a nonsegregating mix with a rapid initial consolidation and reasonably fast long term self-weight consolidation.

The rate and amount of initial consolidation also depends on the mixing procedure and mixing time (Liu *et al.*, 1996). The standpipe tests conducted with CaO showed that as the mixing time increased from 5 minutes to 30 minutes, the initial consolidation rate of the CT increased (FTFC, 1995*g*). However, the shorter mixing time appeared to yield CT with a faster long term self-weight consolidation rate. It may be more favourable to choose a shorter mixing time to encourage a faster initial consolidation rate. As CT is deposited in layers, it is important that the water from the initially deposited layer of CT is quickly released before a following layer is deposited. This would prevent the water from being trapped in the previous layer of CT.

Since CT has a high water content such that it can be transported hydraulically, it should be discharged in a low energy environment so that segregation of the mixture will not occur (FTFC, 1995*g*). Air entrainment during the deposition process causes some segregation of the fine material out of CT (FTFC, 1995*g*). Experiments have shown that the vertical, submerged discharge method is effective in both dispersing energy and preventing air entrainment. Horizontal discharge was found to be ineffective because it caused hydraulic jumps resulting in high turbulence and segregation of CT. Furthermore, it was recommended that the thickness of CT is placed in thin layers to reduce the drainage path during the consolidation stages.

The water initially released from the CT shows a certain level of acute toxicity and therefore needs to be treated before being discharged into the environment (FTFC, 1995*h*). Due to natural detoxification, no acute toxicity was measured after the water had been in storage for a period of time which was determine based on the number of trout and daphnia which survived in the water after three to six months. However, the reduction of chronic toxic level is still currently being researched. Treatment options include the process of initial, passive, biological detoxification of the CT release water in holding ponds, and then releasing the water into another pond for a season until the water has met the discharge requirements (FTFC, 1995*h*). The water can then be discharged through natural wetlands where further detoxification of chemicals in the discharged water occurs. This is to ensure that toxic level is reduced when the water enters the neighbouring off-lease environment.

4.2 Definitions

The terminology used in the *Experimental Program and Design* section are defined in the following and the sample calculation for the terminology are shown in Appendix 1:

1. Fines accounts for all the particles finer than 45μm. In this experiment, approximately 95% of a fine particles in a CT comes from MFT and 5% comes from the sands.
2. *Sands* are being referred as the sand that make up the solids content of CT. This is calculated by subtracting the fines content from 100%.
3. *Sands to Fines* ratio (SFR) is the ratio of the percentage of *Sands* to the amount of fines in CT.
4. *Clay:water* ratio or *clay mineral:water* ratio defined by SOSG (1996) represents the total percentage of available clay mineral surfaces in the CT solids divided by the total percentage of water in CT. They have used methylene blue testing to determine clay mineral surfaces. In this thesis, the *clay:water* ratio was not determined using

methylene blue test. The method in which *clay:water* ratio is calculated for this thesis is described in Section *4.3.4*.

5. *Clay:sand* ratio is the total percentage of clay size material in the CT solids divided by the *Sands* in the solids content of CT.

The terminology used in the *Results* section are defined as follows and the sample calculations are also shown in Appendix 1:

1. The *Actual Fines* and *Solids* are defined as the actual amount of fines and the total solids in the CT. This was obtained from the solids and fines content testing. The samples were collected during the process of making CT for standpipe test. The procedure for standpipe test is described in Section *4.3.5*.
2. CMF(%) stands for Clay Mineral Fraction which is the amount of clay mineral contained in CT. It is the fines content of CT multiplied by the total amount of clay size material contained in both the MFT and sands.
3. F/(F+W) is the ratio of fines content to the sum of fines content and water content in CT. Water content is calculated by subtracting the solids content from100%. As described in Section *4.1.2*, the F/(F+W) describes the amount of fine particles and water between the pore spaces of sand particles.
4. C/(C+W) is the ratio of total clay minerals in CT to the sum of total clay minerals and the water content in CT. The total clay minerals is the CMF multiplied by the solids content. The C/(C+W) ratio describes the amount of clay size particles and water in the voids between the sand particles in a CT.
5. SI represents the Segregation Index (SI) of CT. The index describes the segregation behaviour of the CT and reflects the percentage of fines (particles < 45μm) not

captured in the CT. A SI value that is less than 10% indicates that the tailings is a nonsegregating mix. The formula derived by Suthaker (1997) is found in the Appendix.

6. Fines captured is the amount of fines (<45μm) retained within the sand matrix. It is calculated by subtracting the SI from 100%.

Note that the clay content in *clay:water* and *clay:sand* ratios does not have the same definition as the clay content defined for C/(C+W). The clay content in C/(C+W) is defined as the total clay sized material found in both MFT and sands, but the clay content in *clay:water* and *clay:sand* ratios only considers the clay size material in MFT. This will be explained in Section *4.3.4*.

4.3 Experimental Procedures and Design

The success in creating a CT is also dependent on the amount of clay minerals in the fine tailings or MFT reacting with the added chemicals. Previous experiments performed at Suncor Oil Sands Group have shown that the segregation boundary of CT mixed with 600ppm of agricultural grade gypsum is equivalent to a *clay mineral:water* ratio of 0.1 (SOSG, 1996). The method of determining this ratio is explained in Section *4.3.4*. Their experimental results stated that all the CT with a *clay:water* greater than 0.1 will not segregate. However this ratio requires further investigation and verification.

The investigation of this proposed *clay:water* ratio required standpipe testing on MFT with different clay contents (particles < 2μm). Hence, the purpose of this study was to examine the effects of varying MFT clay content on the segregation and consolidation behaviour of CT.

The chosen clay contents were initially 25%, 55%, and 75% of the MFT fraction which in this study are termed as the low clay content MFT, MFT-55 or 55% clay content MFT, and the high clay content MFT respectively. The procedures of material preparation, the material index testing, and the standpipe tests are described. This is followed by a description of the flow chart which illustrates the strategy of experimental program for determining the segregation boundary through standpipe testing.

4.3.1 Material Preparation

The MFT identified as SY-22 was used in this study. The index test procedures and the characteristics of this tailings have been described in Sections *3.2.1* and *3.3.1* respectively. Recall that the hydrometer test performed on this MFT showed that 55% of the MFT was clay size material (<2μm).

The low and high clay content MFT were obtained by separating the clay size material (<2μm) from the silt size material (>2μm) of the 55% clay content MFT. The method of separation was based on the concept of a hydrometer test. In a hydrometer test, water is added to the solids to achieve a solids content of approximately 5%. At such a low solids content, the coarser particles will settle by gravity at a faster rate than the fine particles. In the procedure used in this study, when the silt size material had settled to the bottom of the container, the clay size particles remained in the liquid were removed, leaving the silt size material in the container.

Prior to the separation process, it was estimated that up to 15 standpipe tests would be performed for each clay content, and each set of tests required approximately 12L of tailings at about 30% solids content. A separation test trial was conducted with 200mL of MFT-55 to determine the amount of clay size material that the MFT could yield. It was found that after 24 hours, 54% of MFT-55 material was still in suspension. Based on this preliminary test, approximately 80L of MFT-55 were used.

Four barrels of 75.6L (20gallons) were used for the separation process. For each barrel, the MFT release water from Syncrude settling basin (pond water) was added to 20L of MFT-55 to achieve a solids content of approximately 5%. The calculation for the required amount of pond water for this separation process is shown in the Appendix. After adding the pond water to the tailings, it was stirred for about 5 minutes with a shovel to thoroughly suspend the particles. Two samples were collected for solids content determination. According to the hydrometer test done on the MFT-55, the clay size particles of the MFT would begin to settle after about 9 hours. Figure 4.6 shows the general layers of the settling solids. Layer 1 consisted mostly of the unsettled clay size particles with a high water content. The interface layer, Layer 2, contained silt size material with about 60% clay size particles. The bottom layer had up to 70% silt size material and a solids content of approximately 25%. Shortly after 9 hours, Layer 1 was siphoned into a barrel, Layer 2 into another barrel, and Layer 3 was poured into a 20L plastic pail. More pond water was later added to the tailings in Layer 2 to repeat the separation process.

The solids content of the tailings in Layer 1 was approximately 4%. Since a solids content of approximately 28% is required for the standpipe tests, the excess water in

Layer 1 was removed by filtering the water through a filter paper with an applied vacuum of approximately 508mm Hg. The filter paper manufactured by the Micron Separation Inc. has pore sizes of 0.22μm. These pore sizes are large enough for the electrolyte to flow through while filtering out the soil particles without increasing the ionic concentration of the pore water. An evaporation process was not implemented because this method would increase the concentration of electrolyte in the pore water which may affect the colloidal behaviour of the clay slurry.

The filter paper trimmed to the desired size was glued on a perforated acrylic plastic tube with a thin piece of geofabric illustrated on Figure 4.7. Silicone gel was then used to seal the edges of the filter paper. The inner diameter of the tube is approximately 70mm and the thickness of the plastic is about 2mm. The base of the tube was plugged with a #12 rubber stopper and then sealed with silicone gel. The purpose of the geofabric was to protect the filter paper from directly contacting the perforated tube, to provide extra support for the filter paper, and to increase the surface area of the filtration. Without the geofabric, the filter paper would tear more easily, and the filtration area would only concentrate at the perforation in the tube resulting in a reduced filtering surface area.

Six to nine filtering tubes were inserted into the 75.6L drum of tailings (Layer 1) and the filtering tubes were connected to the vacuum with a nylon tubing (6mm outer diameter). The pond water was drawn into the tube when the vacuum was applied. The filtered water was either recycled for another separation process or discarded.

The filter paper required cleaning when the MFT soil collected on the surface. As the water content decreased, the hydraulic conductivity decreased, hence the filtering process took approximately 2.5 months to obtain a approximately 16L of clay slurry with a solids content of 30%. After the desired solids content for each clay content was achieved, the slurry was stored and sealed in 20L plastic pails to prevent evaporation of the pore fluid.

4.3.2 Index Tests

The clay contents of each slurry was determined through hydrometer tests performed according to ASTM D422-63 with a slight modification. The modification has been described in Section *3.2.1*. Similarly, each hydrometer test was carried out with wet slurries that had an equivalent dry mass of 50g. Each hydrometer test was terminated after 48 hours because it was sufficient to determine the clay contents of each slurries.

The Atterberg limits tests were performed on both the low clay content MFT, and the high clay content MFT according to ASTM D4318-84. Approximately 1L of both MFT were collected and air-dried in a ventilated oven at 26°C for approximately 48 hours or until the desired water content was achieved. The samples were stirred occasionally to allow the slurry to dry uniformly, and to prevent it from overdrying. Each sample was then divided into two portions for the plastic and liquid limit tests. Following the Atterberg limits tests, the dried samples of both the low, and the high clay content MFT obtained from the liquid limit test were used for Soxhlet extraction to determine the bitumen content of both slurries. The Soxhlet extraction procedure has been described Section *3.2.1*.

The solids content tests performed on these MFT samples were also described in Section *3.2.1*. The specific gravity of these MFT samples were obtained from using equation (2.4) which is based on the amount of bitumen contained in the MFT.

The water chemistry analysis along with the cation exchange capacity tests were done at Norwest Laboratories in Edmonton, Alberta. The ESR value of each MFT were calculated based on the concentrations of Na^+, Ca^{2+}, and Mg^{2+}. Methylene Blue tests, which quantifies the amount of clay minerals in soil material based on the exposed clay surface area, were performed by McMurray Resources (Research and Testing) Limited in Fort McMurray, Alberta.

The sand used in making CT was obtained from the beach at the Mildred Lake Settling Basin in SCL. The sand was delivered to Edmonton in several 250L barrels (45 gallons) but only 18L of sand was used. The sand was first sieved through a #14 sieve and inspected for clumps of clayey soil to ensure that no additional clay size particles were added to the MFT when making CT. The sand was thoroughly mixed with a shovel, and a sample was collected for grain size distribution test. For the grain size distribution, the sand was sieved through a series of sieves #20, #40, #60, #80, #100, #120, #140, and #200. The particles that passed through the #200 sieve were collected for a hydrometer test. The purpose of this test was to obtain the grain size distribution, and to determine the amount of clay size particles left in the sand.

The solids content of the sand was determined according to the procedure described in Section *3.2.1*. The fines content of each pail was determined by washing the sample through a #325 sieve with tap water. The retained solids were dried in an oven for 16 hours at 110°C. The total dry solids in the sand was calculated from the average solids content obtained from the solids content test. The mass of fines (<45μm) in the sand is the difference between the total dry solids and the dry solids retained in the #325 sieve. The fines content is the mass of fines divided by the total dry solids. A sample calculation is shown in Appendix 1.

4.3.3 Slurry Samples Preparation Procedure for SEM

The samples that were prepared for SEM observation are listed on Table 4.1. The method of preparation has been described in *Chapter 3*, Section *3.2.3*. Similarly, approximately 100mL of samples were collected and left undisturbed for two days except for the CT samples which was left undisturbed for 14 days. This was to observed the structure after it underwent consolidation for 14 days. The CT samples were collected during the preparation process in the standpipe tests and it is described in the Section *4.3.5*.

4.3.4 Experimental Program for Standpipe Tests

The purpose of this experimental program was to strategically choose the solids and fines contents that would produce a segregation boundary through standpipe testing. Recall the experimental results of SOSG (1996) stated that all the tailings with a *clay:water* ratio greater than 0.1 were nonsegregating mixes. They have obtained the ratio by performing methylene blue tests on the fine tailings samples used in previous test study shown in Figure 4.8. This test study was to determine the segregation boundary for tailings treated with 600ppm of agricultural grade gypsum. The data at the segregation boundary shown in Figure 4.8 was then recomputed on a clay mineral basis as shown in Figure 4.9 (SOSG, 1996). Unfortunately no methylene blue test data was provided to show how the *clay:water* ratio was obtained. However, it was found that by assuming the fine tailings with a clay content of 45%, similar results as shown in Figure 4.9 were obtained using the following equation:

$$\textit{clay:water ratio} = \frac{C*F*S}{100-S} \tag{4.1}$$

C represents the clay content of a fine tailings, and *F* and *S* describe the fines and solids content of a tailings respectively. Similarly, the *clay:water* ratio of the tailings in the experimental program were calculated according to equation (4.1).

In this experimental program, the proposed solids and fines contents for creating CT ranged from 35% to 60%, and 10% to 30% respectively. The *clay:water* ratios for each clay content MFT were calculated based on these proposed solids and fines contents. A sample calculation of the *clay:water* ratio is shown in the Appendix. Five tailings samples with *clay:water* ratios ranging from 0.05 to 0.3 were initially selected to determine if the *clay:water* ratio segregation boundary was 0.1. Subsequent tests were conducted to refine the previously established segregation boundary or to re-establish another boundary if the experiment results did not agree with the *clay:water* ratio segregation boundary of 0.1. Figure 4.10 shows the *Experimental Program* strategy in a flow chart format. The flow chart illustrates two possible routes in which the experiment could proceed. The first route depended on whether the standpipe tests will produce a *clay:water* ratio segregation boundary of 0.1. If the *clay:water* ratio was not equal to 0.1, the experiment would be directed to the second route.

The only varying parameter in this study was the clay content of MFT, therefore the LGG dosage of each CT was maintained at 900g/m^3. This dosage was chosen based on the results of standpipe tests carried out with agricultural grade gypsum by Suthaker and Scott (1996*a*). Through standpipe testing, they found that the optimum dosage to obtain CT was 900g/m^3. The main difference between the LGG, and agricultural grade gypsum is the amount of $CaSO_4$ that is contained in these chemicals. Approximately 95% of LGG is $CaSO_4$ while agricultural grade gypsum has approximately 85% (Mikula, 1996*b*). The LGG treated CT would not be expected to have a significant difference in the standpipe test results, compared to that of the agricultural grade gypsum treated CT, since the difference in $CaSO_4$ between these chemicals is only 10%.

4.3.5 Standpipe tests

The masses of MFT, sand, and pond water required for standpipe tests were calculated for 1.2L of CT. The extra 200mL of CT was used for solids and fines content tests, methylene blue tests, and for CT microstructure observation using a Scanning Electron Microscope (SEM). The purpose of performing solids and fines content tests was to verify that the correct amount of sand, MFT, and pond water were added according to the *Designed* solids and fines contents.

The MFT was first stirred thoroughly for at least 5 minutes. For each standpipe test, the sand, MFT, pond water were weighed and mixed together in a 5L plastic pail. The ternary mixture was then stirred using a blade mixer shown on Figure 4.11. The blade mixer was connected to a hand held drill. This type of mixing blade has a small area of contact with the soil mixture and therefore provides high shearing of the mixture during stirring (Caughill, 1992).

The stirring speed was adjusted such that the entire soil mixture was suspended during stirring. The stirring time was exactly 5 minutes, during which two 50mL samples were collected for solids content test, and another two for fines content tests. Immediately after the samples were collected, the LGG powder was dissolved in 2 to 3mL of pond water and poured into the soil mixture. This was to prevent the powder from solidifying, and to encourage well mixing of LGG in the soil mixture. The pH of the soil mixture was recorded two minutes after the LGG was added. Only selected CT mixes were collected for SEM observation. The amount of samples collected were approximately 100mL.

Immediately after stirring, the CT was poured into a 1L graduated cylinder (900mm in height), and its initial tailings height, time, and other observations of the CT were recorded. The cylinder was covered to prevent evaporation during the test period.

As the CT consolidated with time, the height of the soil-water interface, time, and the consolidating characteristics of the CT were recorded every half hour for the first two hours followed by every hour for the next three hours. After the first day of the test, the observations were recorded three times a day for 14 days. The test was carried out for 14 days because it was sufficient for examining the segregation and initial consolidation characteristics of the tailings.

All the samples collected for the solids and fines contents tests were weighed prior to the tests. The solids content tests were carried out according to the procedure described in Section *3.2.1*. The fines content tests were obtained by washing the collected tailings samples through a #325 sieve with tap water. The particles that remained in the sieve were dried in the oven at 110°C for 16 hours. The total dry solids in CT was calculated from the average solids content obtained from the solids content test. The mass of fines in the CT is the difference between the total dry solids and the dry solids retained in the sieve. The fines content is the mass of fines divided by the total dry solids. A sample calculation has been shown in the Appendix.

Upon the completion of the standpipe tests, the released water of each test sample was siphoned and discarded. For each sample, the entire cylinder of tailings was sampled for solids and fines content determination which alternated with depth. Layers of samples of approximately 50mL were scooped into a pre-weighed aluminium dish, and the elevation of the collected samples were recorded. A sample calculation of the fines content is shown in the Appendix.

4.4 Results

4.4.1 Material Properties

The hydrometer tests showed that the low clay content MFT had 36% clay size material, and the high clay content MFT contained 70%. The low clay content will also be referred to as 36% clay content MFT, and the high clay content as 70% clay content MFT. These clay contents were acceptable for the standpipe tests even though MFT of 25% and 75% clay contents were initially planned. The grain size distribution of the low clay content MFT, MFT-55, and the high clay contents MFT have been plotted on Figure 4.12. The figure indicates that approximately 100% of the MFT soil particles were finer than 45μm. The grain size distribution of the beach sand is shown on Figure 4.13. This figure shows that about 91% of the material was sand size, 5% was silt size, and the remaining 4% was clay size.

Table 4.2 lists the solids, fines, and clay contents for the low, high, 55% clay content MFT, sand, and the pond water. It also lists the bitumen contents of the aforementioned MFT. The specific gravity was obtained using equation (2.4) which is based on the bitumen content of the MFT. This equation gave a specific gravity of approximately 2.5 for each MFT. The specific gravity of the sand obtained from Suthaker (1997) is approximately 2.6.

The Atterberg limits test results for the aforementioned MFT are tabulated on Table 4.3. Table 4.4 lists the results of cation exchange capacity (CEC), methylene blue tests, and the ESR for both 36%, and 70% clay content MFT. The ESR was calculated using the Gapon equation which has been illustrated in the Appendix and discussed in Section *3.1.1*.

Table 4.5 shows the results of CMF obtained from hydrometer tests and methylene blue test. These results showed a slight discrepancy in the CMF between the two tests. The CMF of the 36% and 70% clay content MFT presented the largest difference compared to the 55% clay content MFT. The difference in these results will be discussed in Section *4.5.1*.

The water chemistry analysis, electric conductivity (EC), and the ionic strength (I) of the 36%, MFT-55, and 70% clay content MFT are listed on Table 4.6. The data shows that the 36% and 70% clay content MFT have a much higher concentration in Ca^{2+}, Na^{+},

Mg^{2+}, and HCO_3^-. The ionic strength of each MFT was calculated using the following equation derived by Griffin and Jurinak (1973):

$$I\ (\text{moles/L}) = 0.0127\ EC \tag{4.2}$$

The difference in the aforementioned chemical concentrations and its effect on the MFT *card-house* structure of MFT will be discussed in Section *4.5.1*.

4.4.2 Scanning Electron Micro-graphs of CT

The structure of the MFT at the aforementioned clay contents, and the effects of LGG on the three MFT structures were observed. The resulting structure of CT mixes were also examined. The SEM used in this study was the same equipment described in *Chapter 3*. Three sets of samples (Table 4.1) were prepared for SEM observation:

1. 36%, 55% (MFT-55), and 70% clay content MFT
2. LGG mixed with the above mentioned MFT
3. CT samples (treated with LGG) with 36%, 55%, or 70% clay content MFT.

Figures 4.14a and b show the clay structure of MFT at 36%, and 70% clay content respectively. The 36% clay content MFT structure has thinner rows of clay particles with spacings between clay alignment averaging at approximately 5μm. The cross-linking clay particles appeared to be randomly distributed between each row of clay particles. The 70% clay content MFT structure has thicker rows of clay particles. The cross-linking clay particles are also randomly distributed. The spacing between clay alignments were not measured because the micro-graph does not show a plan view of the structure that can be accurately measured. However, the spacing observed appeared to be similar to that of 36% clay content MFT structure. The structure of MFT at 55% clay content presented in Figure 3.6 (*Chapter 3*) showed thick alignments of clay particles with spaces averaging at about 5μm. This structure appeared to be quite similar to the 70% clay content MFT structure.

The effects of LGG on the structure of MFT at the aforementioned clay contents were examined using the SEM. Figures 4.15, 4.16, and 3.18 (*Chapter 3*) show the structures of 36%, 70%, and 55% clay content MFT treated with 2500g/m^3 of LGG respectively. The structures of the latter two samples appeared to be more aggregated than that of the 36% clay content MFT.

The final set of SEM micro-graphs displays the structures of CT prepared for the standpipe tests. Figures 4.17, 4.18, and 4.19 present the CT structures at 36%, 55%, and 70% clay content MFT respectively. Notice that the magnification of these micro-graphs are 200 times so that the arrangement of sand particles can be better observed. These figures show the embedded sand grains within the clay matrix, and the grains did not appeared to be in contact with each other. The clay structures of each micro-graph possessed distinct rows of clay particles as seen previously in the structure of the untreated MFT samples. Furthermore, the rows of clay particles of the CT with 36% clay content MFT were thinner compared to the CT with 55% or 70% clay content MFT. These are better illustrated in figures 4.20, 4.21, and 4.22 respectively at a magnification of 500 times.

4.4.3 Standpipe Tests Results for Tailings with 36%, 55%, and 70% Clay Content MFT

Table 4.7 tabulates the calculated *clay:water* ratios using equation (4.1) for the 36%, 55%, and 70% clay content MFT. It shows a matrix with the solids content listed on the left and the fines content, SFR, and *Sand* are listed across the bottom. From this table, the solids and fines content were chosen for standpipe tests. The selection procedure has been described in Section *4.3.4*.

Morgenstern and Scott (1994) have defined a CT with 90% of fines captured or greater as a nonsegregating mix, and a CT with a 50% of fines captured or less as a segregating mix. In this study, the segregating mix is classified as any tailings that has a fines captured less than 90%. During the standpipe tests, a distinct MFT-sand interface were observed in mixes with fines captured less than 90%, hence the modification in the definition. *Somewhat segregated* mixes are tailings with fines captured greater than 90% but their solids contents profiles and the observed consolidating behaviour during the test suggested that the tailings had segregated.

During the standpipe tests, it was observed that the segregated tailings usually developed a layer of foam after the tailings was being poured into the cylinders. After the first few hours of the test, the segregated tailings exhibited three distinct layers which composed of release water, MFT, and sand. By inspection, the nonsegregating mixes usually had a uniformly distributed soil mass with a layer of water at the surface of the tailings. As the pore water escaped to the surface of the CT soil mass, several channels or flow paths were seen throughout the column of soil, and dome shaped soil mounds formed on the surface of the soil mass.

Table 4.8 tabulates the summary data of 12 standpipe tests carried out with the 36% clay content MFT. The table includes the data for the D*esign* and the *Actual* fines and solids content of the tailings, CMF, initial and final void ratios, F/(F+W), C/(C+W), *clay:sand* ratio, and *clay:water* ratio. Table 4.9 lists the resulting Segregation Index, and the percent fines captured for each tailings. These parameters were used to determine if the tailings had segregated.

The *clay:water* ratio segregation boundary of the tailings with 36% clay content MFT is plotted on Figure 4.23. It shows the *clay:water* ratio boundary at 0.085 separating the segregated mixes from the non-segregated ones. Figure 4.24 illustrates a distinct segregation boundary plotted on a non-triangular SPD. The boundary followed along the F/(F+W) path at approximately 19%. The solids contents profile of each tailings has been plotted on Figure 4.25. In order to compare the profiles, the solids contents were plotted against the normalised height, H/Hf, which is defined as the sampling height divided by the final height recorded on the last day of the experiment. CTs were identified by their fairly vertical line while the segregated mix has a bi-liner profile. Figure 4.26 illustrates the initial consolidation behaviour of tailings as the self-weight consolidation progressed with time. Here, the elapsed time was plotted with the normalised height, H/Ho, which is defined as the consolidating height divided by the initial height of the tailings recorded at the beginning of the test.

The summary data of the 13 standpipe tests results obtained for the tailings with 55% clay content MFT are tabulated on Table 4.10 with the same headings as Table 4.8. Table 4.11 summarises the Segregation Index, Fines Captured, and the status of the segregating behaviour.

The *clay:water* ratio segregation boundary for 55% clay content MFT illustrated on Figure 4.27 indicated that the ratio is 0.09. The segregation boundary plotted on a non-triangular SPD in Figure 4.28 shows a distinct boundary at a F/(F+W) of approximately 16.5%. The solids content profiles of each standpipe tests were plotted with normalised heights and solids contents (Figure 4.29). Similarly, the normalised height was defined as the sampling height divided by the final height. The sedimentation progress of the tailings with 55% clay content MFT is plotted on Figure 4.30. For comparison purposes, the consolidating heights were converted to the normalised height of H/Ho.

Tables 4.12 and 4.13 summarise the 13 standpipe tests results obtained for the tailings with 70% clay content MFT. The tables list the same parameters which have been identified above. Figure 4.31 plots the *clay:water* ratio segregation boundary at 0.118. The boundary was set at 0.118 instead of 0.1 because two segregated samples were plotted near 0.118 whereas only one non-segregated sample was plotted on 0.1. Hence the 0.118 is a better representative of the segregation boundary than 0.1. Similar to the other two sets of results (36% and 55% clay content tailings), the segregation boundary of the 70% clay content tailings is better illustrated when graphed on a non-triangular SPD shown on Figure 4.32. The boundary lies along the F/(F+W) contour line at approximately 15%. Figures 4.33 and 4.34 illustrate the solids contents profiles and the initial consolidation behaviour of the tailings respectively.

The segregation boundaries of all the tailings with 36%, 55%, and 70% clay content MFT are plotted on Figure 4.35. It is evident that the segregation boundary of the tailings with 70% clay content MFT plots the highest on the SPD and the 36% clay content plots the lowest. Figure 4.36 shows the same results plotted with initial void ratio on the y-axis instead of solids content. The contour lines of the F/(F+W) and the segregation boundaries plot as straight lines when void ratio is used compared to that of Figure 4.35. Figure 4.37 summarised all the tailings results by plotting a ternary diagram which contains initial void ratio on the y-axis, CMF on the x-axis, and the contour lines of C/(C+W). This diagram illustrates a unique segregation boundary for CT treated with 900g/m^3 of LGG based on the clay mineral fraction in the tailings, and the initial void ratio. C/(C+W) indicates the amount of clay particles and water contained in the pore spaces of tailings.

Figure 4.38 compares the segregation boundaries of LGG treated tailings and agricultural grade gypsum treated tailings. The segregation boundary of the tailings treated with agricultural grade gypsum were performed by Suthaker and Scott (1996*b*), and the tailings has approximately 55% clay content. The dosage for both of these chemicals was 900g/m^3. The result showed that both chemicals produced similar segregation boundaries and this is further discussed in the following section.

4.5 Discussion

4.5.1 Material Properties

Prior to the analysis of the standpipe test results, it was necessary to confirm that the intent of varying the clay content in the tailings was fulfilled. The clay contents of the MFT determined by hydrometer tests were 36% and 70%. This was acceptable for the standpipe tests even though the experimental program was designed for clay contents of

25% and 75%. Methylene blue testing was also performed on both MFT and CT samples to determine their clay contents. For the MFT samples, methylene blue test results listed in Table 4.4 show a slightly higher amount of clay minerals compared to the hydrometer test results. For the CT samples, the results of methylene blue test compared to the clay mineral fraction (CMF) calculated based on hydrometer test were quite inconsistent. These results are shown in Table 4.5. The difference in the results obtained by hydrometer test method and methylene blue test method may be due to the difference in the level of sensitivity in detecting the amount of clay minerals in MFT. Whether or not one test method is more precise than the other has yet to be confirmed. Since hydrometer testing has been vastly used to reliably characterise the grain size distribution of soil samples, and the exact methodology for calibration of the methylene blue test are unknown, this study will rely more on the test results obtained by the hydrometer test.

Plasticity of a soil mass is mainly determined by the amount and the nature of the clay minerals present in the soil mass. The plasticity results of the 36%, and 70% clay content MFT confirmed that the latter MFT has a higher amount of clay mineral. This is confirmed by the CEC test. The CEC of the low clay content MFT was only 6.8 meq/L compared to the CEC of 14.3 meq/L for the high clay content MFT. Compared to the 36%, and 70% clay content MFT, the results of Atterberg limits, CEC test showed that the 55% clay content MFT had an intermediate amount of clay minerals. The separation process has proven to be successful and hence the analysis of the standpipe tests could proceed as planned.

The difference in bitumen content between the low and the high clay content MFT listed in Table 4.2 was approximately 0.9%. The higher bitumen content found in the

36% clay content MFT may be due to the adhesion of the bitumen to the larger soil particles surfaces than the finer particles of the 70% clay content MFT. As mentioned in Section *2.2.1*, the bitumen content has an effect on the plasticity characteristics of MFT. The higher the bitumen content of MFT, the higher the Atterberg limits. This effect was not observed in both of these MFT because the difference in bitumen content was too low to cause an effect. The plasticity characteristics of these MFT were mostly controlled by the differences in their clay content. The specific gravity calculated using equation (2.4) for the low, and high clay content MFT were 2.53 and 2.52 respectively. They are close to the anticipated specific gravity of 2.5 since the specific gravity of the 55% clay content MFT was also 2.5.

The water analysis of the 36% and 70% clay content MFT showed an abundant concentration of Na^+, and HCO_3^-. The ions in the latter MFT had a higher concentration compared to the 36% clay content MFT except for the Ca^{2+} and SO_4^{2-} (Table 4.6). In comparison to the water analysis of the 55% clay content MFT, the concentration of all the ions except perhaps SO_4^- found in the 36%, and 70% clay content MFT were much higher than expected as shown in Table 4.6. The increase in these concentrations may have occurred during the separation process of MFT-55 because the MLSB pond water with higher concentrations of anions and cations than that of the MFT pore water was used. Unfortunately a water chemistry analysis of the pond water was not performed because it was discarded.

Further investigation of the ionic strength of all three MFT showed that the 36% clay content MFT had the highest ion activity while the 50% clay content MFT had the lowest. The ionic strength is introduced to assess the combined effect of the activities of several electrolytes in the solution, and the ion activity describes the reactivity in a chemical reaction (Tan, 1993). The water chemical analysis therefore showed that the pore water of the 36% clay content MFT has the highest amount of reactivity which is directly related to the high chemical concentrations. However, the difference in ionic strengths between the MFT does not seem to affect their clay structure. The ESR of 1.04, 1.1, and 1.56 indicated that all the 36%, 55%, and 70% clay content MFT respectively are highly dispersed and this is evident in their SEM micro-graphs presented in Figure 4.14a, 3.6 (*Chapter 3*), and 4.14b. It is concluded that the difference in ionic strengths in all the above MFTs do not appear to have an effect on the structure of MFT.

As explained in Section *3.3.1*, the ESR of the above MFTs are overestimated because K_G of 0.015 (mmol/L)$^{-1/2}$ was used in the calculation. For this study, the ESRs gave sufficient indication that the MFTs' structures are dispersed as shown in the SEM micro-graphs. In order to accurately predict the ESR of MFT, it is necessary to determine K_G through laboratory testing. The testing were not performed because it is beyond scope of the thesis.

4.5.2 Composite Tailings Micro-structure Examination

The 36%, and 70% clay content MFT exhibited a similar *card-house* structure to that of a 55% clay content MFT shown in *Chapter 3*. The chemical that was found to be mainly responsible for the *card-house* structure in MFT was HCO_3^-. Other chemicals which appeared to have an effect on the *card-house* structure were, NaOH, bitumen and the *strongly bound* organic matter.

The effects of LGG on the structure of MFT were examined in *Chapter 3*. It was found that the LGG treated MFT had a *card-house* structure that was more aggregated compared to an untreated MFT structure. The similar structure was also observed in the 36%, and 70% clay content MFT that were treated with 2500g/m^3 of LGG. The replacement of Na^+ by the Ca^{2+} introduced via LGG compressed the double diffuse layer which increased the attraction forces between the clay particles resulting in a less dispersed structure. This enhanced the ability of the MFT to retain sand grains within the structure creating a nonsegregating tailings.

In *Chapter 3*, the cavity expansion test showed that the addition of LGG had strengthened the MFT clay structure by approximately four times. The strengthened *card-house* structure was the key to the formation of CT. A CT can only be created when the MFT *card-house* structure is strong enough to hold the sand grains within its matrix. If the clay structure is not strong enough, the sands grains will fall through the clay matrix producing a segregated tailings. In Figures 4.17, 4.18, and 4.19, the sand particles appear to be suspended within the MFT structure. The sand grains were not in contact with each other because the CT had not yet undergone sufficient initial consolidation to reach a sand matrix where the grains would be in contact.

4.5.3 Segregation Boundary

The *Actual* fines and solids contents of the CT with 36%, 55%, and 70% clay content MFT were acceptable. The results showed very slight deviations from the *Design* fines and solids contents. Recall that the *clay:water* ratio segregation boundary of 0.1 proposed by SOSG (1996) stated that any CT with a *clay:water* ratio less than 0.1 will segregate. However, the results obtained through standpipe testing in this thesis show that the proposed *clay:water* ratio segregation boundary of 0.1 can be affected by the amount of clay size particles in the CT. For comparison purposes, the *clay:water* ratio of the CTs with 36%, 55%, and 70% clay contents were calculated according to equation (4.1). The *clay:water* ratio segregation boundary for 36%, 55%, and 70% clay content are 0.085, 0.090, and 0.118 respectively. These ratios showed that the proposed ratio of 0.1 by the SOSG is conservative in predicting the segregation characteristics for the CTs with 36% or 55% clay content MFT. However, the ratio is not conservative in predicting the segregation characteristics for the CTs with higher clay contents. This is evident in the results generated from the CTs with 70% clay content MFT which showed that CTs with *clay:water* ratio of 0.1 will likely to segregate.

Although the difference between these *clay:water* ratios is only 0.005 between the CT with 36% and 55% clay content MFT, and 0.028 between the latter two clay contents, the segregation behaviour was observed to be sensitive to these boundaries. For example, characteristics of segregation were observed at a *clay:water* ratio of 0.080 for CTs with 36% clay content MFT. Similar behvaiour was observed for the other two clay contents as their *clay:water* ratio is lowered.

Figure 2.7 in *Chapter 2* illustrates a typical range of clay size material in MFT ranges from 45% to 60%. It is expected that at these ranges, the *clay:water* ratio segregation boundary will also be around 0.1 with an optimum dosage of 900g/m^3 LGG. Tailings that has MFT with clay content less than 45% is expected to have a *clay:water* ratio segregation boundary of around 0.085, and tailings with a clay content MFT greater than 60% are expected to have a *clay:water* ratio segregation boundary of approximately 0.118.

Although different types of gypsum have been used in CT, they appeared to have little effect on the segregation boundaries. As shown in Figure 4.38, the segregation boundary for the CT treated with 900g/m^3 of agricultural grade gypsum or laboratory grade gypsum were quite similar. The MFT, which was treated with agricultural grade gypsum to make CT, was also obtained at the same location and time as SY-22 MFT. From this experiment, it appears that different types of gypsum have little effect on the tailings segregation boundary. Comparison of other types of gypsum were not carried out because it is beyond the scope of this thesis.

The experimental results also show that the tailings with 36% clay content MFT required significantly higher solids content than the tailings with 55% or 70% clay content MFT to form nonsegregating mixes. The CT with 36% clay content MFT segregation boundary plots at a higher position on a SPD as seen on Figures 4.35 and 4.36. Compared to the tailings with 55% or the 70% clay content MFT, the 36% clay content MFT did not have sufficient clay minerals to react with gypsum to form a strong enough clay structure to hold the sand grains within its matrix. At the same fines content, the tailings with 36% clay content MFT would therefore require a higher solids content or a lower void ratio to form a nonsegregating mix. In general, as the clay content in MFT increased, a greater amount of clay minerals would be available to react with gypsum forming a strong enough clay structure to hold the sand grains. Consequently, a lower solids content is required as exhibited in the CT with 70% clay content MFT.

Only a slight improvement was observed in the segregation boundary of the CT with MFT at 70% clay content compared to that of the CT with 55% clay content MFT. This may be due to the small difference in the amount of cation exchangeable sites between the 55% and the 70% clay content MFT. Table 4.4 showed that the 55% clay content MFT has a CEC of 11.5meq/L and the latter MFT has a CEC of 14.3meq/L. The difference between their CEC is only 2.8meq/L compared to a difference of 4.7meq/L between the CEC of 36% and 55% clay content MFT. Hence, the slight improvement in the segregation boundary of CT with 70% clay content MFT may be inferred by the slight difference in the CECs.

Instead of using the *clay:water* ratios to describe the segregation boundary of the CTs with the aforementioned clay contents, a unique segregation boundary is plotted to describe the segregation behaviour. The unique segregation boundary is shown in Figure 4.37 which is plotted with initial void ratio, CMF, and C/(C+W). Similar to all the above described segregation boundaries, the curve was drawn in "by hand" separating the segregated samples from the non-segregated samples. The boundary describes the segregation status for all the tested tailings based on their CMF and the initial void ratio regardless of the fines contents in the tailings. All the tailings that plot above the segregation boundary will segregate and the tailings that plot below the boundary will not segregate. This plot may act as a guide to predict whether the tailings will segregate given the initial void ratio, and the clay mineral fraction contained in tailings. The application of this segregation boundary will be explained in Section *4.5.5*.

4.5.4 Initial Consolidation Behaviour

The observed initial consolidation behaviour of the tailings with 36%, 55%, and 70% clay content MFT exhibited similar trends. Both the segregating and nonsegregating tailings underwent a fairly rapid consolidation in the first 48 hours and then slowed down as the tailings continued to consolidate. It was observed that a segregated tailings consolidated at a faster rate in the first 48 hours than a CT. In a segregated tailings, the sand grains fall through the clay structure without being held within its clay matrix. Hence, their initial consolidation rate observed in the first 48 hours were faster.

The experimental results showed that the for each clay content, the CTs with higher fines contents underwent a slower initial consolidation rate than that with a lower fines content. The CTs with higher fines contents have a gradual sloping curve as shown in the initial consolidation progress plots, Figures 4.26, 4.30, and 4.34. Majority of the CTs exhibited poor initial consolidation at fines content ranging from 25% to 30% regardless of the solids contents.

The CTs with 36%, 55%, and 70% clay content MFT that consolidated at the fastest rate were identified as *50S/25F*, *55S/15F*, and *50S/15F* respectively. These CTs have fines content ranging from 15% to 25%. Although most of the CT with a fines content of 25% exhibited poor initial consolidation behaviour, it appeared that the initial consolidation rate of CT with 36% clay content MFT was not affected by the high fines content. This may be due to the lower amount of clay minerals that is available to react with LGG compared to the higher clay content MFTs. Hence a higher fines content was necessary for the 36% clay content MFT to achieve similar results as the other two CTs with higher clay contents.

The total change in void ratio after 250 hours of testing for the above CTs that consolidated the fastest were 0.99, 0.75, and 1.12 respectively (Table 4.14). For the CT that consolidated at the slowest rate, the total change in void ratios after 250 hours of testing were 0.32, 0.12, and 0.70 respectively and the fines contents of these CTs ranged from 25% to 30%. More importantly, $\Delta e/(1+e_i)$, was calculated to rank the CT's initial consolidation behaviour from the slowest to the fastest.

These results agreed with the initial consolidation theory of CT described by Liu *et al.* (1996). They explained that the initial consolidation of CT depends on its fines content. Hence, when the fines content of a CT exceeds 25%, the initial consolidation slows down dramatically. Furthermore, the higher the fines contents in CT, the lower the hydraulic conductivity because the fine grained material blocks the flow paths. This inhibits the water from escaping quickly to the surface of the tailings, thus lowering the initial consolidation rate of CT.

Consider the consolidation behaviour of the non-segregated CT at each clay content. Within each clay content, Table 4.14 ranks the CT from the slowest rate to the fastest rate of consolidation with their corresponding initial void ratios, final void ratios, total change in void ratios, CMF, and the initial consolidation normalised heights. For each clay content, the initial void ratios of CT were not arranged in any particular order. It appears that the initial void ratio of CT has little effect on its initial consolidation rate.

The comparison between 36%, 55%, and 70% clay content CTs showed that the 70% clay content CT has the highest change in void ratio and has the highest initial consolidation rate after 250 hours of standpipe test on Table 4.14. Recall from *Chapter 2*, the permeability of tailings is dependent on the bitumen content. As the bitumen content of the fine tailings or MFT increases, the hydraulic conductivity decreases and consequently the consolidation of the fine tailings or MFT under self-weight decreases. Since the initial consolidation of CT is controlled by the properties of the fines tailings or MFT that make up the CT, the initial consolidation of CT is therefore affected by the bitumen content in the fine tailings or MFT. Hence a CT that has a MFT with the highest bitumen content will be expected to consolidate the slowest.

In this study, 36%, 55%, and 70% clay content MFT had bitumen contents of 2.5%, 3.3%, and 1.6% respectively. However, the accuracy of the Soxhlet extraction test in obtaining the bitumen contents of these samples needs to be verify. This can be done by repeating number of tests on the same MFT sample to ensure that the test results are repeatable. This exercise was not performed in this study and should be done for future study. Nevertheless, the 70% clay content MFT appeared to have the lowest bitumen content amongst the clay slurries and the CT created with this MFT was observed to have the highest initial consolidation rate. On the contrary, the CT with 55% clay content MFT had the highest bitumen content and the observed initial consolidation rate was the lowest. These results indicate that the MFT with a higher bitumen content has a lower hydraulic conductivity because the bitumen is blocking the pore fluid flow paths and therefore reducing the initial consolidation rate of the CT. Hence, the initial consolidation rate of CT is highly dependent on the characteristics of the fine tailings or MFT that make up the CT. In this study, the bitumen content of the fine tailings or MFT had the largest effect on the initial consolidation of CT.

Comparison of the behaviour of the tailings within a given clay content showed that the nonsegregating tailings had higher amounts of clay mineral fractions (CMF) than the segregating ones. It was observed that the CT with a higher clay mineral fraction generally had a lower rate of initial consolidation (Table 4.14). This is most evident between the slowest and the fastest consolidating CT for each clay content. It was also observed that the CT with a higher CMF had a higher fines content. Consequently, the increase in fines content with CMF in the MFT resulted in the blockage of flow paths thus reducing the hydraulic conductivity of the CT giving a reduction of initial consolidation rate.

The above mentioned trend was not observed when the CMF were compared between CTs with 36%, 55%, and 70% clay content MFT. It was observed that the CT with 70% clay content MFT had the fastest consolidation rate compared to the other two CT. Table 4.14 shows that the CT with 70% clay content MFT at a CMF of 7.2 consolidated faster than the CT with 55% clay content MFT at a CMF of 5.7. This behaviour can also be explained by the difference in bitumen content which affects the initial consolidation rate of the CT. The CT with 70% clay content MFT had the lowest bitumen content and was observed to have the highest initial consolidation rate. As it was previously concluded, the initial consolidation rate of CT is dependent on the bitumen content of the fine tailings or MFT that make up the CT.

The consolidation rate of CT can be qualitatively predicted by both the F/(F+W) and the C/(C+W) ratio plotted on a SPD. Recall that an increase of F/(F+W) ratio indicates a decrease in the hydraulic conductivity of CT resulting in a lower initial consolidation rate. Since the CMF increases with the fines content, an increase of C/(C+W) ratio will also indicate a decrease in the hydraulic conductivity of CT. As seen in this experiment, the segregation boundaries normally plots along a F/(F+W) ratio path on a SPD. For the CT with 36%, 55%, and 70% clay content MFT, the optimum F/(F+W) were 19%, 16.5%, 15% respectively. The C/(C+W) plotted on Figure 4.37 ranged from 3% to 9%. When the CT increased in F/(F+W) or C/(C+W) ratio, they plotted further away (below) from the segregation boundary which inferred that the CT had higher amount of fines (<45μm) within the void spaces of CT and therefore had a lower consolidation rate. Hence, the experimental results showed that the closer a CT plots to the segregation boundary, the faster its initial consolidation rate. At the boundary, the CT has an optimum C/(C+W) or F/(F+W) ratio whereby the initial consolidation rate is the highest.

4.5.5 Engineering Application

Figures 4.35 and 4.36 illustrate the effect of varying clay contents in MFT on the segregation boundary of tailings. These plots are replotted in Figure 4.37 which shows the relationship between the clay mineral fraction, initial void ratios, and the C/(C+W) ratio.

The segregation boundary is derived for tailings treated with 900g/m^3 of LGG. For example, a tailings with a CMF of 10% and an initial void ratio of 4 is expected to be a segregated mix. At the same CMF, the tailings has an initial void ratio of 2 is expected to be a non-segregated mix. A sample calculation of CMF is shown in the Appendix.

The initial consolidation characteristics of a tailings treated with 900g/m^3 of LGG can also be qualitatively predicted using this plot provided that the bitumen content is constant. Using the above example, a CT with a CMF of 10% and an initial void ratio of

2 has a C/(C+W) of approximately 12%. Another CT that has the same CMF but with an initial void ratio of 3 has a C/(C+W) of approximately 8%. The latter CT is expected to consolidate at a faster rate because it has a lower C/(C+W) ratio and it is plotted closer to the segregation boundary.

If the bitumen content of the MFT used for making CT is not constant, the above analysis in the immediate preceding paragraph cannot be used to predict the initial consolidation behaviour. The bitumen content in MFT, rather than the clay mineral fraction in the CT, will dominate the initial consolidation behaviour of CT. This was observed in the initial consolidation behaviour of the CTs with 70% clay content MFT which exhibited the fastest initial consolidation rate and the lowest bitumen content. This finding inferred that regardless of the amount of clay size minerals in the MFT, the initial consolidation rate of CT can be increased by reducing the amount of bitumen in the MFT. It may therefore be favourable to re-extract the bitumen from the existing MFT in the containment pond to improve the initial consolidation characteristics of CT.

4.6 Summary

The effects of varying MFT clay contents (<2μm) on segregating and consolidating behaviour of CT were examined. Clay contents of 36% and 70% were obtained through a separation process in which MFT was diluted to a solids content of approximately 5% causing the fine particles to separate from the coarser particles by gravity. The clay contents were confirmed by hydrometer test and methylene blue test results. The methylene blue test was not found to be helpful in CT samples since the results were inconsistent. Due to the inconsistency in the methylene blue results, the hydrometer test results were used.

The 36% and 70% clay content MFT had the same *card-house* structure as seen on the SEM micro-graphs in *Chapter 3*. In a CT, it is this *card-house* structure that holds the sand grains. The SEM of a LGG treated MFT exhibited a more aggregated clay structure than an untreated one. It was observed that the addition of LGG further strengthened the MFT clay structure such that a high solids content would not be necessary to form a nonsegregating tailings compared to a untreated tailings. As a result, this segregation boundary plots at a higher position on a SPD than the segregation boundary of an untreated tailings stream.

Standpipe test results showed that the *clay:water* ratio segregation boundary of 0.1 proposed by SOSG (1996) can be affected by the amount of clay size particles in the CT. Instead of a unique *clay:water* ratio of 0.1, the *clay:water* ratio segregation boundary for 36%, 55%, and 70% clay content was determined to be 0.085, 0.090, and 0.118 respectively. These ratios showed that the proposed *clay:water* ratio of 0.1 is conservative in predicting the segregation behaviour of CTs with less than 55% clay content and not as conservative in predicting the behaviour of CTs with greater than 55% clay content MFT.

It appeared that different types of gypsum has little effect on the tailings segregation boundary provided that the same dosage was used. This is inferred by comparing tests results obtained using laboratory grade gypsum and agricultural grade gypsum. Comparison of other types of gypsum is beyond the scope of this thesis.

It was observed that the tailings with 36% clay content MFT required a higher solids content than the tailings with 55% or 70% clay content MFT to form nonsegregating mixes. The 36% clay content MFT did not have sufficient clay minerals to react with gypsum, hence the clay structure was not strong enough to hold the sand grains. At the same fines content, the tailings with 36% clay content MFT would require a higher solids content or a lower void ratio to form a nonsegregating mix. Hence on a SPD, the segregation boundary of this tailings plots at a lower position than that of the tailings with 55% or 70% clay content MFT.

A summary plot was generated for all the tailings at each clay content. A unique segregation boundary was observed on a non-triangular SPD describing the relationship between clay mineral fraction, C/(C+W) ratio and the initial void ratio. This plot may act as a guidance to predict whether the tailings will segregate given its clay mineral fraction and initial void ratios.

The initial self-weight consolidation test results showed that the consolidation rate was the highest in the first 48 hours and the rate decreases with increasing fines content. Within each clay content, the experimental results showed that the CT generally consolidated the fastest with a lower clay mineral fraction. However, this behaviour is not true when comparing all clay contents. The CT with 70% clay content MFT exhibited the fastest consolidation rate and highest change in void ratio. This was unexpected because it was initially assumed that MFT with the highest clay content would have the lowest hydraulic conductivity. This behaviour may be due to the effect of bitumen content in the MFT. The higher the bitumen content in MFT that makes up the CT, the lower the hydraulic conductivity and hence a lower initial consolidation rate of CT. The

70% clay content MFT had the lowest bitumen content and the highest initial consolidation rate was observed in the CT with this MFT.

The initial consolidation rate of CT can be qualitatively predicted by both the F/(F+W) and the C/(C+W) ratio plotted on a SPD. At the segregation boundary, the CT has an optimum C/(C+W) or F/(F+W) ratio whereby the consolidation rate is the higher compared to another CT that plots further away form the boundary.

The application of the above findings is discussed in Section *4.5.5*. It describes the usage and the limitations of the ternary diagram which relates the initial void ratio, CMF in tailings, and C/(C+W) ratio. Suggestions were also made for improving the initial consolidation behaviour of the CT.

Table 4.1: Samples collected for SEM.

Samples	Solids Content(%)	Fines Content(%)	pH
MFT			
36% MFT	29.5	95	8.09
55% MFT	27.3	95	8.6
70% MFT	33	100	8.54
MFT treated with LGG			
36% MFT	29.5	95	8.2
55% MFT	27.3	95	8.5
70% MFT	33	100	8.4
CT samples			
36% MFT	55	25	8.15
55% MFT	55	20	8.75
70% MFT	40	25	8.35

Table 4.2: Solids, fines, clay, bitumen contents of MFT, sands, and pond water used in CT.

Material	Solids (%)	Ave Solids (%)	Fines (%)	Ave Fines (%)	Clay (%)	Bitumen (%)
Sand						
Bucket #						
1	89.09	89.4	6.7	5.6	4	0
2	89.43	89.4	5.62	5.6	4	0
3	89.19	89.4	4.64	5.6	4	0
MFT-55						
Bucket #						
#10	27.3		95		55	3.3
#11	27.3		95		55	3.3
MFT (LC)	29.5		95		36	2.5
MFT (HC)	33		100		70	1.6
Pond Water	0		0		0	0

LC = low clay content MFT
HC = high clay content MFT

Table 4.3: Atterberg limits test results for 36% clay content MFT, and 70% clay content MFT.

Sample	LL(%)	PL(%)	PI(%)	Activity
36%	38.3	18.7	19.6	0.54
55%[1]	47.6	21.4	26.2	0.47
70%	63.0	26.8	36.2	0.52

[1] air-dried

Table 4.4: Colloidal properties of the 36% clay content MFT, MFT-55, and 70% clay content MFT.

Sample	CEC (meq/L)	MB[1] (%)	ESR
36%	6.8	43.0	1.04
55%	11.5	63.3	1.10
70%	14.3	74.1	1.56

[1] clay mineral quantified by methylene blue test

Table 4.5: The comparison between the clay mineral fraction (CMF) obtained from hydrometer test and methylene blue test.

Clay Content (%)	CMF[1] (%)	CMF from MB[2] test (%)
36	7.6	10.1
	9.5	18.5
55	8.6	8.3
	11.5	12.5
70	11.5	17.8
	14.6	23.9

[1] CMF calculated from hydrometer test results
[2] MB = methylene blue

Table 4.6: Water chemistry analysis results for the 36%, and 70% clay content MFT.

Components	36% MFT (mg/L)	55% MFT (mg/L)	70% MFT (mg/L)
Ca^{2+}	17.2	1.2	13.3
Mg^{2+}	11.8	1.1	13.1
Na^{+}	1530	450	2230
SO_4^{2-}	243	225	224
HCO_3^{-}	1130	665	1660
pH	8.09	8.60	8.54
EC(dS/m)	5.83	1.86	8.15
I (moles/L)	0.076	0.024	0.11

Table 4.7: ***Clay:water*** **ratios for 36%, 55%, and 70% clay content MFT. The shaded and italised** ***clay:water*** **ratios were chosen for standpipe tests.**

Clay Content = 36%

Solids Content (%)	Clay/Water					
60	0.054	***0.081***	***0.108***	0.135	0.162	
55	0.044	***0.066***	***0.088***	***0.110***	***0.132***	
50	0.036	0.054	***0.072***	***0.090***	***0.108***	
45	0.029	0.044	0.059	***0.074***	***0.088***	
40	0.024	0.036	0.048	***0.060***	0.072	
35	0.019	0.029	0.039	0.048	0.058	
	10	15	20	25	30	Fines (%)
	90	85	80	75	70	Sand (%)
	9	5.67	4	3	2.33	SFR

Clay Content = 55%

Solids Content (%)	Clay/Water					
60	0.083	***0.124***	0.165	0.206	0.248	
55	0.067	0.101	***0.134***	0.168	0.202	
50	***0.055***	***0.083***	***0.110***	***0.138***	***0.165***	
45	***0.045***	***0.068***	***0.090***	***0.113***	0.135	
40	0.037	0.055	***0.073***	0.092	0.110	
35	***0.030***	0.044	0.059	0.074	0.089	
	10	15	20	25	30	Fines (%)
	90	85	80	75	70	Sand (%)
	9	5.67	4	3	2.33	SFR

Clay Content = 70%

Solids Content (%)	Clay/Water					
60	0.105	0.158	0.210	0.263	0.315	
55	***0.086***	***0.128***	0.171	0.214	0.257	
50	0.070	***0.105***	***0.140***	0.175	0.210	
45	0.057	***0.086***	***0.115***	0.143	0.172	
40	0.047	0.070	***0.093***	***0.117***	***0.140***	
35	0.038	0.057	***0.075***	0.094	***0.113***	
	10	15	20	25	30	Fines (%)
	90	85	80	75	70	Sand (%)
	9	5.67	4	3	2.33	SFR

Table 4.8: **Summary data of the sedimentation test for tailings samples with 36% clay content MFT**

Chemical Dosage: 0.99 g (900g/m3) of Laboratory Grade Gypsum for 1.1L of sample

Clay Content in MFT : 36%

Sample	Date (start-finish)	Design (%)		Actual (%)				e_i	e_f	F/(F+W) (%)	C/(C+W) (%)	Clay/Sand ratio	Clay/Water ratio
		Solid	Fines	Solid	Fines	Sand	CMF						
Clay36-1	April 9-23	55	15	53.6	16.8	83.2	3.8	2.25	1.28	16.25	4.20	0.07	0.07
Clay36-2	April 9-23	55	20	49.8	19.6	80.4	5.7	2.61	1.77	16.28	5.35	0.09	0.07
Clay36-3	April 9-23	55	25	53.1	24.3	75.7	7.6	2.30	1.76	21.58	7.92	0.12	0.10
Clay36-4	April 9-23	55	30	54.4	31.8	68.2	9.5	2.18	1.80	27.50	10.18	0.17	0.14
Clay36-5	April 15-28	50	25	50.2	25.7	74.3	7.6	2.58	1.57	20.58	7.11	0.12	0.09
Clay36-6	April 15-28	50	30	49.8	31.3	68.7	9.5	2.62	2.13	23.69	8.61	0.16	0.11
Clay36-7	April 15-28	60	15	60.2	16.2	83.8	3.8	1.72	0.84	19.68	5.43	0.07	0.09
Clay36-8	April 15-28	60	20	60.7	20.2	79.8	5.7	1.68	1.23	23.78	8.09	0.09	0.11
Clay36-9	May 2-14	40	25	40.4	27.68	72.32	7.6	3.84	1.83	15.80	4.90	0.14	0.07
Clay36-10	May 2-14	45	25	45.93	25.5	74.5	7.6	3.06	1.66	17.80	6.06	0.12	0.08
Clay36-11	May 2-14	50	20	50.3	21.38	78.62	5.7	2.57	1.54	17.79	5.45	0.10	0.08
Clay36-12	May 2-14	45	30	44.3	30.35	69.65	9.5	3.27	1.74	19.44	7.02	0.16	0.09

Table 4.9: **Determination of a segregated or non-segregated mix using segregation index and fines captured parameters for 36% clay content in MFT.**

Sample	Date (start-finish)	SI (%)	Fines Captured (%)	Comments
Clay36-1	April 9-23	23.03	76.97	segregated
Clay36-2	April 9-23	2.54	97.46	did not segregate
Clay36-3	April 9-23	0.40	99.60	did not segregate
Clay36-4	April 9-23	1.84	98.16	did not segregate
Clay36-5	April 15-28	7.09	92.91	did not segregate
Clay36-6	April 15-28	1.67	98.33	did not segregate
Clay36-7	April 15-28	0.35	99.65	did not segregate
Clay36-8	April 15-28	2.34	97.66	did not segregate
Clay36-9	May 2-14	31.48	68.52	segregated
Clay36-10	May 2-14	29.10	70.90	segregated
Clay36-11	May 2-14	23.32	76.68	segregated
Clay36-12	May 2-14	8.49	91.51	somewhat segregated

Table 4.10: Summary data of sedimentation test for tailings samples with 55% clay content MFT

Chemical Dosage: 1.08g (900g/m3) of Laboratory Grade Gypsum
Clay Content in MFT: 55%

Sample	Date (start-finish)	Design (%)		Actual (%)			CMF	e_i	e_f	F/(F+W) (%)	C/(C+W) (%)	Clay/Sand ratio	Clay/Water ratio
		Solid	Fines	Solid	Fines	Sand							
Clay55-1	Feb 10-25	35	10	32.0	14.0	86.0	2.8	5.55	2.35	6.98	1.29	0.09	0.04
Clay55-2	Feb10-25	50	15	49.0	16.0	84.0	5.7	2.65	1.43	13.32	5.19	0.10	0.08
Clay 55-3	Feb10-25	50	20	50.0	21.0	79.0	8.6	2.60	2.06	17.36	7.92	0.15	0.12
Clay55-4	Feb10-25	50	25	47.0	22.0	78.0	11.5	2.93	2.61	16.32	9.26	0.16	0.11
Clay55-5	Feb10-25	50	30	49.0	27.0	73.0	14.4	2.71	2.59	20.60	12.17	0.20	0.14
Clay55-6	Feb 12-26	50	10	49.0	14.0	86.0	2.8	2.71	1.51	11.86	2.61	0.09	0.07
Clay55-7	Feb 12-26	40	20	38.0	20.0	80.0	8.6	4.24	3.87	10.92	5.01	0.14	0.07
Clay55-8	Feb 15-25	45	15	41.0	13.0	86.0	5.7	3.74	2.15	8.29	3.81	0.08	0.05
Clay55-9	March 11-26	45	25	43.3	24.0	76.0	11.5	3.41	2.87	15.49	8.08	0.17	0.10
Clay55-10	March 11-26	45	20	43.5	20.3	79.7	8.6	3.38	1.94	13.52	6.21	0.14	0.09
Clay55-11	March 11-26	55	15	54.1	14.4	85.6	5.7	2.21	1.44	14.51	6.29	0.09	0.09
Clay55-12	March 11-26	55	20	54.3	19.6	80.4	8.6	2.19	1.84	18.89	9.27	0.13	0.13
Clay55-13	March 11-26	60	15	60.0	15.1	84.9	5.7	1.73	1.19	18.47	7.87	0.10	0.12

Table 4.11: **Determination of a segregated or non-segregated mix using segregation index and fines captured parameters for 55% clay content in MFT.**

Sample	Date (start-finish)	SI (%)	Fines Captured (%)	Comments
Clay55-1	Feb 10-25	42.94	57.1	segregated
Clay55-2	Feb10-25	53.44	46.6	segregated
Clay55-3	Feb10-25	17.77	82.2	somewhat segregated
Clay55-4	Feb10-25	0.74	99.3	did not segregate
Clay55-5	Feb10-25	1.63	98.4	did not segregate
Clay55-6	Feb 12-26	70.20	29.8	segregated
Clay55-7	Feb 12-26	64.86	35.1	segregated
Clay55-8	Feb 15-25	44.91	55.1	segregated
Clay55-9	March 11-26	0.08	99.9	did not segregate
Clay55-10	March 11-26	19.02	81.0	somewhat segregated
Clay55-11	March 11-26	4.43	95.6	did not segregate
Clay55-12	March 11-26	1.79	98.2	did not segregate
Clay55-13	March 11-26	2.85	97.2	did not segregate

Table 4.12: **Summary data of sedimentation tests for tailings samples with 70% clay content MFT**

Chemical Dosage: 0.90 g (900g/m3) of Laboratory Grade Gypsum for 1L of sample
Clay Content in MFT : 70%

Sample	Date	Design (%)		Actual (%)				e_i	e_f	F/(F+W)	C/(C+W)	Clay/Sand	Clay/Water
	(start-finish)	Solid	Fines	Solid	Fines	Sand	CMF			(%)	(%)	ratio	ratio
Clay70-1	May 13-23	45	15	45.2	15.0	54.8	7.2	3.15	1.52	11.01	7.97	0.19	0.09
Clay70-2	May 13-23	50	15	49.6	14.6	50.4	7.2	2.64	1.52	12.56	9.14	0.20	0.10
Clay70-3	May 13-23	40	25	40.6	24.9	59.4	14.6	3.80	2.79	14.54	10.65	0.29	0.12
Clay70-4	May 13-23	35	20	34.9	19.0	65.1	10.9	4.85	2.57	9.24	6.66	0.20	0.07
Clay70-5	May 17-27	55	10	54.0	8.3	46.0	3.7	2.21	0.87	8.88	6.38	0.13	0.07
Clay70-6	May 17-27	40	20	37.3	22.4	62.7	11.5	4.37	2.74	11.76	8.53	0.25	0.09
Clay70-8	May 17-27	45	20	42.5	19.2	57.5	11.5	3.52	2.30	12.43	9.04	0.23	0.10
Clay70-7(2)	May 20-31	35	30	35.0	31.3	65.0	18.3	4.83	3.01	14.41	10.54	0.34	0.12
Clay70-8(2)	May 20-31	45	20	44.7	20.7	55.3	10.9	3.22	1.90	14.33	10.48	0.26	0.12
Clay70-9	May 20-31	55	15	55.0	15.0	45.1	7.2	2.13	1.49	15.47	11.35	0.23	0.13
Clay70-10(2)	May 21-June2	40	30	39.8	30.4	60.2	18.3	3.93	2.86	16.73	12.33	0.35	0.14
Clay70-11	May 21-June2	50	20	49.9	22.7	50.1	10.9	2.61	1.91	18.44	13.66	0.32	0.16

Table 4.13: Determination of a segregated or non-segregated mix using segregation index and fines captured parameters for 70% clay content in MFT.

Sample	Date (start-finish)	SI (%)	Fines Captured (%)	Comments
Clay70-1	May 13-23	23.33	76.67	segregated
Clay70-2	May 13-23	1.97	98.03	did not segregate
Clay70-3	May 13-23	1.15	98.85	did not segregate
Clay70-4	May 13-23	46.97	53.03	segregated
Clay70-5	May 17-27	35.07	64.93	segregated
Clay70-6	May 17-27	36.93	63.07	segregated
Clay70-8	May 17-27	15.04	84.96	segregated
Clay70-7(2)	May 20-31	17.37	82.63	segregated
Clay70-8(2)	May 20-31	23.29	76.71	segregated
Clay70-9	May 20-31	1.04	98.96	did not segregate
Clay70-10(2)	May 21-June2	0.62	99.38	did not segregate
Clay70-11	May 21-June2	0.50	99.50	did not segregate

Table 4.14: Comparison between the void ratios, CMF, and consolidation behaviour for CT at 36%, 55%, and 70% clay content

Consolidation Behaviour	Clay Contents (%)	*Design*		*Actual*		e_i	e_f @ 250hr	Δe	Δe/(1+e_i)	CMF (%)	H/Ho @ 250 hours
		Solids (%)	Fines (%)	Solids (%)	Fines (%)						
Slowest	36	55	30	54.4	31.8	2.18	1.86	0.32	0.10	9.5	0.9
		50	30	49.8	31.3	2.62	2.17	0.45	0.12	9.5	0.88
		55	25	53.1	24.3	2.30	1.82	0.48	0.15	7.6	0.86
		60	20	60.7	20.2	1.68	1.26	0.42	0.16	5.7	0.85
		55	20	49.8	19.6	2.61	1.79	0.82	0.23	5.7	0.78
		60	15	60.2	16.2	1.72	1.07	0.65	0.24	3.8	0.77
Fastest		50	25	50.2	25.7	2.58	1.59	0.99	0.28	7.6	0.73
Slowest	55	50	30	49.0	27.0	2.71	2.59	0.12	0.03	14.4	0.98
		55	20	54.3	19.6	2.19	1.9	0.29	0.09	8.6	0.92
		50	25	47.0	22.0	2.93	2.61	0.32	0.08	11.5	0.92
		45	25	43.3	24.0	3.41	2.95	0.46	0.10	11.5	0.9
		60	15	60.0	15.1	1.73	1.22	0.51	0.19	5.7	0.82
Fastest		55	15	54.1	14.4	2.21	1.46	0.75	0.23	5.7	0.78
Slowest	70	55	15	49.9	22.7	2.61	1.91	0.70	0.19	10.9	0.8
		40	25	55.0	15.0	2.13	1.49	0.64	0.20	7.2	0.79
		50	20	40.6	24.9	3.80	2.79	1.01	0.21	14.6	0.81
		40	30	39.8	30.4	3.93	2.86	1.07	0.22	18.3	0.79
Fastest		50	15	49.6	14.6	2.64	1.52	1.12	0.31	7.2	0.69

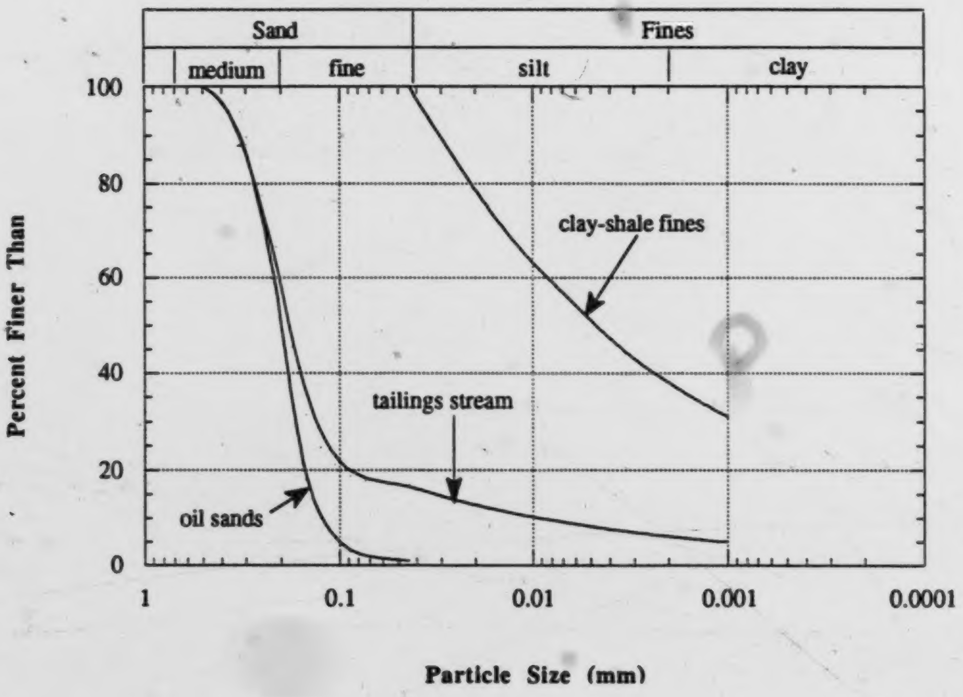

Figure 4.1: Grain size distribution of tailings stream, clay-shale fines, and oil sands (Scott *et al.*, 1993).

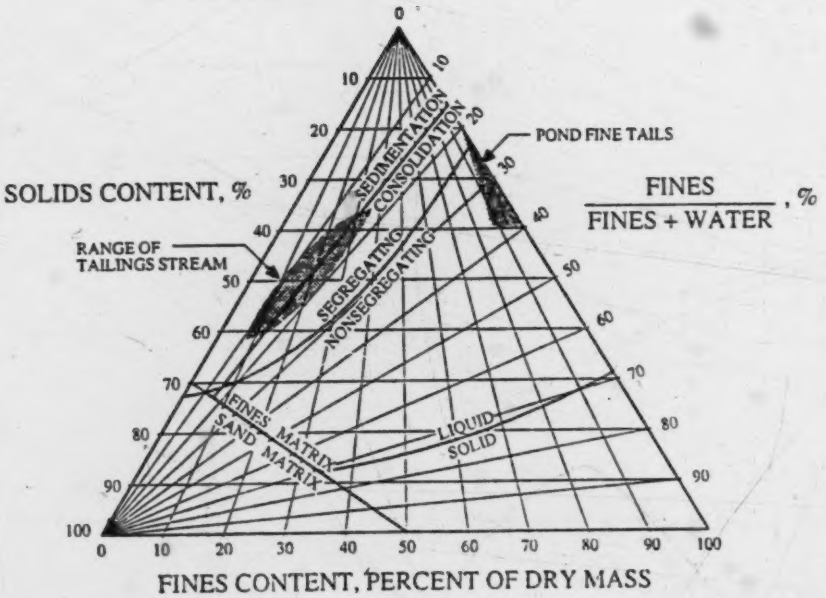

Figure 4.2: Slurry Property Diagram for Syncrude Tailings (Morgenstern and Scott, 1994).

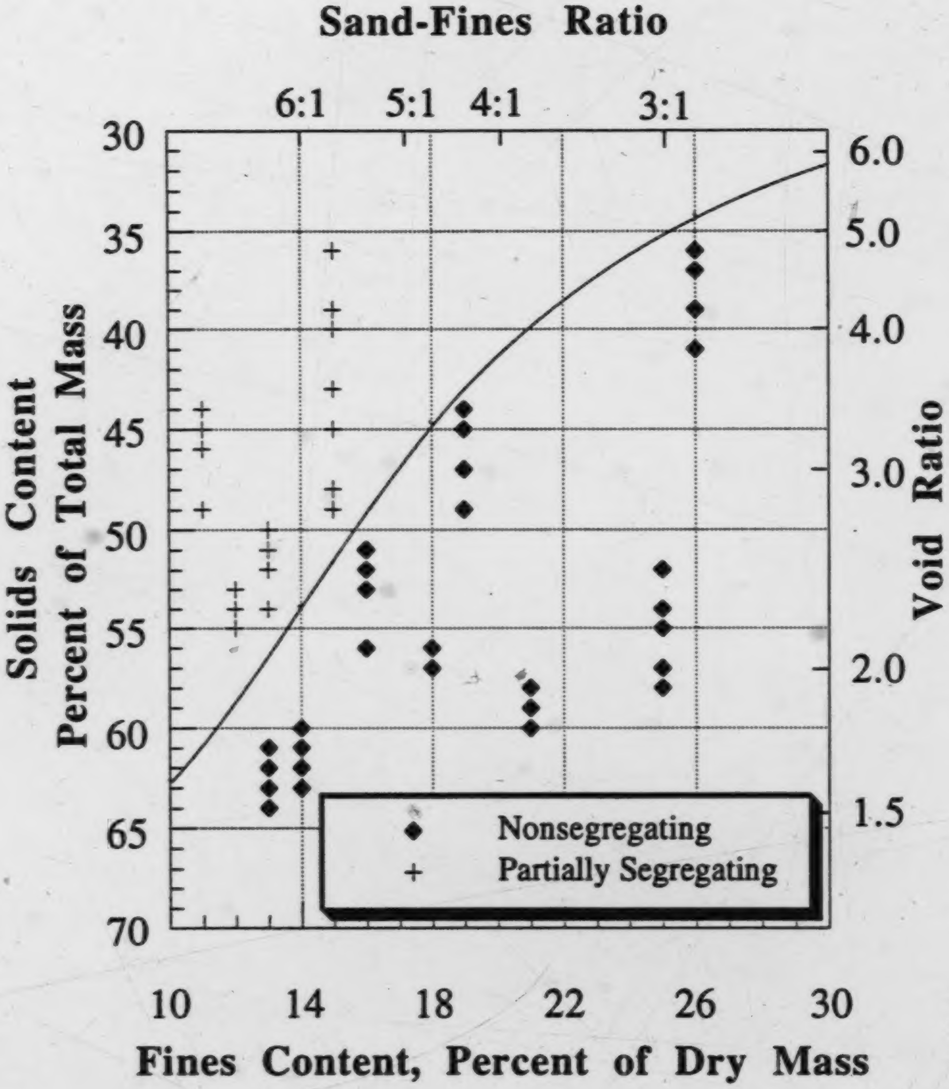

Figure 4.3: Segregation of CaO tailings (Scott *et al.*, 1993)

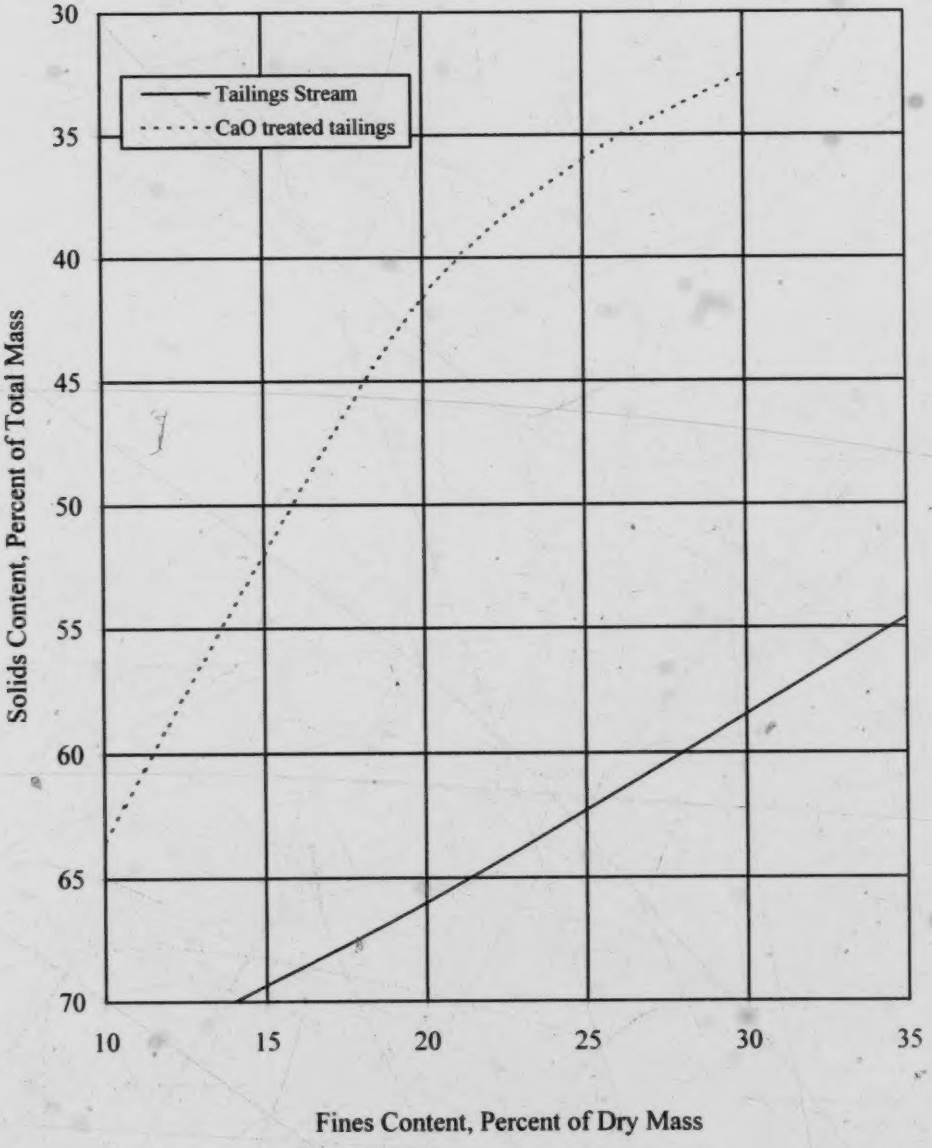

Figure 4.4: Segregation boundaries for Syncrude tailings stream and CaO treated tailings (Scott *et al* ., 1993) - *modified*

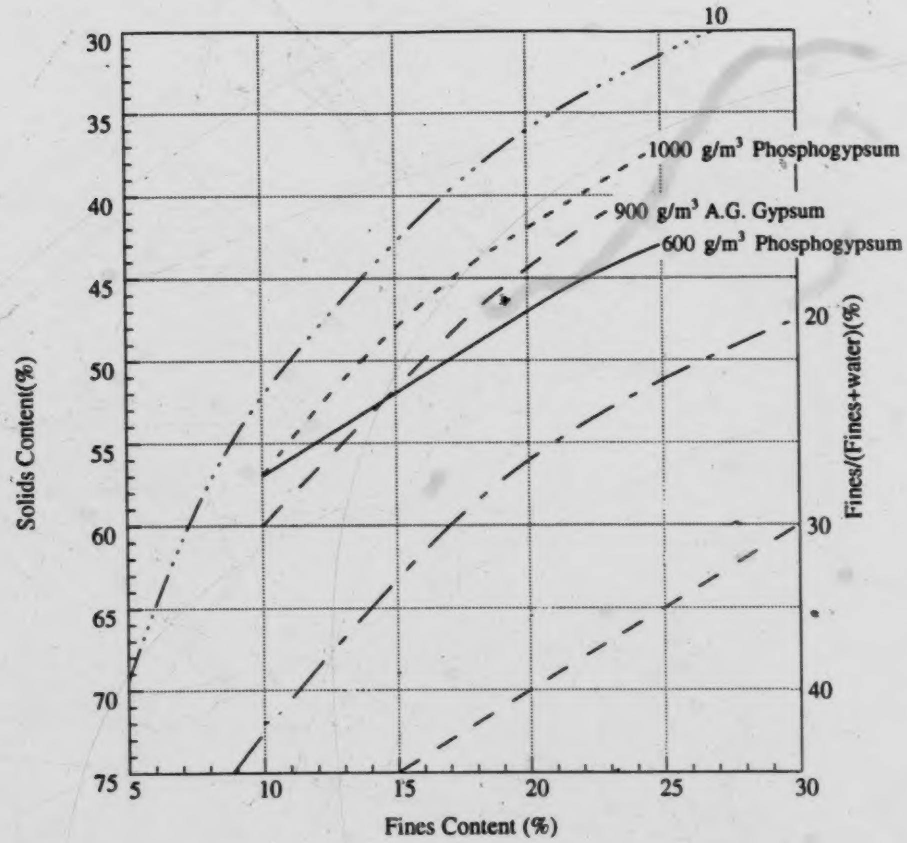

Figure 4.5: Segregation boundary for Syncrude Composite Tailings (Suthaker, 1996*a* and 1996*b*).

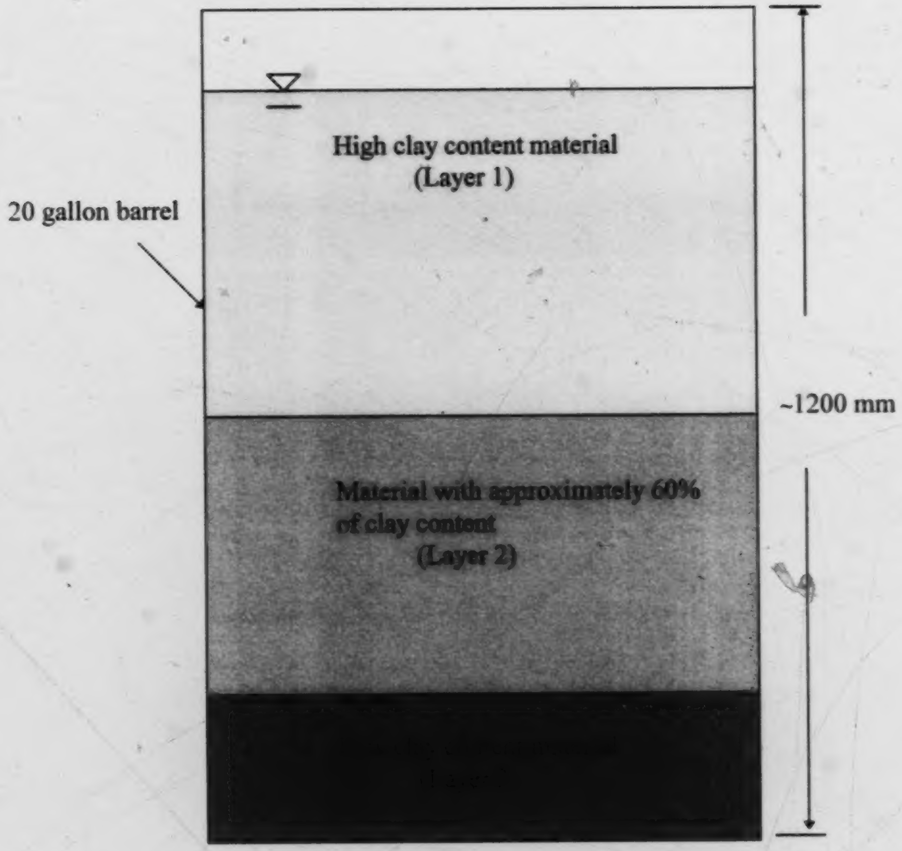
High clay content material
(Layer 1)
20 gallon barrel
~1200 mm
Material with approximately 60% of clay content
(Layer 2)
[illegible] clay content material
(Layer 3)

Figure 4.6: Schematic of the separated layers. The thickness of the layers depends on the amount of MFT-55 and water added.

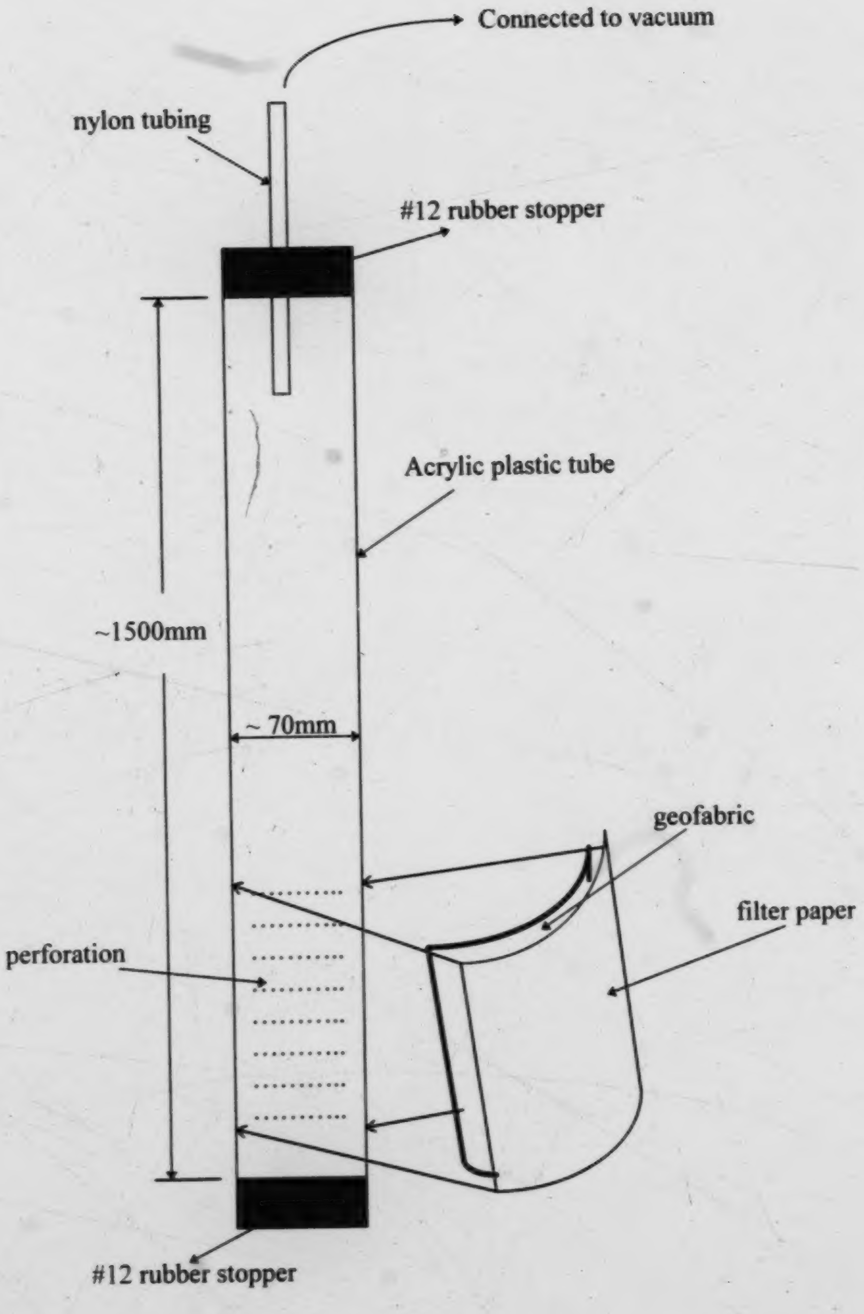
Connected to vacuum
nylon tubing
#12 rubber stopper
Acrylic plastic tube
~1500mm
~ 70mm
geofabric
filter paper
perforation
#12 rubber stopper

Figure 4.7: Filtering tube used during the separation process.

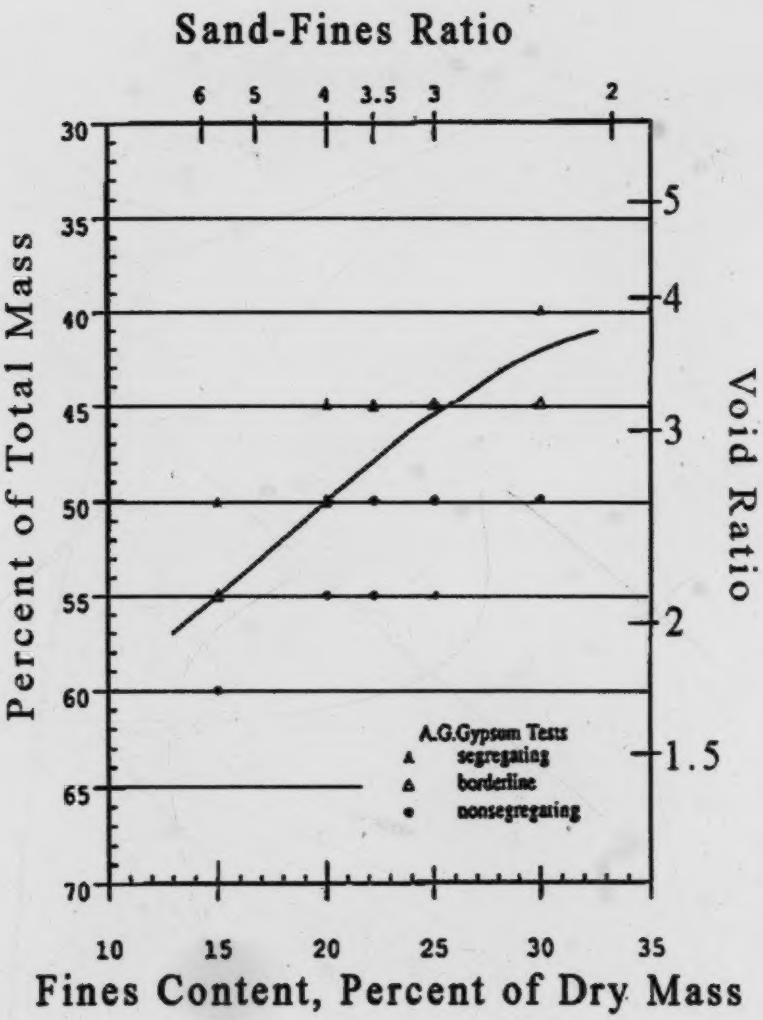

Figure 4.8: Suncor segregation test results for 600 ppm of agricultured grade gypsum (SOSG, 1996).

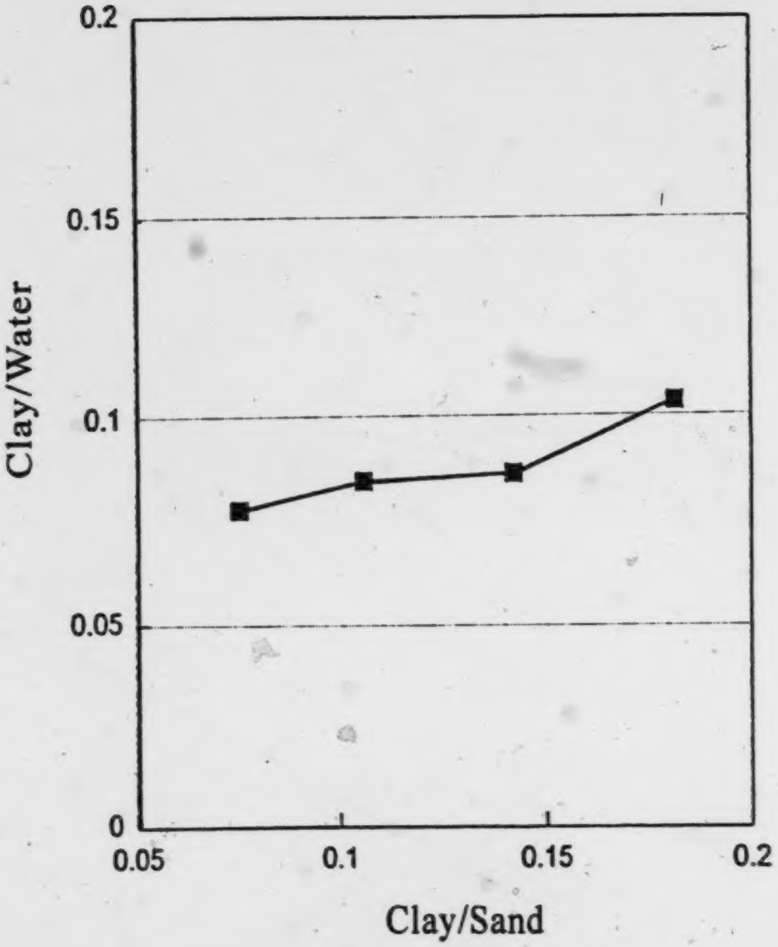

Figure 4.9: Segregation boundary obtained from data in Figure 4.8 (SOSG, 1996).

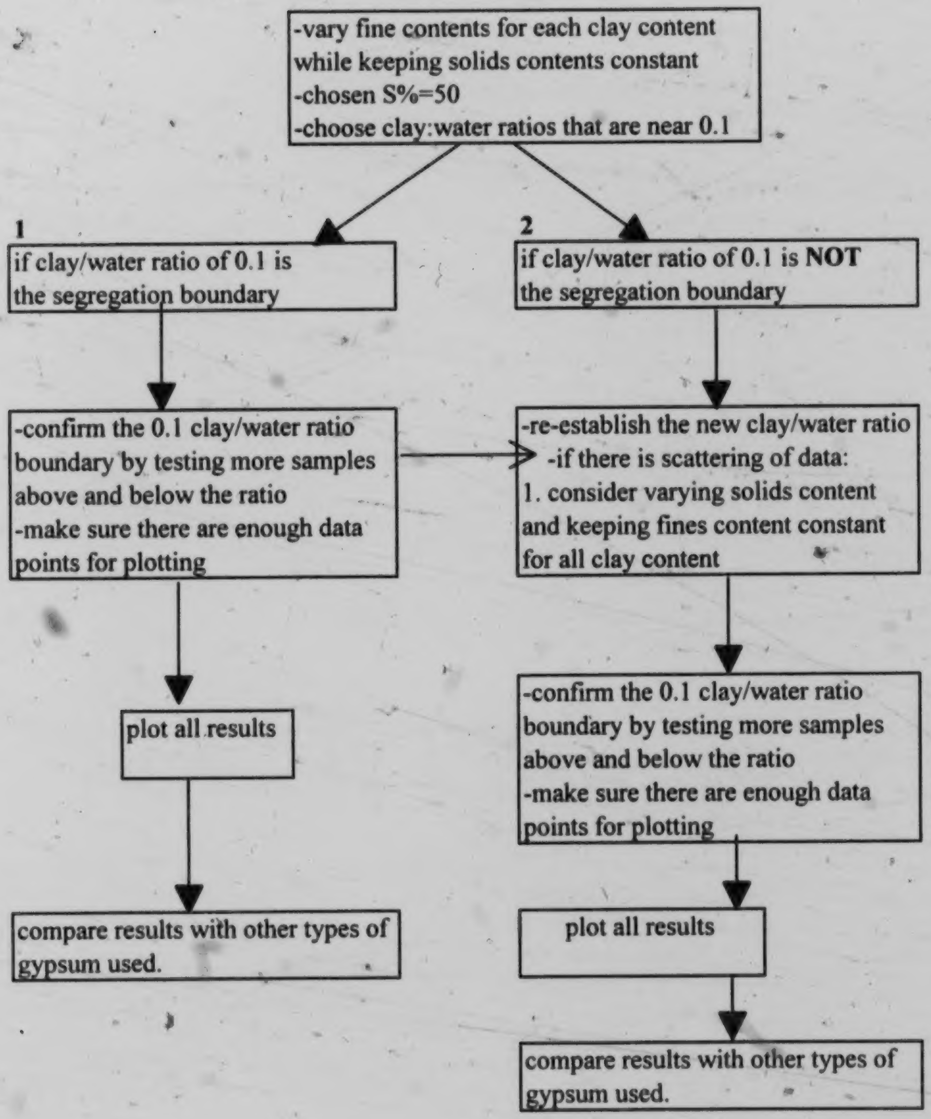
-vary fine contents for each clay content while keeping solids contents constant
-chosen S%=50
-choose clay:water ratios that are near 0.1
1
if clay/water ratio of 0.1 is the segregation boundary
2
if clay/water ratio of 0.1 is NOT the segregation boundary
-confirm the 0.1 clay/water ratio boundary by testing more samples above and below the ratio
-make sure there are enough data points for plotting
-re-establish the new clay/water ratio
-if there is scattering of data:
1. consider varying solids content and keeping fines content constant for all clay content
plot all results
-confirm the 0.1 clay/water ratio boundary by testing more samples above and below the ratio
-make sure there are enough data points for plotting
compare results with other types of gypsum used.
plot all results
compare results with other types of gypsum used.

Figure 4.10: Flow chart illustrating the experimental program

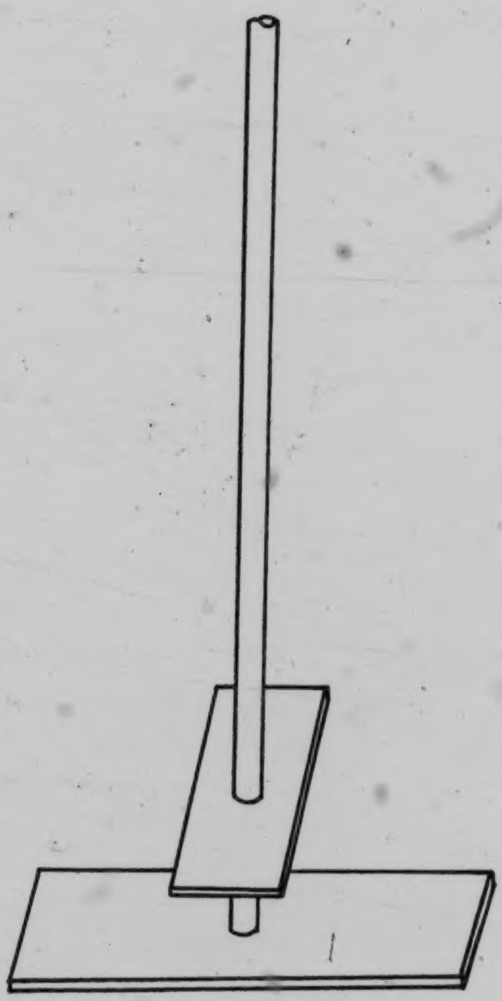

Figure 4.11: Blade used for mixing CT (Caughill, 1992).

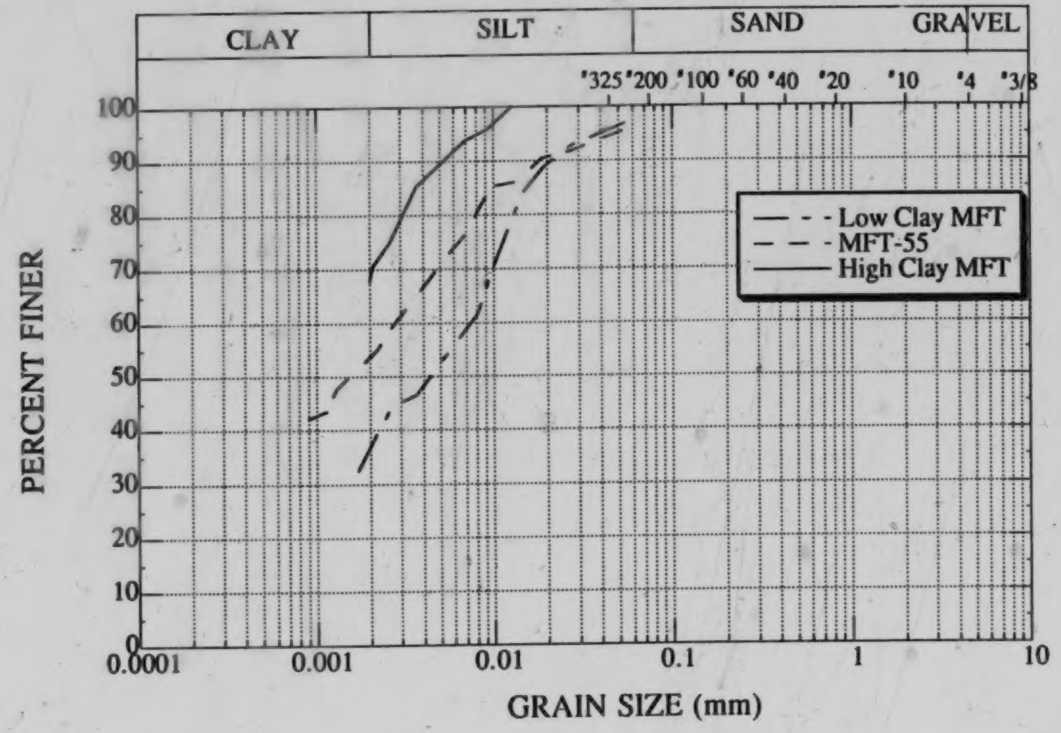

Figure 4.12: Grain size distribution of low clay content MFT, MFT-55 (SY-22), and high clay content MFT.

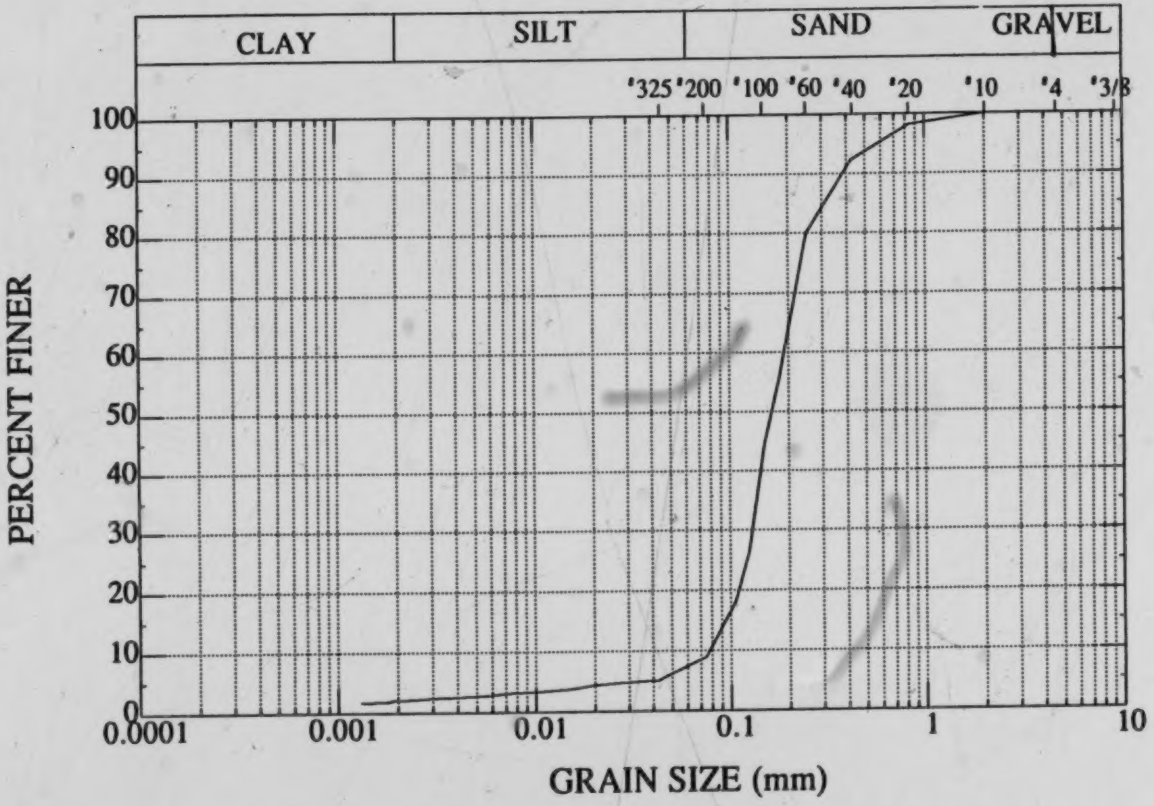

Figure 4.13: Grain size distribution of beach sand.

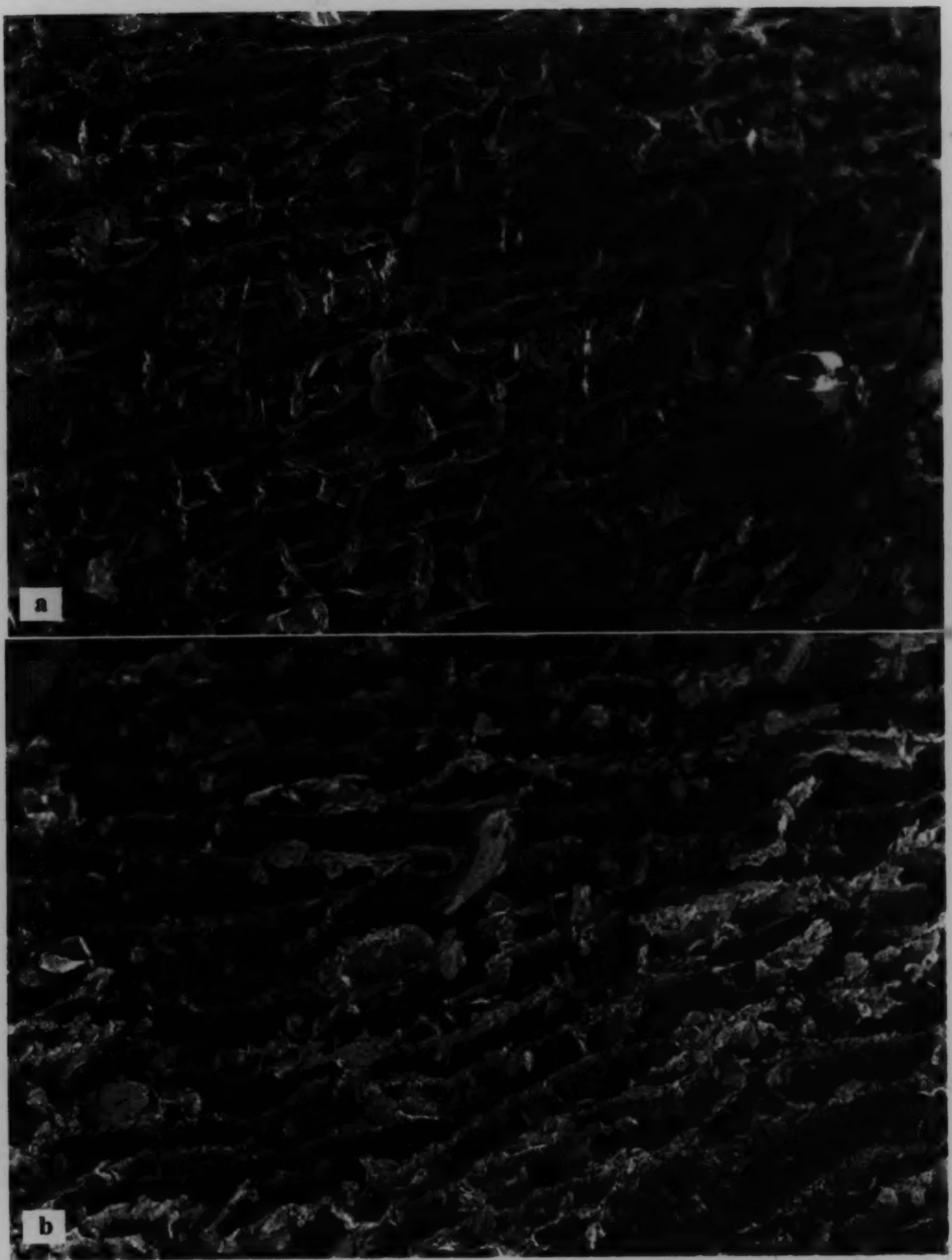

Figure 4.14 : a) 36% clay content MFT
b) 70% clay content MFT
(Magnification at 500X: ▬ 10 microns)

Figure 4.15: 36% clay content MFT mixed with 2500g/m3 of laboratory grade gypsum
(Magnification at 500X: —— 10 microns)

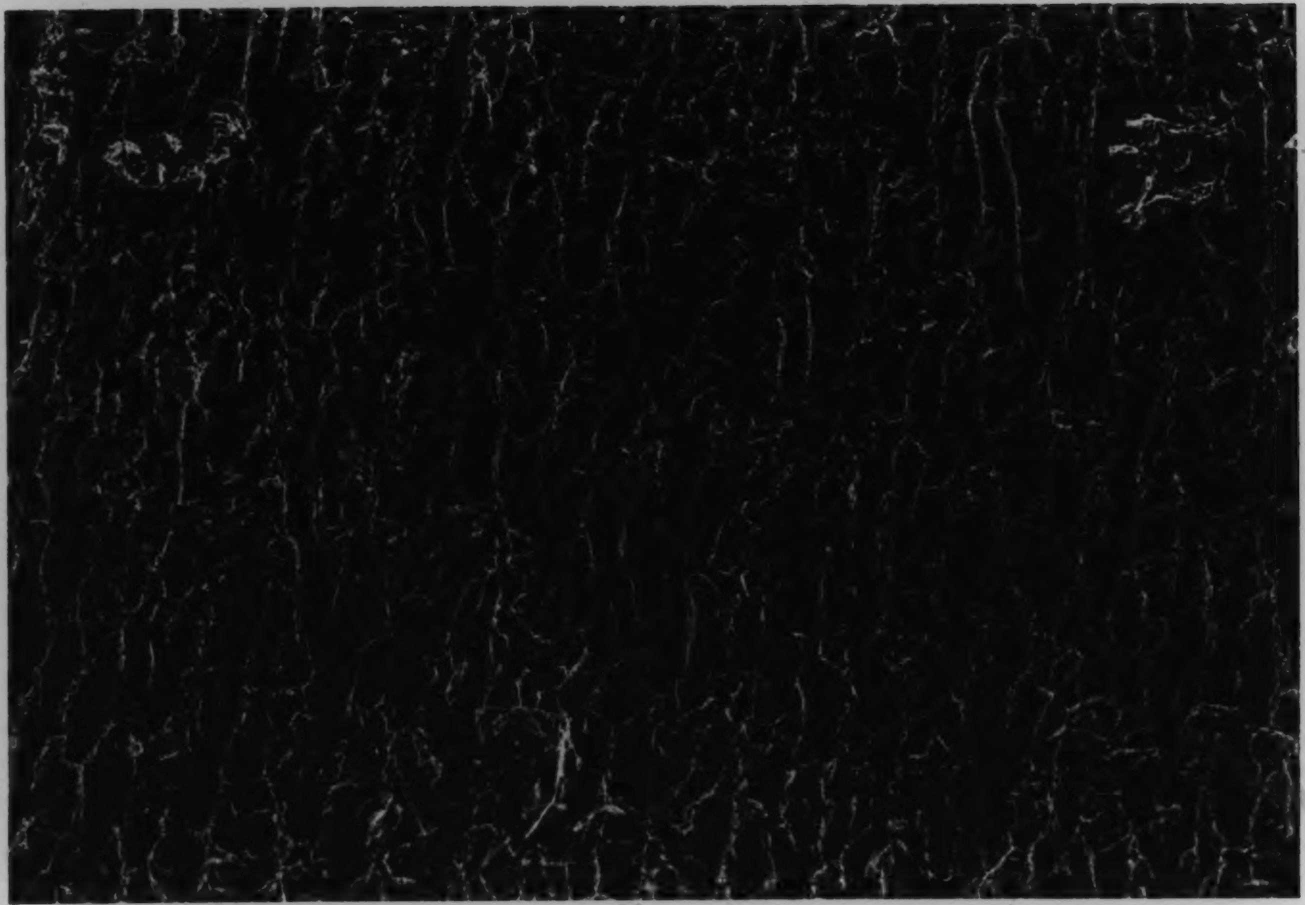

Figure 4.16: 70% clay content MFT mixed with 2500g/m3 of laboratory grade gypsum (Magnification at 500X: —— 10 microns)

Figure 4.17: CT with 36% clay content MFT mixed with 2500g/m3 of laboratory grade gypsum (Magnification at 200X: — 10 microns)

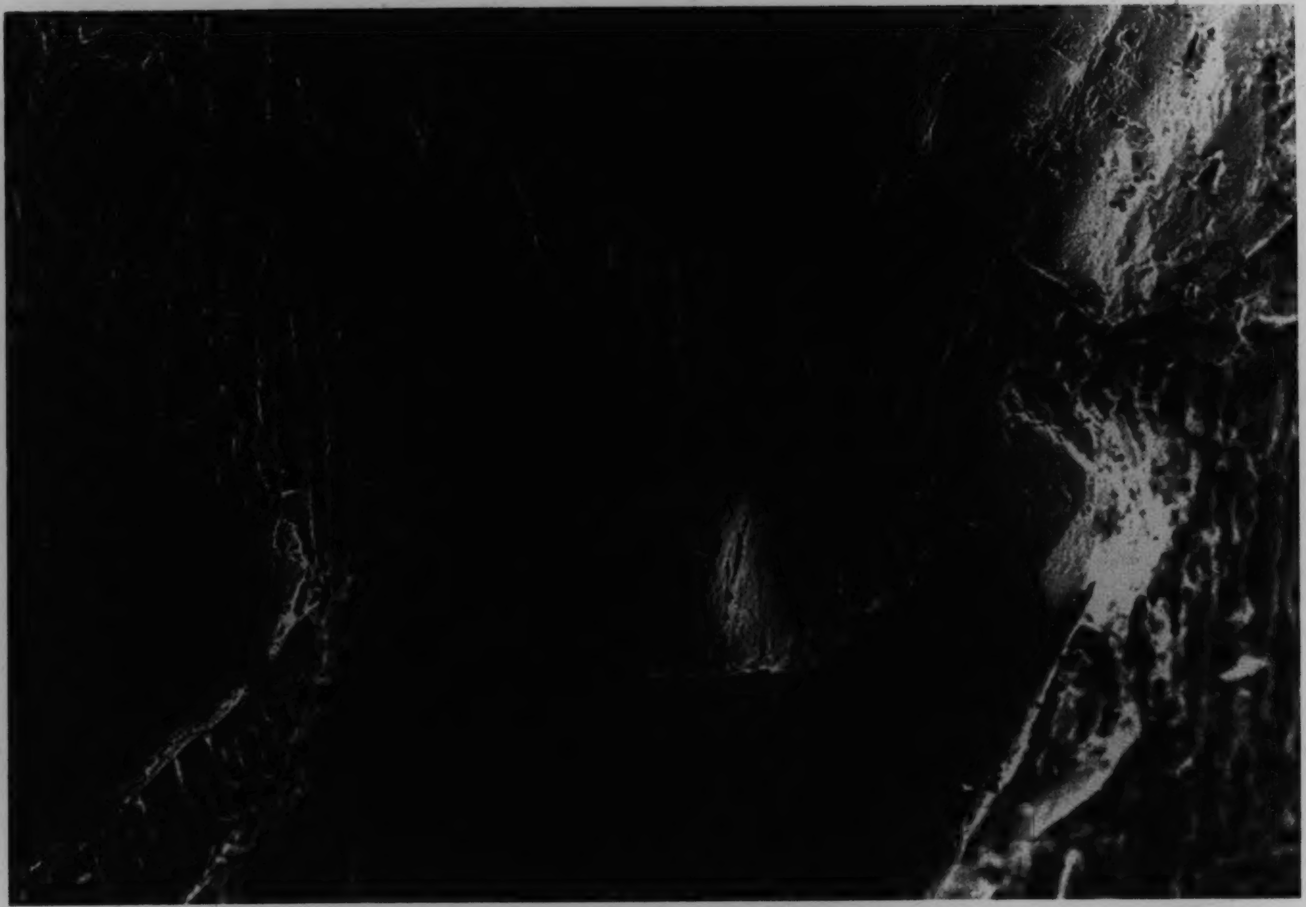

Figure 4.18 : CT with 55% clay content MFT mixed with 2500g/m3 of laboratory grade gypsum
(Magnification at 200X: — 10 microns)

Figure 4.19 : CT with 70% clay content MFT mixed with 2500g/m3 of laboratory grade gypsum. (Magnification at 200X: — 10 microns)

Figure 4.20: CT with 36% clay content MFT mixed with 2500g/m3 of laboratory grade gypsum. (Magnification at 500X: ——10 microns)

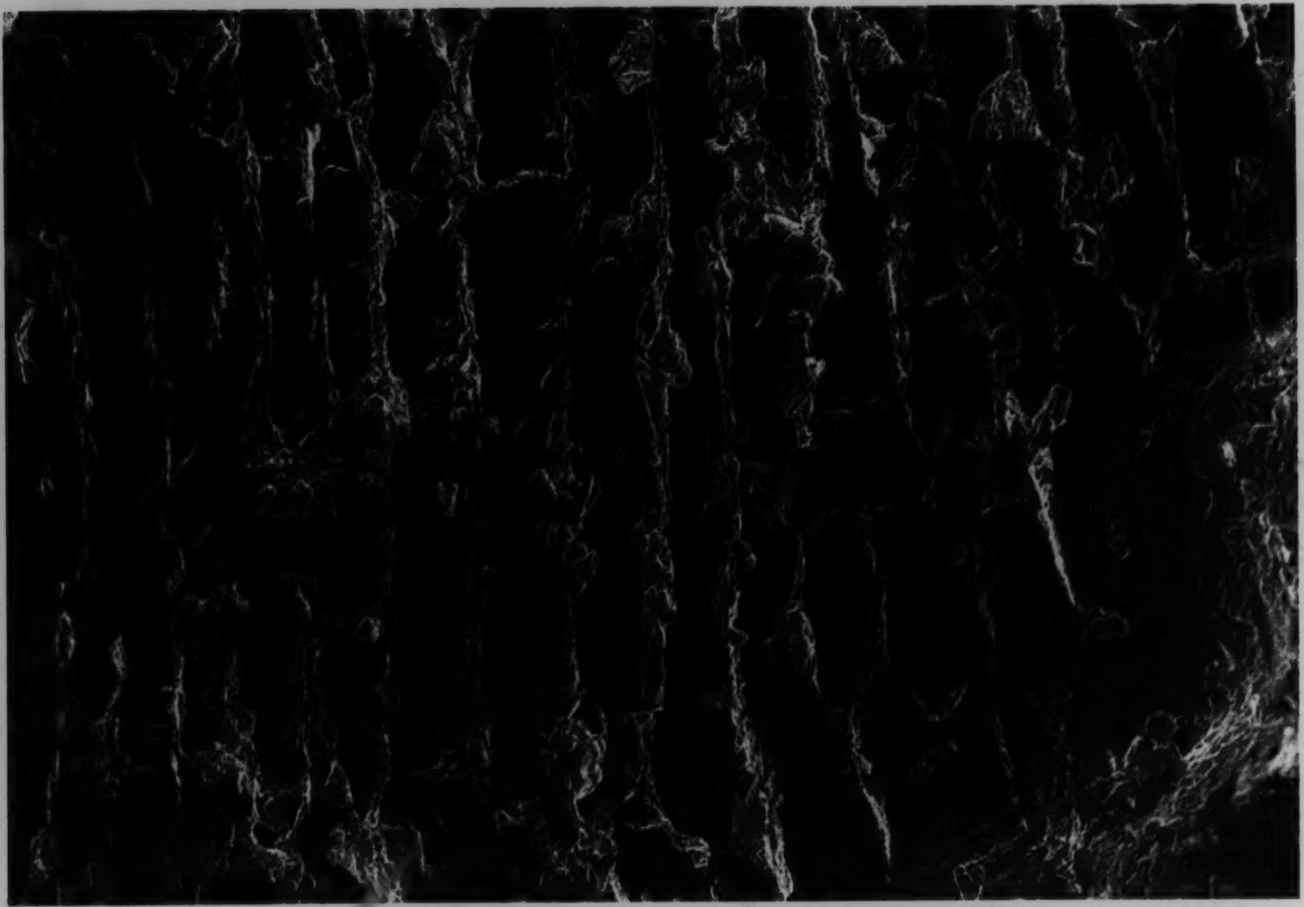

Figure 4.21: CT with 55% clay content MFT mixed with 2500g/m3 of laboratory grade gypsum. (Magnification at 500X: —— 10 microns)

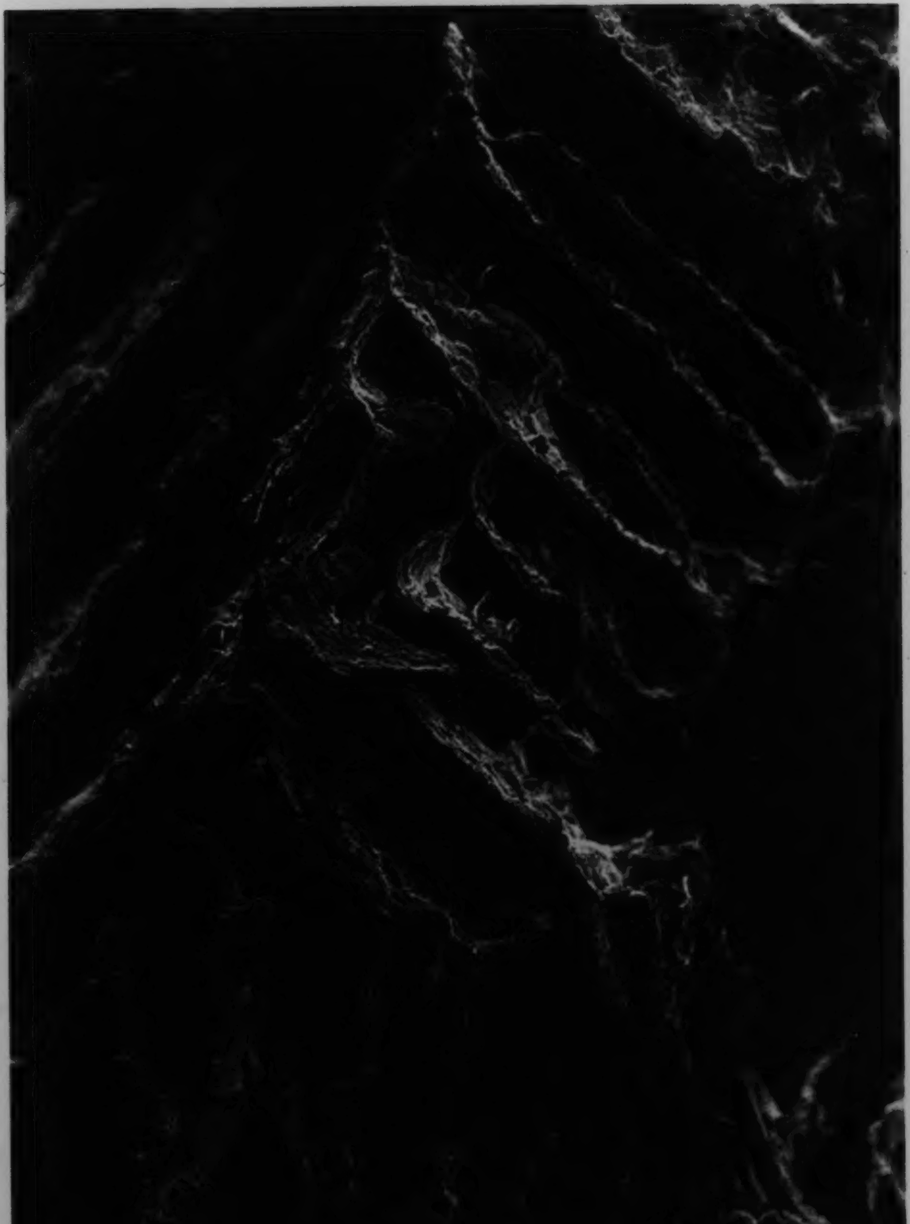

Figure 4.22: CT with 70% clay content MFT mixed with 2500g/m3 of laboratory grade gypsum. (Magnification at 500X: ——— 10 microns)

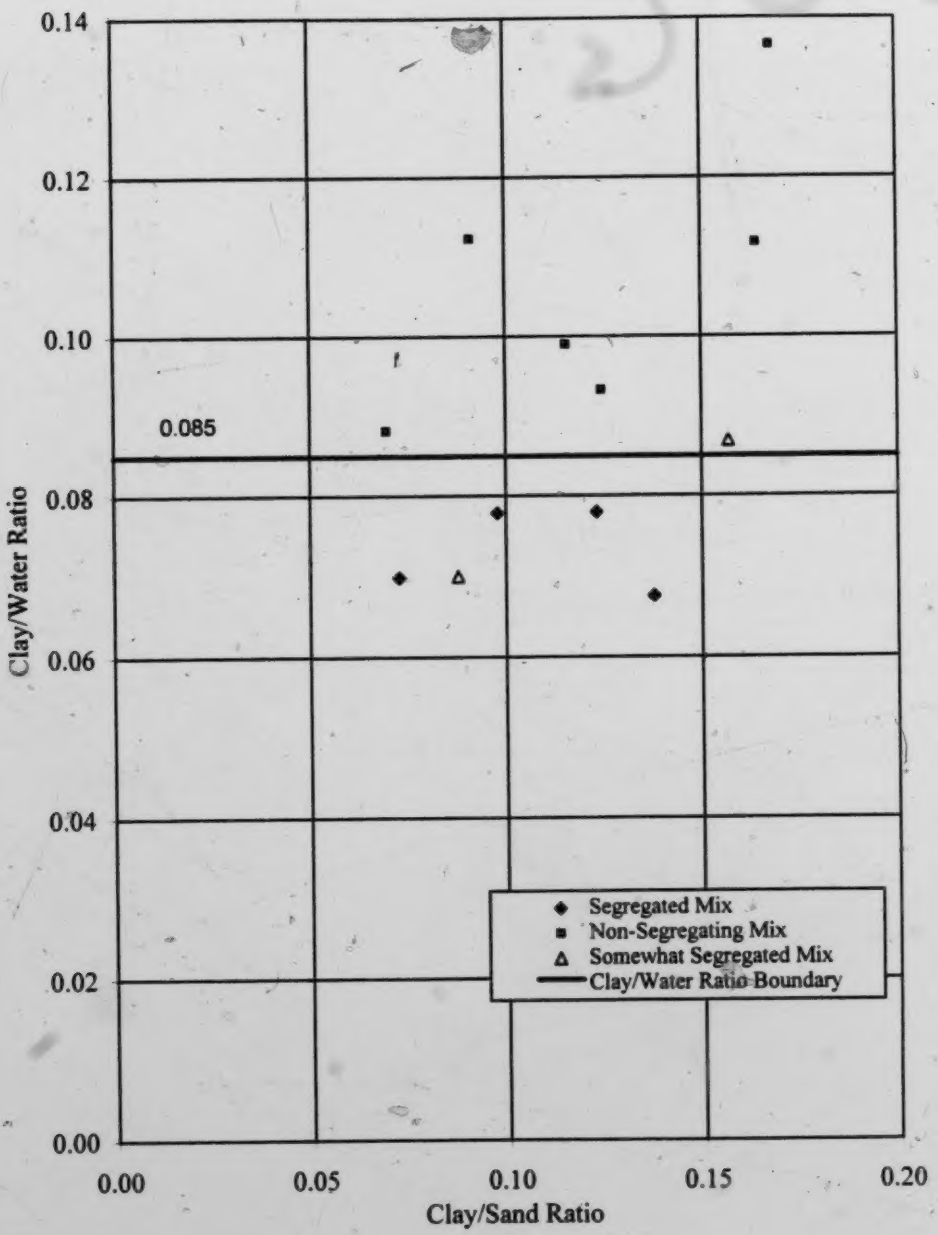

Figure 4.23: Clay/Water ratio boundary for tailings with 36% clay content MFT.

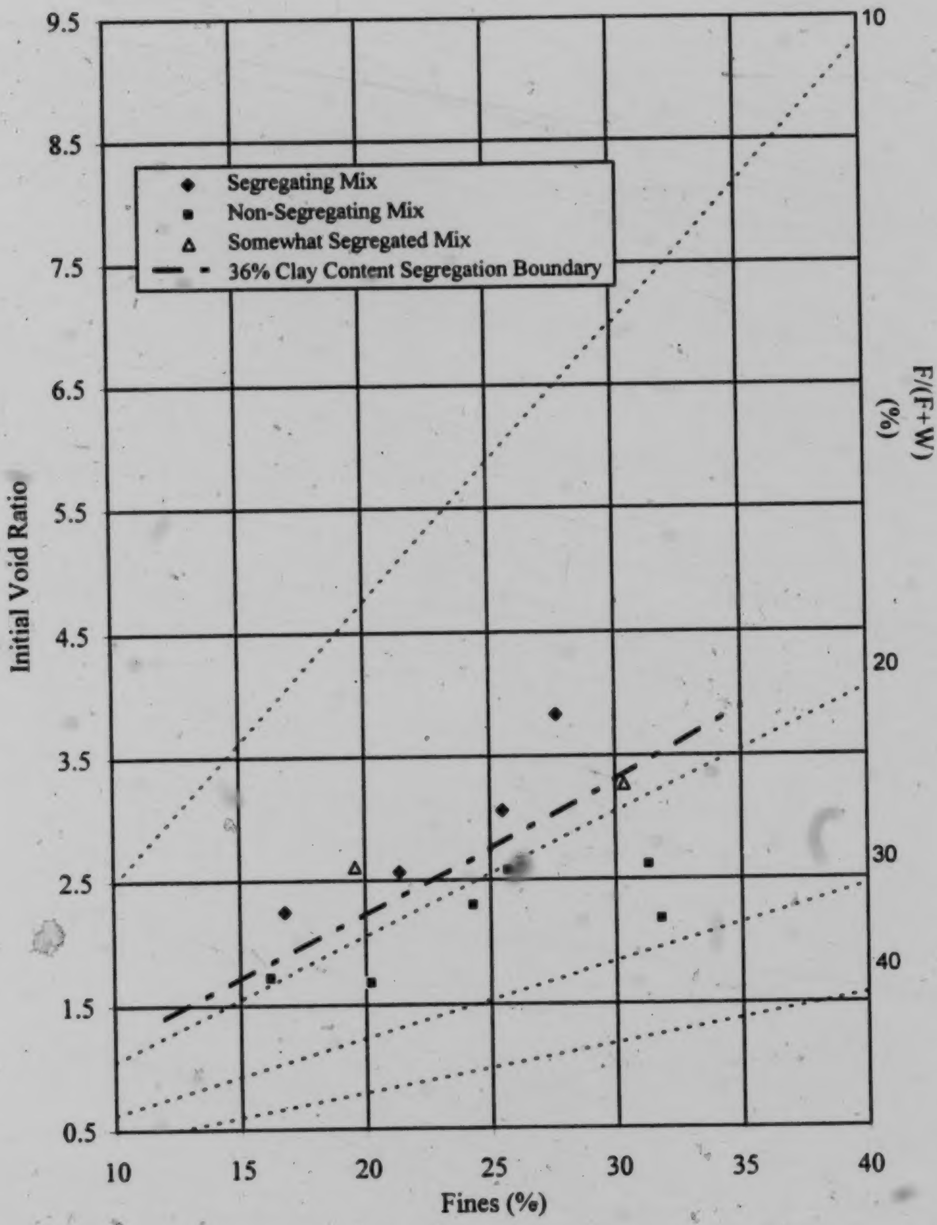

Figure 4.24: Fines vs. Initial Void Ratio and F/(F+W) for tailings with 36% clay content MFT.

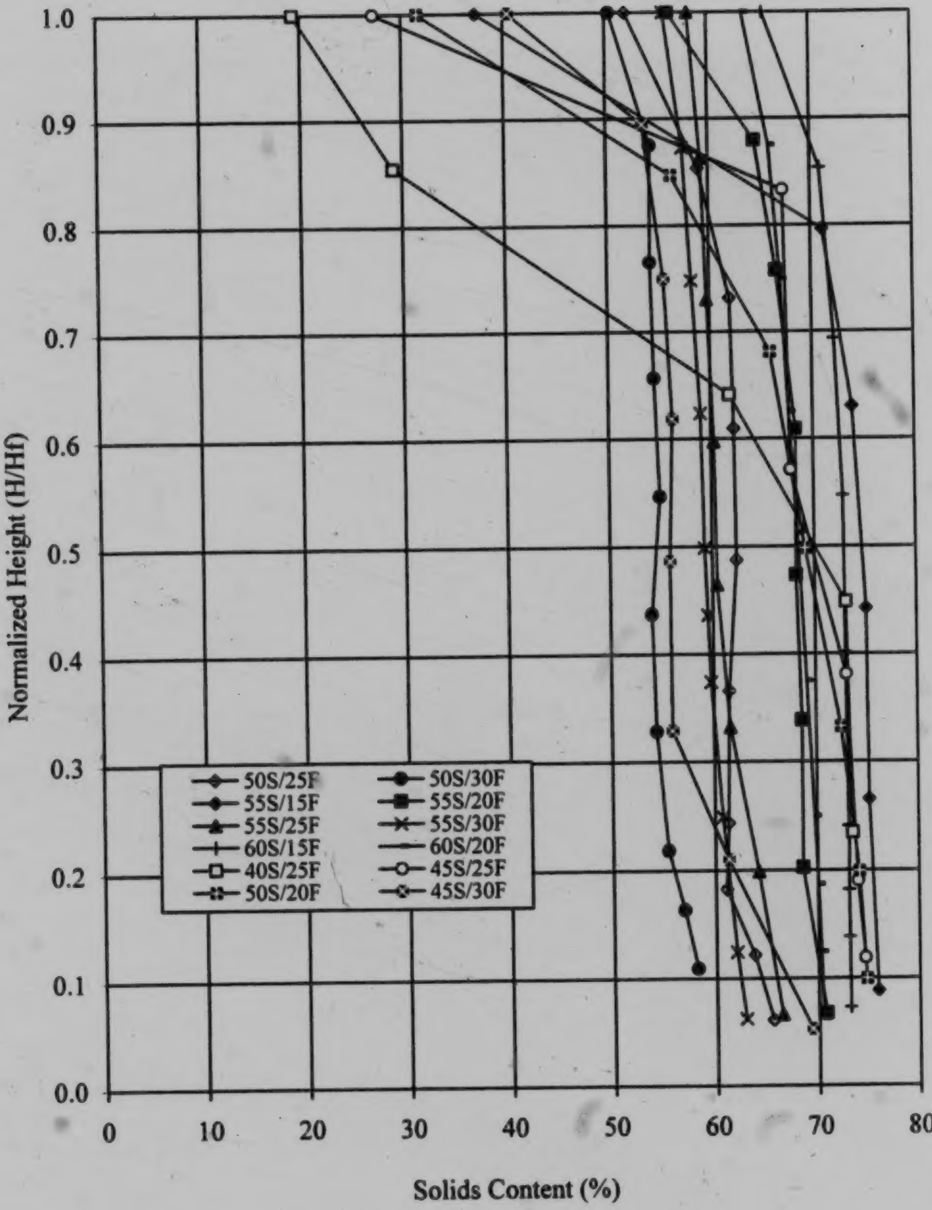

Figure 4.25 : Solids content profile for tailings with 36% clay content MFT.

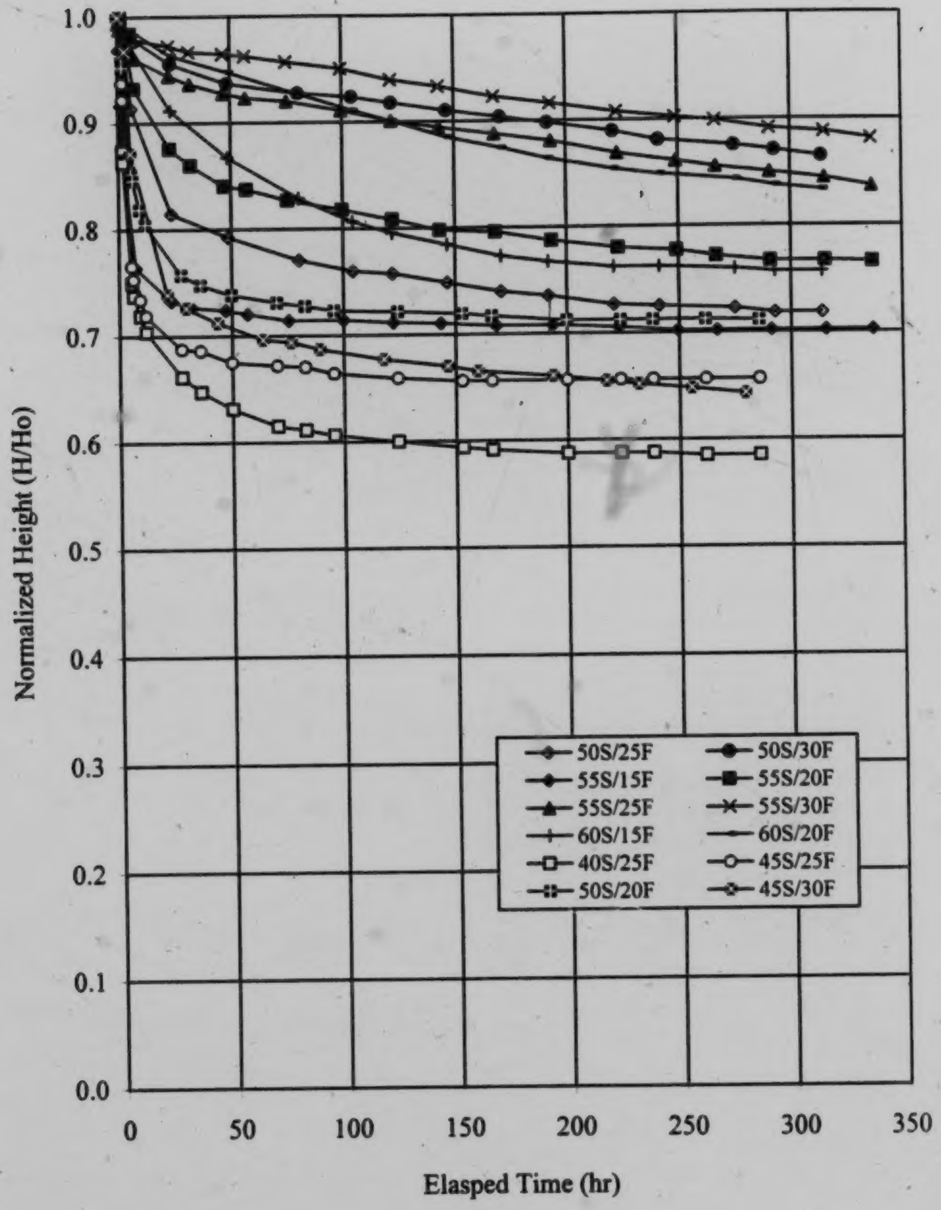

Figure 4.26: Standpipe testing progress for tailings with 36% clay content MFT.

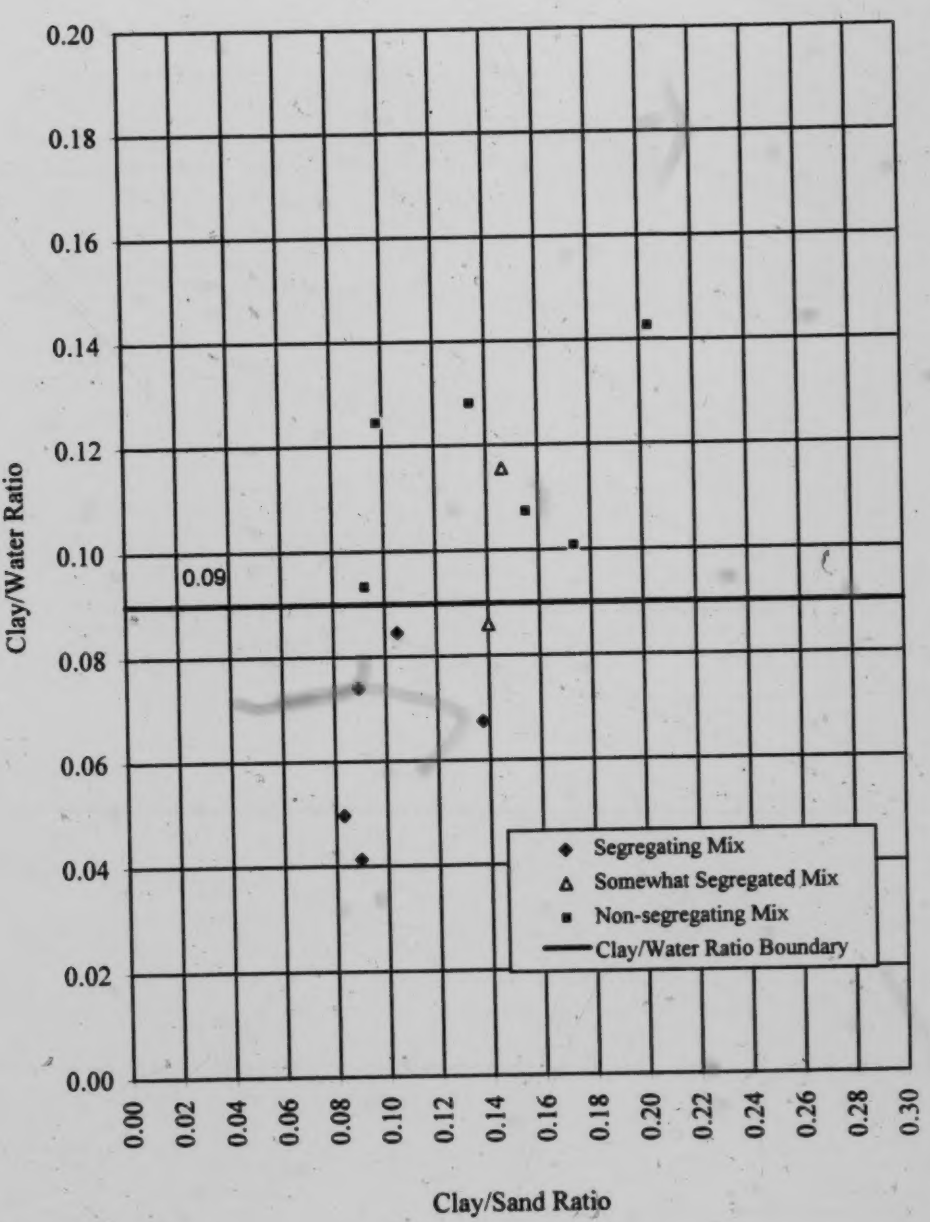

Figure 4.27: Clay/Water ratio boundary for tailings with 55% clay content MFT.

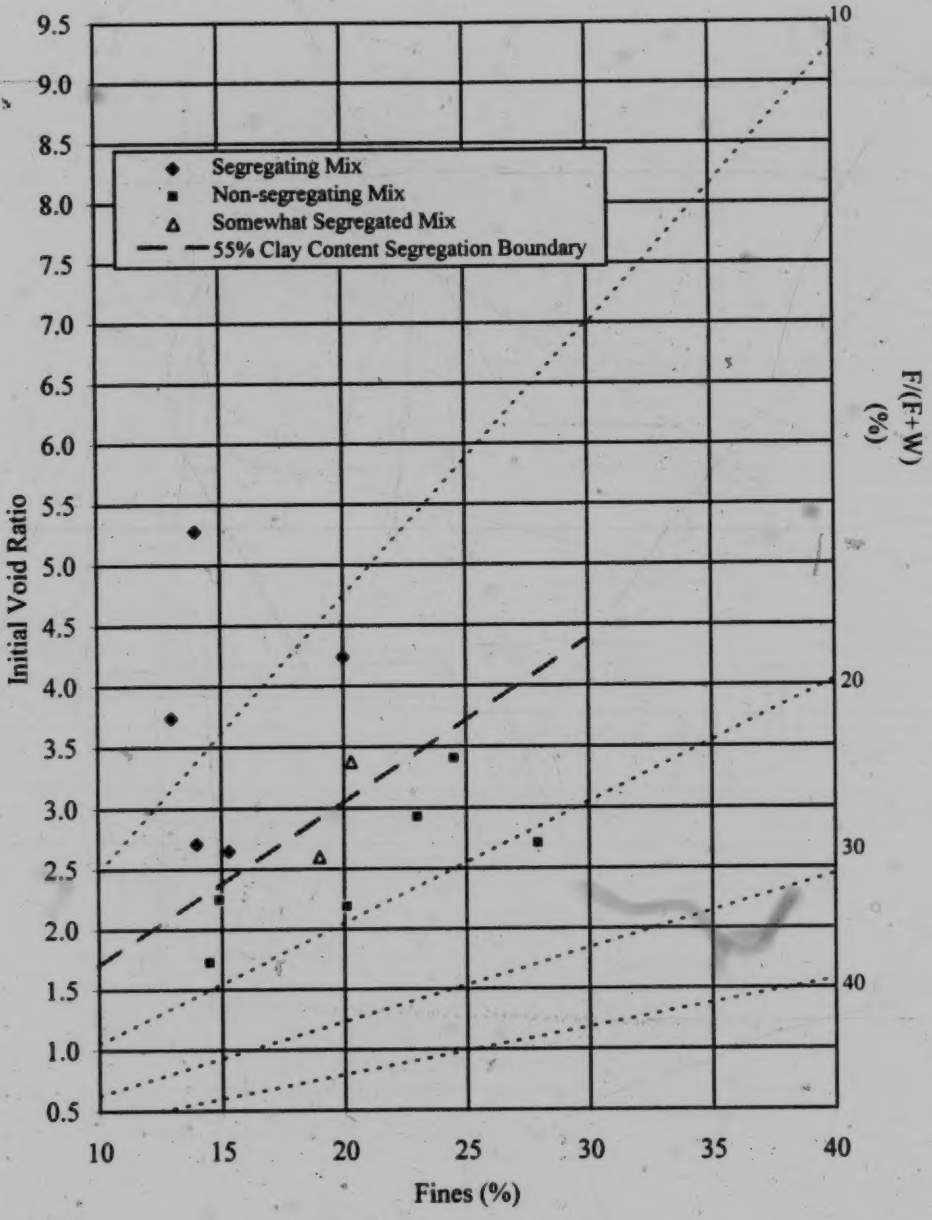

Figure 4.28: Fines vs. Initial Void Ratio and F/(F+W) for tailings with 55% clay content MFT.

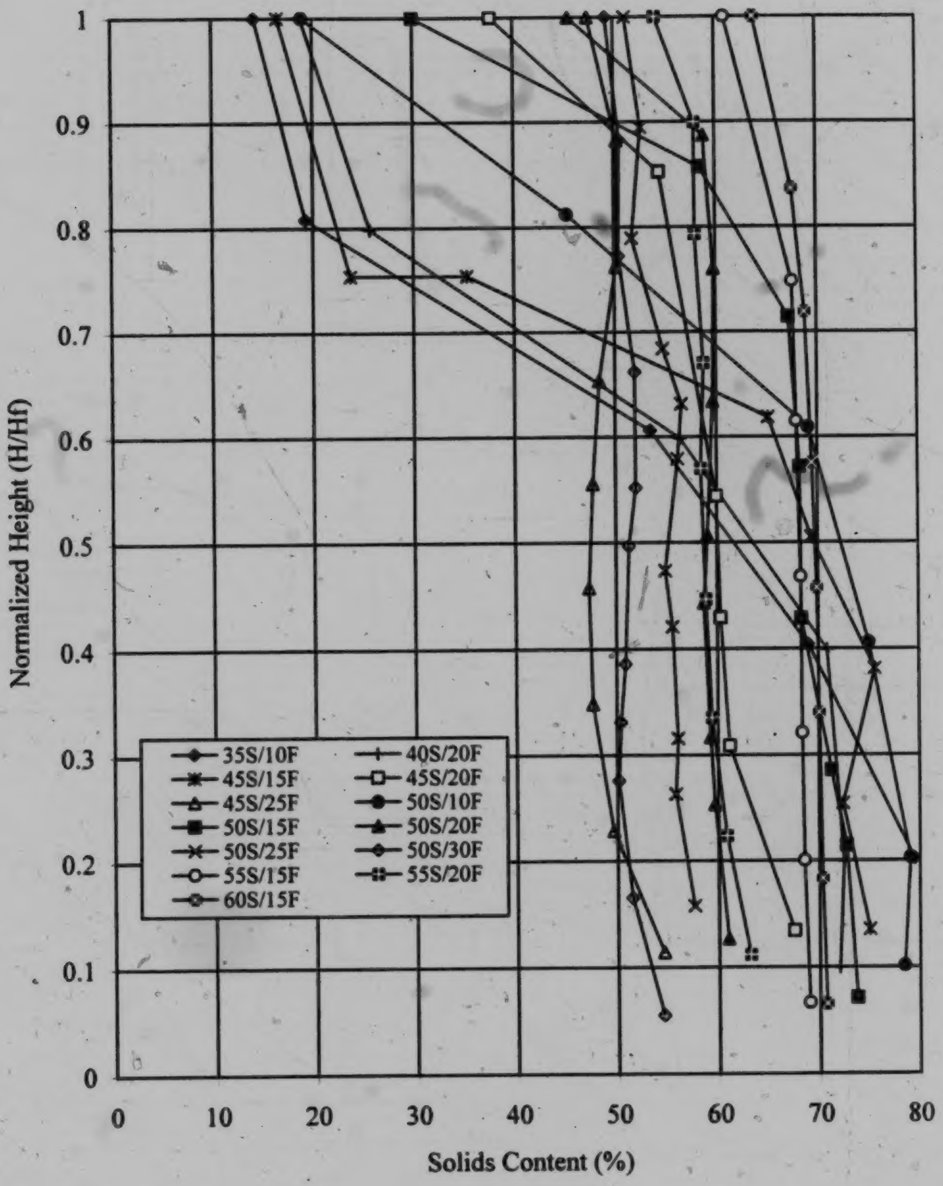

Figure 4.29: Solids content profile for tailings with 55% clay content MFT.

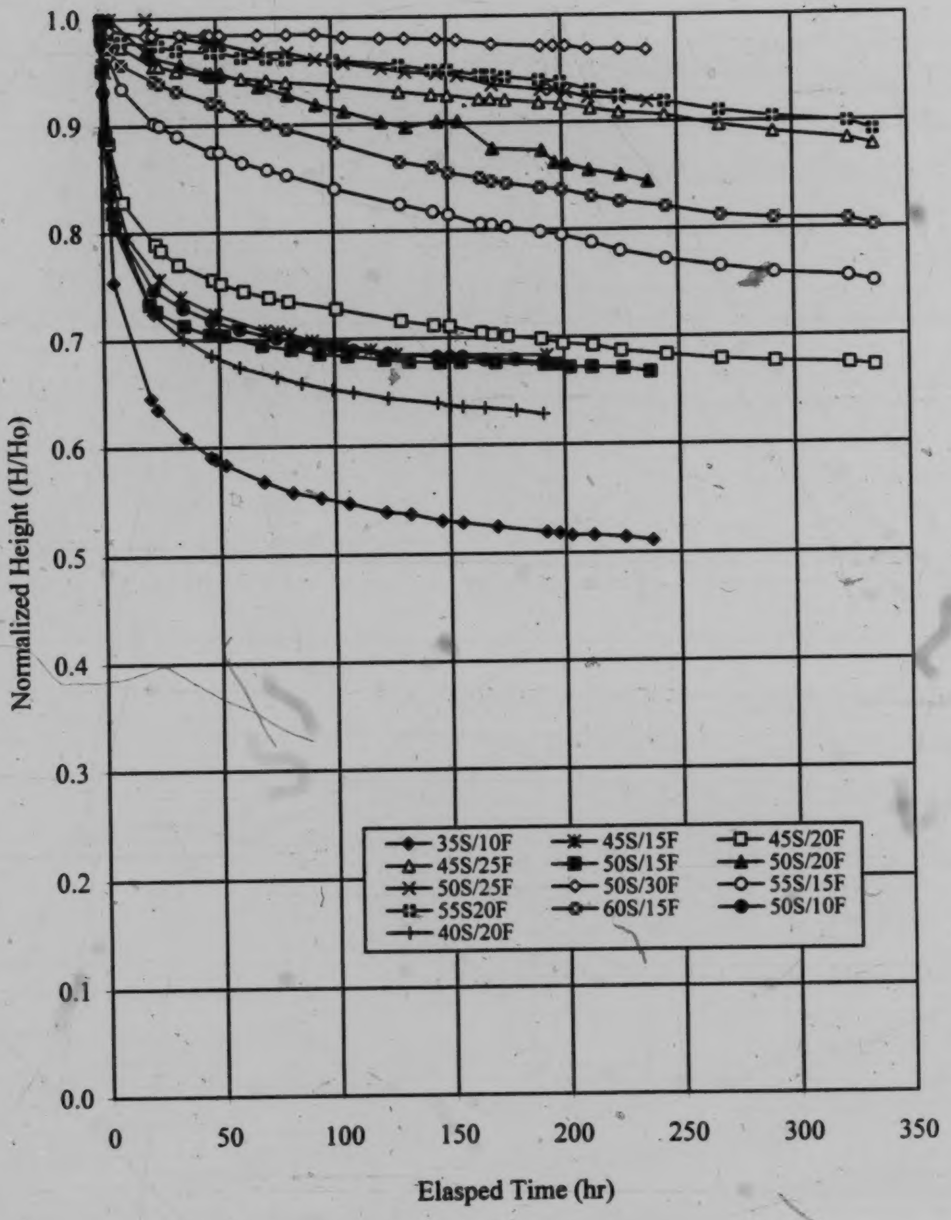

Figure 4.30: Standpipe testing progress for tailings with 55% clay content MFT.

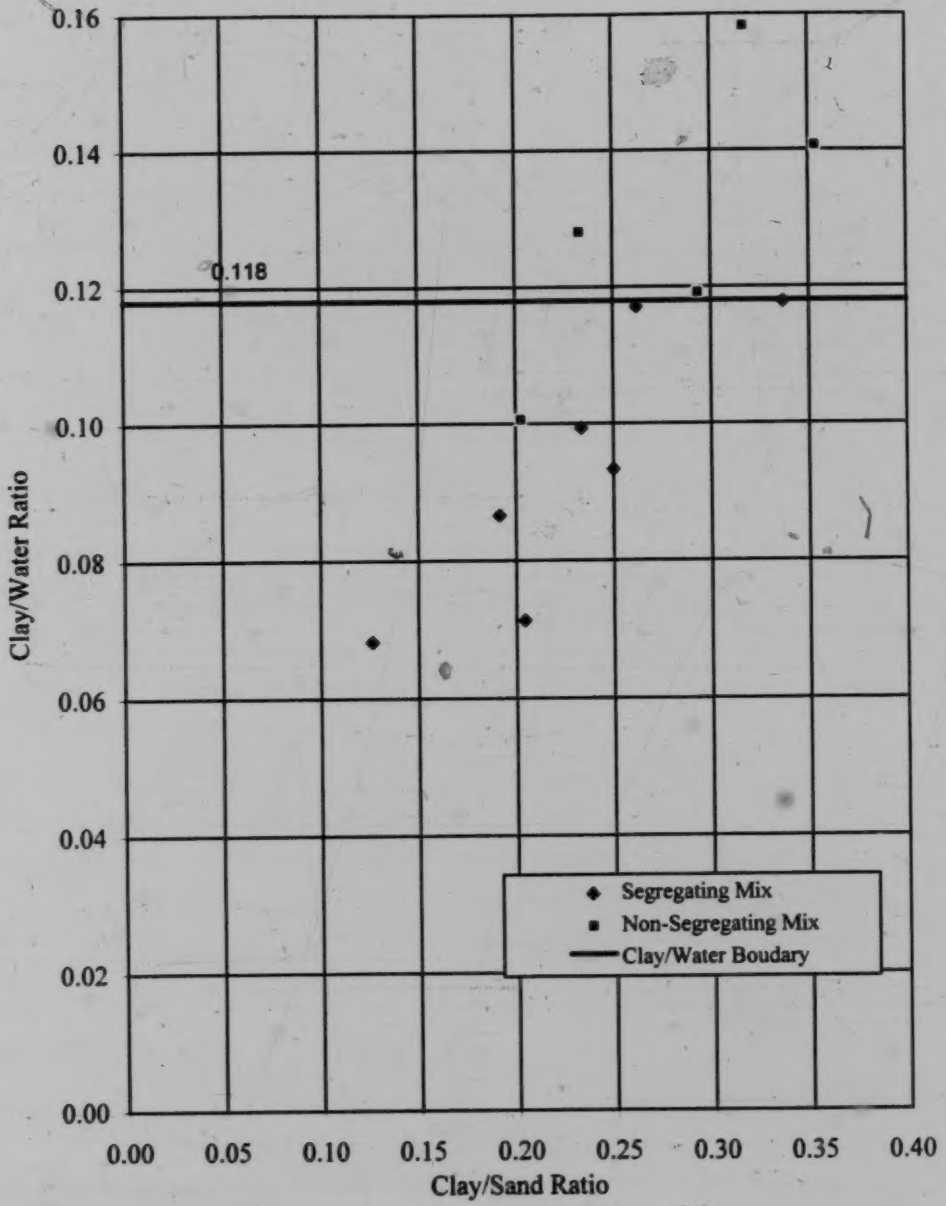

Figure 4.31 : Clay/Water ratio boundary for tailings with 70% clay content in MFT.

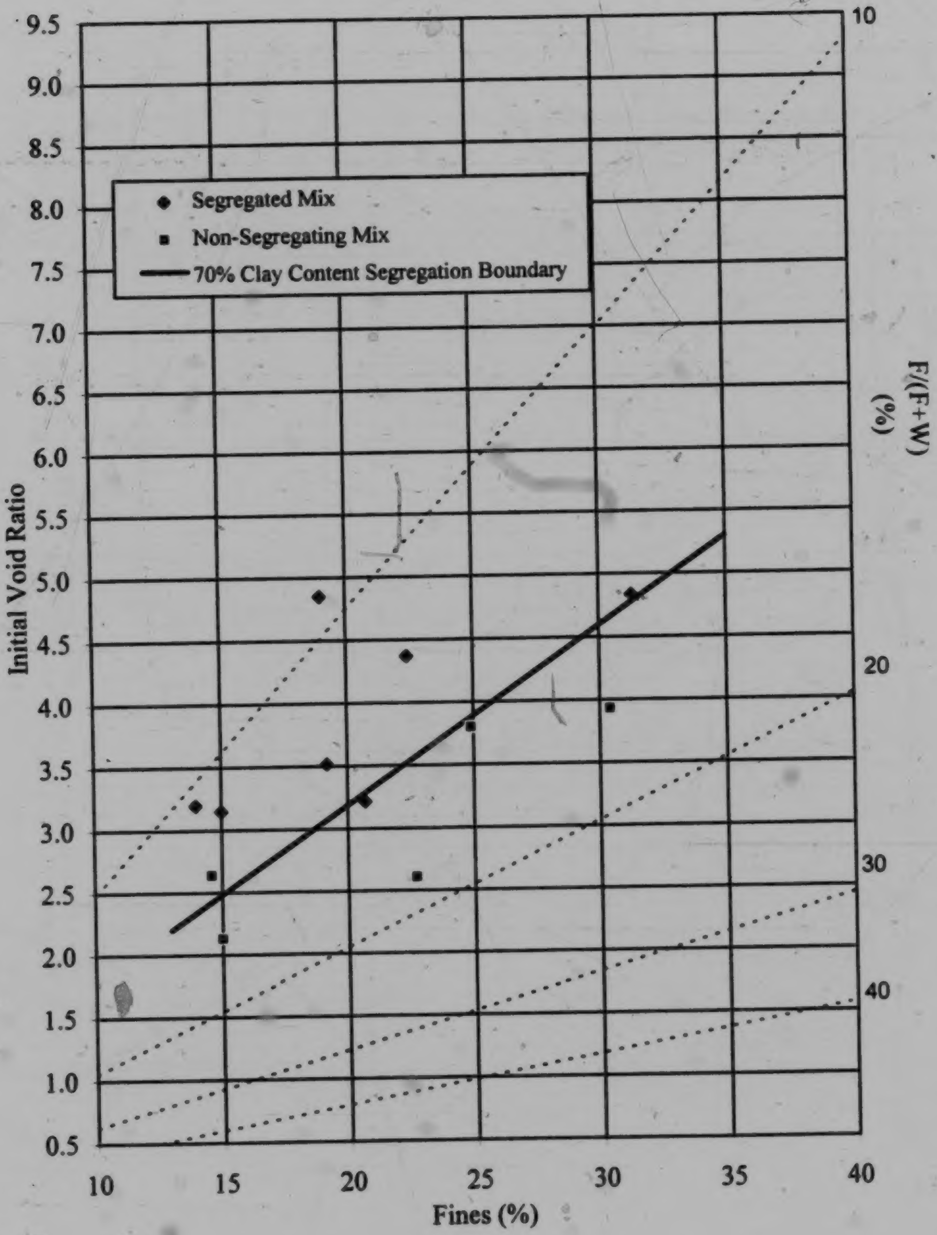

Figure 4.32: Fines vs. Initial Void Ratio and F/(F+W) for tailings with 70% clay content MFT.

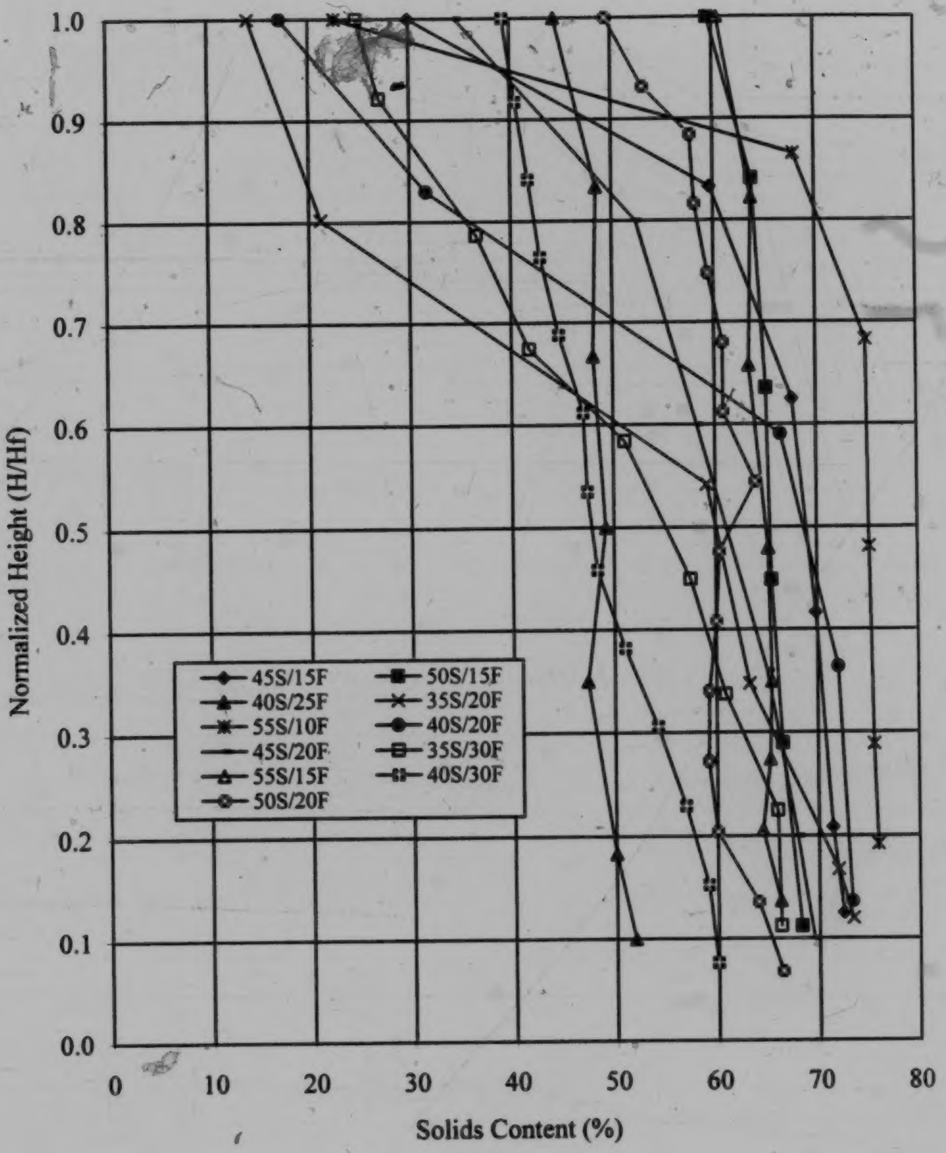

Figure 4.33: Solids content profile for tailings with 70% clay content MFT.

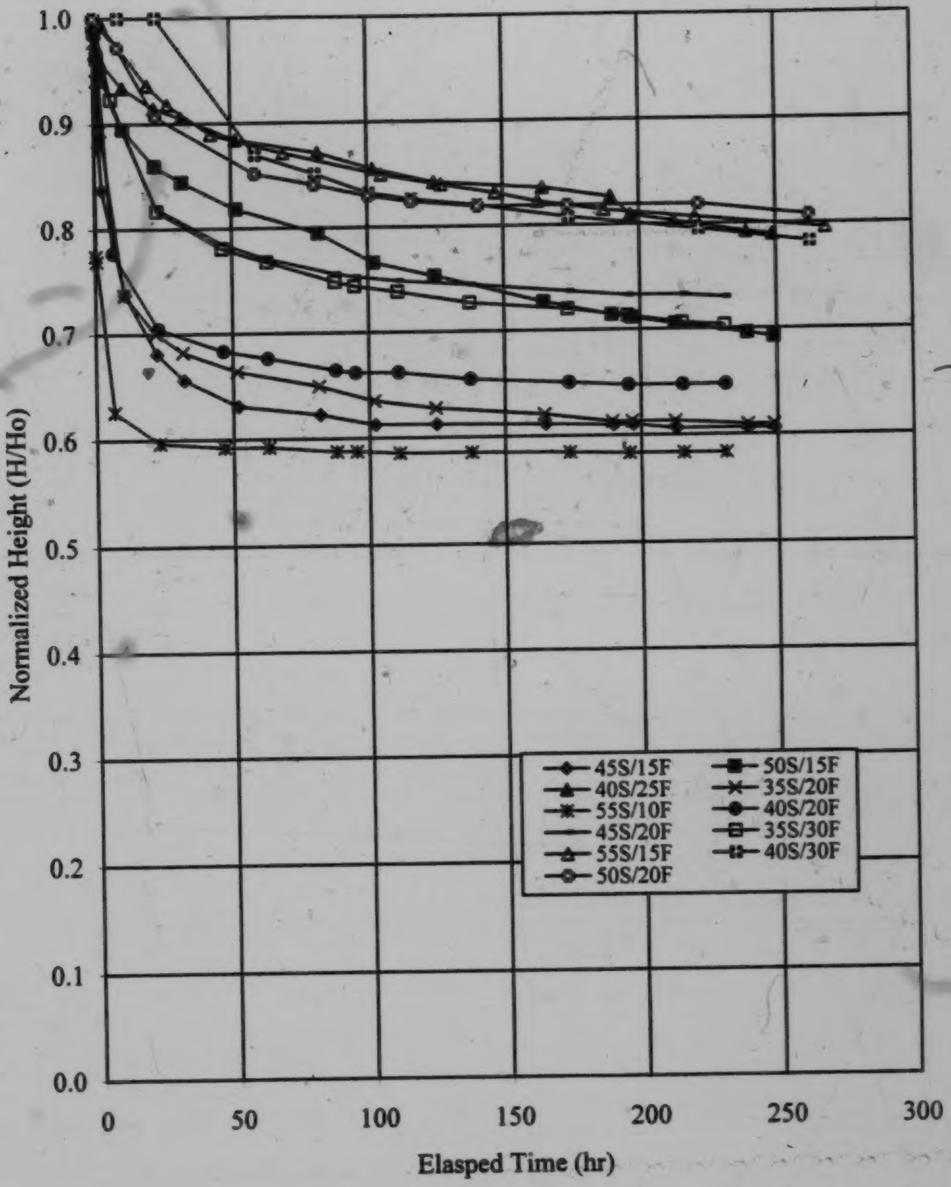

Figure 4.34: Standpipe testing progress for tailings with 70% clay clay content MFT.

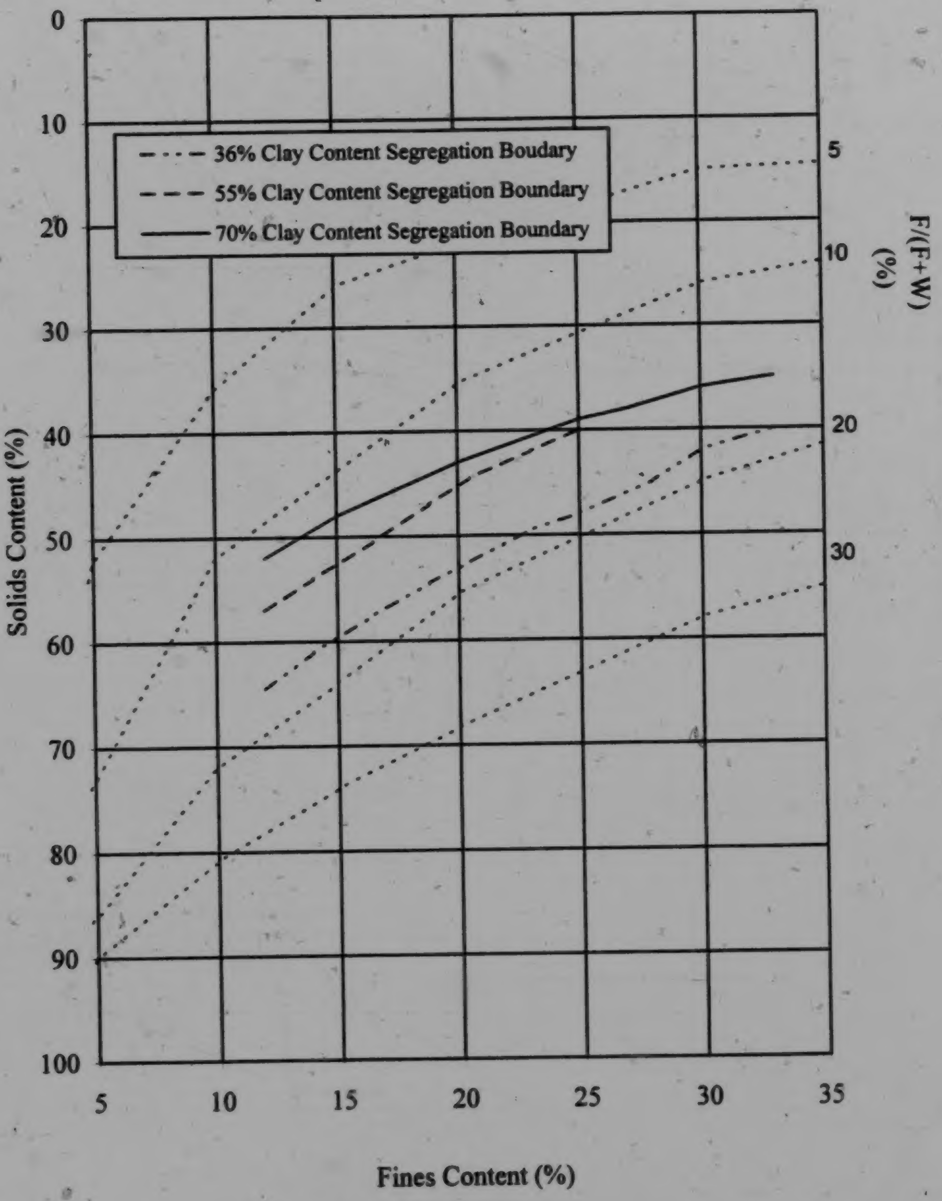

Figure 4.35: Segregation boundaries for tailings with 36%, 55% and 70% clay content MFT.

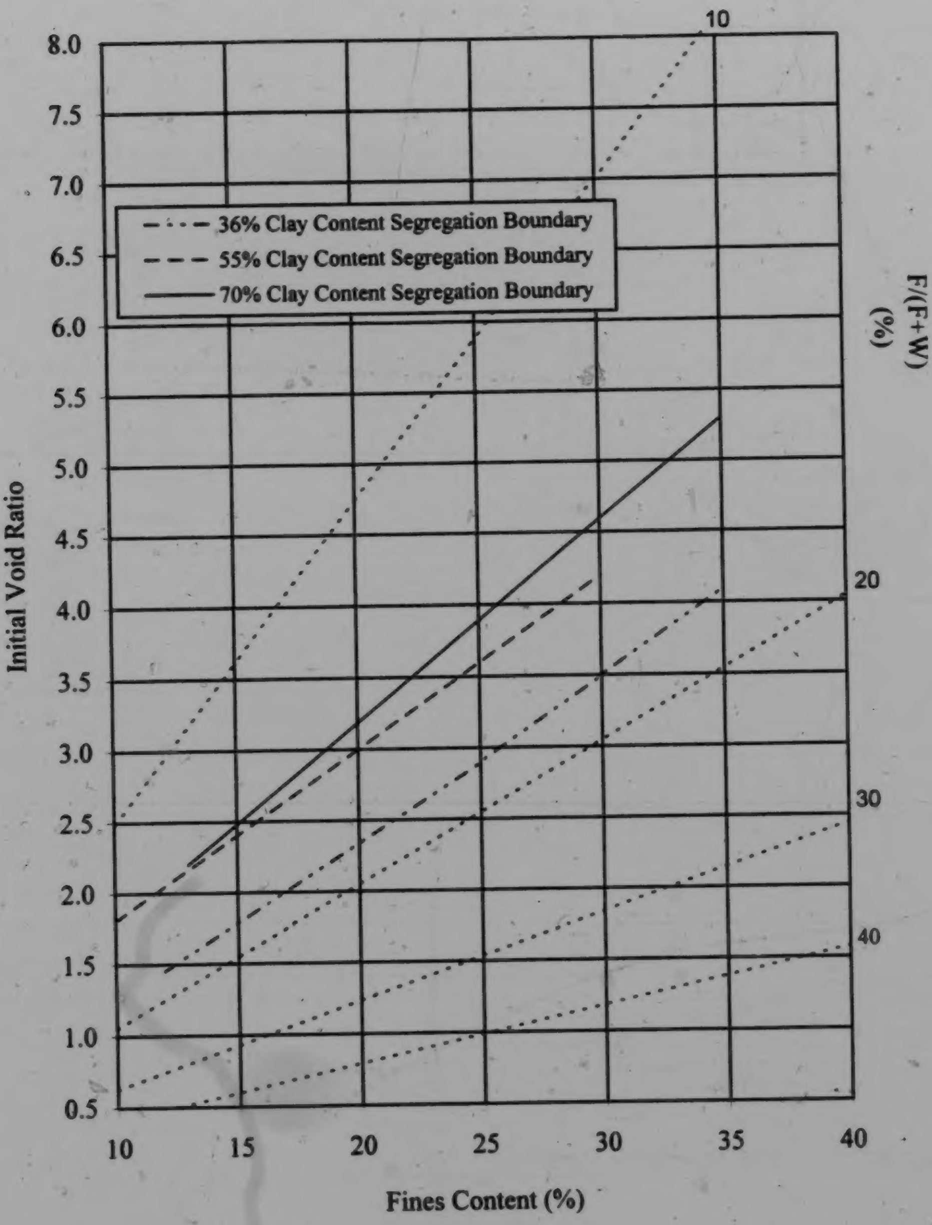

Figure 4.36: Segregation boundaries for CTs with 36%, 55% and 70% clay content MFT.

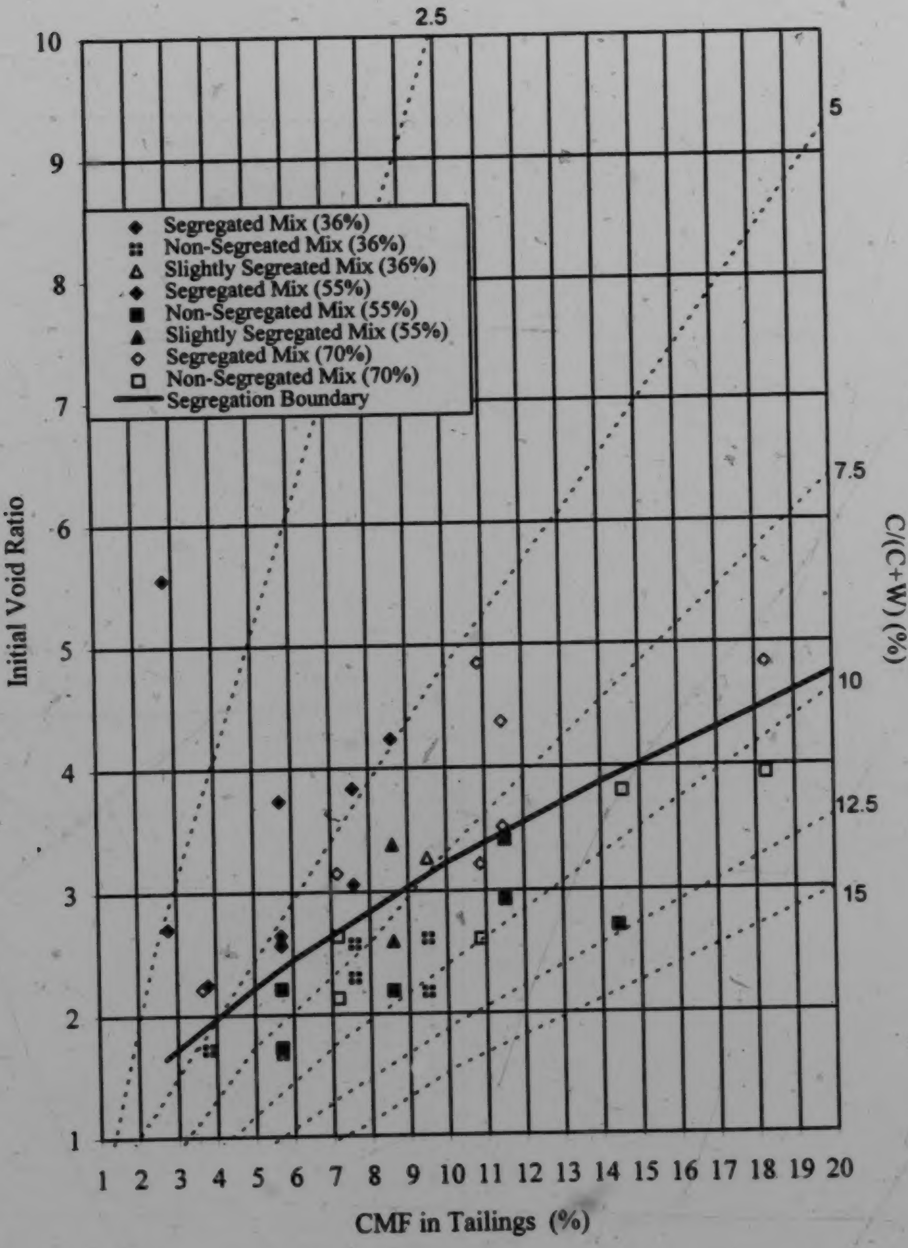

Figure 4.37: Segregation boundary for tailings treated with 900g/m3 of laboratory grade gypsum.

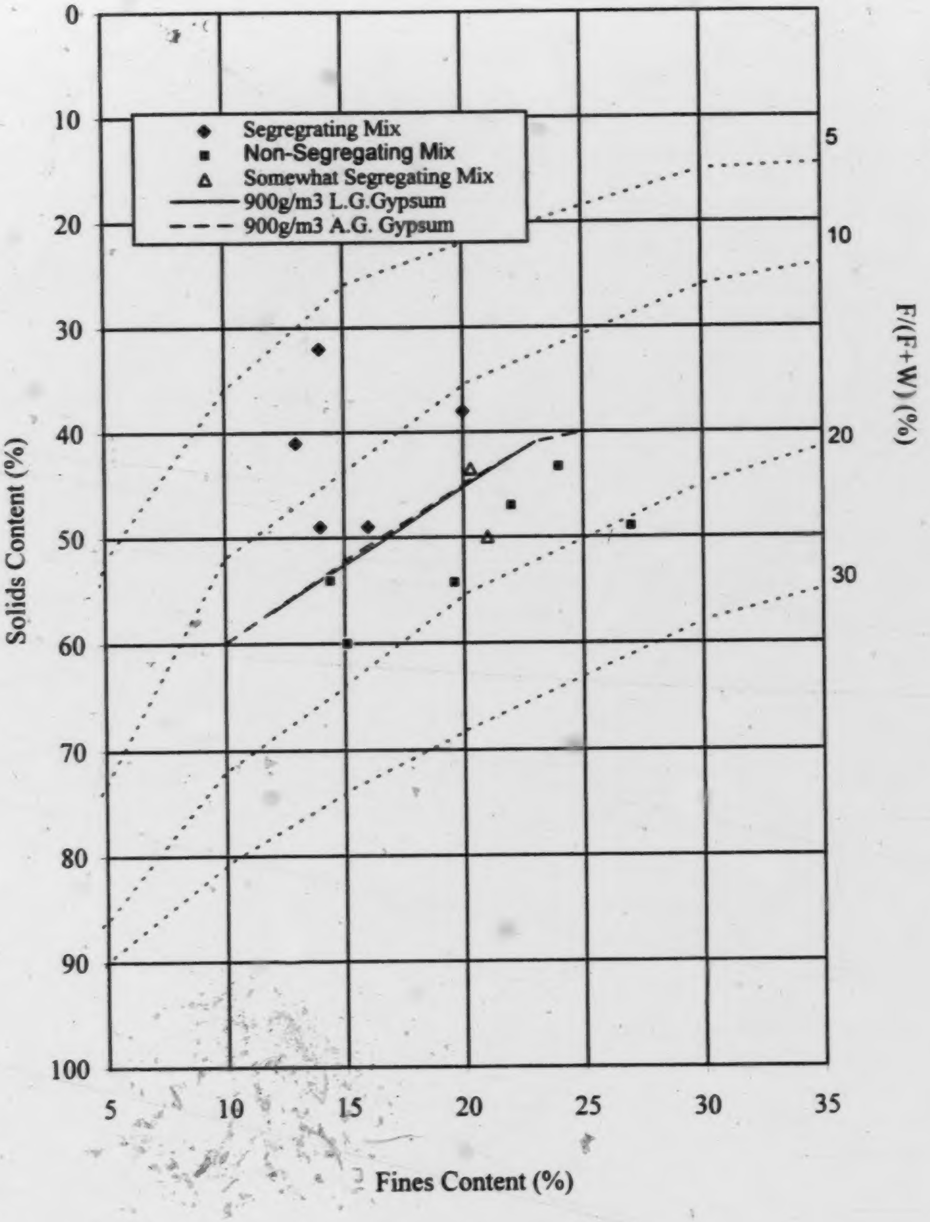

Figure 4.38: Segregation boundaries for tailings treated with laboratory grade, and agricultured grade gypsum.

5.0 Conclusions and Recommendations

The *card-house* structure of MFT is one of the characteristics that is responsible for its poor consolidation behaviour. It is important to understand how the MFT pore water chemistry can be altered to accelerate the rate of consolidation. A technique used in SCL to encourage rapid consolidation of MFT is by creating a composite tailings (CT). The success in creating a CT depends on the solids content, fines content, type and amount of chemical additives, and the clay content (particles < 2μm) of MFT.

There are two main studies in this thesis herein identified as the introductory and the principal studies. The purpose of the introductory study was to better understand the interaction between clay minerals and various pore water chemistry in MFT. This aids in understanding of the water chemistry-clay mineral interactions in CT. The study examined the effects of pore water chemistry, chemical additives and processing temperature on the formation of MFT *card-house* structure. This led to the principal study which examined the effects of varying amounts of clay content in MFT on the segregation and initial consolidation behaviour of CT.

Section 5.1 and 5.2 list the conclusion from the introductory and the principal studies respectively. These are followed by Section 5.3 which lists several recommendations for future work.

5.1 Conclusions to the Introductory Study (Chapter 3)

The Scanning Electron Microscope (SEM) was found to be a useful tool for examining the structures of both MFT and CT clay structures. In this chapter, the MFT structure was first examined to understand which chemicals found in MFT pore water are mainly responsible for the formation of the highly dispersed *card-house* structure. Prior to the examination of the structures, it was necessary to verify if the structures observed were artefacts of freezing during the sample preparation of SEM. Experiments performed in this study showed that the observed structures were not artefacts. The freezing temperature and the agents used during the SEM sample preparation process produced sufficiently rapid freezing rate to inhibit large ice crystal growth. When the samples were frozen at a slower rate, large ice crystal formation can distort the clay structure.

Examination of MFT structures found that the inorganic chemical in the MFT pore fluid that may contribute to the formation of the MFT *card-house* structure is HCO_3^-. However, it is argued that the pH level of MFT could be responsible for the formation of the structure instead of the HCO_3^-. NaOH, to a lesser extent, also appeared to contribute to the formation of MFT structure.

The bitumen and the strongly bound organic matter in MFT also appeared to be responsible for the *card-house* structure even though the exchangeable sodium ratio (ESR) of this sample suggested that a flocculated system should exist. It is also possible that the HCO_3^- in this sample was high enough to form the structure or under the influence of the pH. Further investigation of this matter is discussed in Section **5.3**. Sodium naphthenate, an organic compound that is responsible for the toxicity and poor consolidation of MFT, did not appeared to be responsible for the dispersed MFT *card-house* structure.

The addition of laboratory grade gypsum (LGG) to the MFT does not change the structure but made it finer and much stronger. That is a *card-house* structure was still evident however the particles were more aggregated.

The higher processing temperature used in the Clark Hot Water Extraction process enhances the *card-house* structure. Large spacing between rows of clay particles was observed in the heated sample.

Due to the scope of the thesis, standpipe tests were not performed to examine the effects of the above chemicals on the self-weight consolidation behaviour. However, it was observed that the slow self-weight consolidation rate of MFT is not controlled solely by the dispersed *card-house* structure. Although a *card-house* structure was observed in a kaolinite clay-HCO_3^- system, the particles settled in 3 hours leaving a clear layer of water. Conversely, NaOH and sodium naphthenates acted as dispersing agents preventing the particles from settling as quickly.

5.2 Conclusion to the Principal Study (Chapter 4)

As discussed in *Chapter 3*, the addition of LGG strengthened the MFT structure. In a non-segregating CT, the strengthened MFT structure supports sand particles that act as an internal surcharge compressing the MFT structure. As a result, the water is squeezed out of the MFT at a quicker rate increasing the self-weight consolidation rate of

MFT. This is evident in the SEM micro-graphs of the CTs which showed embedded sand particles within the MFT *card-house* structure.

MFT with 36%, 55% and 70% clay content along with the LGG treated MFTs were prepared. Both sets of MFT structures were examined under a SEM and the structures were compared. The LGG treated MFT samples showed a more aggregated *card-house* structure than the untreated samples.

Suncor Oil Sands Group conducted experiments suggesting that the segregation behaviour of CT is dependent on the parameter, *clay:water* ratio. They explained that all CTs with a *clay:water* ratio greater than 0.1 will not segregate. In this principal study, standpipe tests performed on CT with 36%, 55%, and 70% clay content MFT showed that the *clay:water* ratio of 0.1 was not unique. The *clay:water* ratio of the CT at the aforementioned clay contents were 0.085, 0.090, and 0.118 respectively. These ratios showed that the proposed *clay:water* ratio of 0.1 is conservative in predicting the segregation behaviour of CTs with less than 55% clay content and not as conservative in predicting the behaviour of CTs with greater than 55% clay content MFT.

Further investigation showed that the segregation boundary of CT with 36% clay content MFT plotted at the lowest position and CT with 70% clay content MFT plotted at the highest position on a Slurry Properties Diagram. This result indicated that the 36% clay content MFT did not have sufficient clay minerals to react with LGG, thus the clay structure formed was insufficiently strong to hold the sand grains. Consequently, this CT would require a higher solids content or a lower void ratio to form a non-segregating mixture.

The standpipe test results also showed that CT with 70% clay content MFT has the highest initial consolidation rate and change in void ratio. CT with 55% clay content MFT displayed the lowest initial consolidation rate and change in void ratio. This observed behaviour appeared to be mainly due to the bitumen content in the MFT. Bitumen blocks pore throats or flow channels preventing the pore fluid from escaping, hence decreasing the initial consolidation of the CTs. In this experiment, CT with 70% clay content MFT had the lowest bitumen content and the 55% clay content MFT had the highest. Consequently, the higher bitumen content was the cause of the slower initial consolidation rate in CT with 55% clay content MFT.

Majority of the CTs exhibits poor consolidation behaviour at fines content ranging from 25% to 30%. The higher the fines content in CT, the lower the hydraulic conductivity because the fine grained material blocks the flow channels inhibiting the water to flow out of the soil. Thus reducing the rate of initial consolidation.

A summary plot, which describes the relationship between clay mineral fraction (CMF), C/(C+W) ratio and the initial void ratio instead of *clay:water* ratio, was developed for all the standpipe test results. This plot can be used as a guide to predict the segregation behaviour of CT based on the amount of clay size particles. The plot can also be used to qualitatively predict the initial consolidation rate of CT. Provided that the bitumen content is constant, a CT plotted nearest to the segregation boundary has an optimum C/(C+W) ratio, and would undergo a higher initial consolidation rate than another CT that is plotted further away from the boundary. The engineering application of this plot is described in Section *4.5.5*.

5.3 Recommendations

5.3.1 Recommendations for Field Operations

In *Chapter 3*, it is suggested that HCO_3^- in the MFT pore water may be responsible for the formation of the *card-house* structure. HCO_3^- comes from the connate water of the oil sands ore, and from the Athabasca River. The formation of the *card-house* structure in MFT is therefore unavoidable. In the tailings water (or any water system), HCO_3^- exists between a pH of 8.3 and 10.6. Beyond this range of pH, HCO_3^- converts to H_2CO_3 at lower pH and CO_3^{2-} at a higher pH. However, it is also suggested that the pH of the MFT may have caused the formation of the structure rather than the HCO_3^-. It is recommended to lower or increase the pH of the tailings pore water to remove the HCO_3^- from the system or to modify the pH of MFT such that the *card-house* structure would be destroyed. However, it is necessary to predict and evaluate any adverse effects that may be caused by changing the pH of the tailings water or processing water.

The bitumen and *strongly bound* organic matter both appear to be responsible in part for the formation of the *card-house* structure. It is recommended that by re-extracting the bitumen from the MFT, the effects of these organic compounds on the MFT structure can be lessened. It is also advantageous to re-extract the bitumen from the MFT because the initial consolidation rate of CT is found to be highly dependent on the bitumen content. Thus it is recommended that the bitumen be extracted from the fine tailings or MFT before creating CT to optimise the initial consolidation rate.

5.3.2 Recommendations for Future Research

In *Chapter 3*, the particles settling behaviour of the kaolinite clays in slurries mixed with bicarbonate, sodium hydroxide, and sodium naphthenates were observed in this study. However, it is recommended to perform standpipe tests to study the effects of the above pore water chemicals on the initial consolidation characteristics of these kaolinite clay slurries. This would provide a better understanding of how these pore water chemicals affect the initial consolidation characteristics of MFT.

In a standpipe test, solids content of the kaolinite slurry should be similar to that of MFT and the soil-water interface is recorded with time as the soil material consolidates under self-weight. Other observations such as flow channels, development of foam, clarity of release water, and distinct layers of soil should also be recorded throughout the test period. A test period of two weeks may be sufficient to analyse the initial consolidation behaviour of the slurries.

Recall in *Chapter 3*, a sample of MFT was centrifuged twice to remove its pore fluid. The pore fluid was later replaced with deionized water. The SEM micro-graph of this sample indicated that the bitumen and the *strongly bound* organic matter may be responsible for the formation of the *card-house* structure. However, it is possible that the HCO_3^- (83ppm) that remained in the sample was high enough to form the structure. It is recommended to verify what concentration of HCO_3^- is sufficient to cause the structure in kaolinite clay. The experiment involves the addition of approximately 83ppm (by weight) of $NaHCO_3^-$ to kaolinite clay-deionised water slurry. The mixture will be prepared according to the procedure as described for Sample 4 listed in Table 3.1. The structure will then be observed under a SEM.

This leads to the discussion of whether the *card-house* structure is mainly influenced by the pH level or the HCO_3^-. The first test would involve varying the pH levels of MFT by adding acid or a base and then examine the structures under a SEM. This is to understand how the change in pH would affect the MFT structure. The second test is to vary concentration of HCO_3^- in kaolinite-deionized water slurry but maintaining the pH of the slurry at about 8.5. The samples will then be collected and examined under a SEM. This test is to understand the effect of varying concentration of HCO_3^- have on the structure without the influence of pH levels.

The exchangeable sodium ratio (ESR) of the 36%, 55%, and 70% clay content MFTs were overestimated because the Gapon exchangeable coefficient, K_G of 0.015 $(mmol/L)^{-1/2}$ was used. Recall that the coefficient decreases as sodium adsorption ratio (SAR) exceeds 30. However, these MFT had SARs greater than 30. In order to predict the ESR of these MFT accurately, laboratory testing is required to obtain an approximate value of K_G. However, information on the testing procedure still require further research and therefore will not be discussed in this thesis.

In *Chapter 4*, the bitumen content of the MFT with 36%, 55%, 70% clay content were performed using the Soxhlet extraction method. The results showed that the MFT with 70% clay content has the lowest bitumen content and the 55% clay content MFT has the highest. However, the accuracy of the Soxhlet extraction test results need to be verify. It is suggested that the test be performed on 5 to 10 samples from the same barrel of MFT to determine if the results are repeatable.

6.0 REFERENCES

Banas, L.C. 1991. Thixotropic Behaviour of Oil Sands Tailings Sludge. MSc. Thesis, University of Alberta, Department of Civil Engineering, Edmonton, Alberta, Canada. 394 p.

Babchin, A., Reitman, V., and Rispler, K. 1991. Settling of Synthetic Sludges and Kaolinites. Petroleum Society of CIM and AOSTRA 1991 Technical Conference, Banff, Alberta, April 21-24, 1991. Paper no. 91-127.

Braybrook, G., 1997. Personal Communications. Earth and Atmospheric Sciences Department, University of Alberta, Edmonton, Alberta.

Caughill, D.L. 1992. Geotechnics of Non-segregating Tailings. M.Sc. Thesis. University of Alberta, Department of Civil Engineering, Edmonton, Alberta, Canada. 243p.

Dusseault, M.B., Scott, J.D., Soderberg, H., and Moran, S. 1984. Swelling Clays and Post-Reclamation Mine Subsidence in Alberta. Fifth International Conference on Expansive Soils, Adelaide, South Australia. May 21- 23, 1984. pp 171-176.

Dudas, M. 1996. Soils 450 Course Notes. Department of Earth and Atmospheric Science. University of Alberta, Edmonton, Alberta.

Everhart, T.E., and Hayes, T.L. 1972. The Scanning Electron Microscope. Scientific Am. **226**:54.

Erol, O, Lohnes, R.A., Demirel, T. 1976. Preparation of Clay-type, Moisture-containing Samples for Scanning Electron Microscope. Proceedings of the Workshop on Techniques for Particulate Matter Studies in SEM (Part III), Chicago, Illinois, April 1976. pp 769-776.

FTFC (The Fine Tailings Fundamentals Consortium). 1995*a*. Geotechnical Properties of Mature Fine Tailings in Advances in Oil Sands Tailings Research. Alberta Department of Energy Oil Sands and Research Division. Vol. 1. Chap. 5.

FTFC (The Fine Tailings Fundamentals Consortium). 1995*b*. Quality of Fine Tails" in Oil Sands Tailings Research in Advances in Oil Sands Tailings Research. Alberta Department of Energy Oil Sands and Research Division. Vol. 2. Chap. 2.

FTFC (The Fine Tailings Fundamentals Consortium). 1995*c*. Extraction Factors in Advances in Oil Sands Tailings Research. Alberta Department of Energy Oil Sands and Research Division. Vol.1, Chap 2.

FTFC (The Fine Tailings Fundamentals Consortium). 1995*d*. Fine Tails and Process Water Reclamation in Advances in Oil Sands Tailings Research. Alberta Department of Energy Oil Sands and Research Division. Vol. 2, Chap. 1.

FTFC (The Fine Tailings Fundamentals Consortium). 1995*e*. Water Capped Fine Tails Lake in Advances in Oil Sands Tailings Research. Alberta Department of Energy Oil Sands and Research Division. Vol. 2. Chap. 3.

FTFC (The Fine Tailings Fundamentals Consortium). 1995*f*. Fundamental Properties of Fine Tails in Advances in Oil Sands Tailings Research. Alberta Department of Energy Oil Sands and Research Vol. 1, Chap. 4.

FTFC (The Fine Tailings Fundamentals Consortium). 1995*g*. Volume Reduction of CHWE Fine Tailings Utilizing Nonsegregating Tailings in Advances in Oil Sands Tailings Research. Alberta Department of Energy Oil Sands and Research Division. Vol. 3. Chap. 3.

FTFC (The Fine Tailings Fundamentals Consortium). 1995*h*. Environmental Discharge of NST Release Water in Advances in Oil Sands Tailings Research. Alberta Department of Energy Oil Sands and Research Vol. 3, Chap. 6.

Griffin, R.A. and Jurinak, J.J. 1973. Estimation of Activity Coefficients From Electrical Conductivity. Soil Science **116**: 26-30.

Gully, J.R. and MacKinnon, M. 1993. Fine Tails Reclamation Utilizing a Wet Landscape Approach. Proceeding, Oil Sands - Our Petroleum Future Conference, Edmonton, Alberta, April 4-7, 1993. F23.

Hereygers, C. 1997. Personal Communications. Civil and Environmental Engineering Department, University of Alberta, Edmonton, Alberta.

Ignasiak, T.M., Zhang, Q., Kratochvil, B., Maitra, C., Montgomery , D.S., and Stausz, O.P., 1985. Chemical and Mineral Characterization of the Bitumen-Free Athabasca Oil Sands Related to the Bitumen Concentration in the Sand Tailings from the Syncrude Batch Extraction Test. AOSTRA Journal of Research. **1**:21.

Kasperski, K.L., 1992. A review of Properties and Treatment of Oil Sands Tailings. AOSTRA Journal of Research. **8**:11-53

Kotlyar, L. S., and Sparks, B.D. 1990. Isolation and Characterization of Organic-Rich Solids Present in Athabasca Tailings Pond Sludge. AOSTRA Journal of Research **6**: 41-51.

List, B.R. and Lord, E.R.F. 1997. Syncrude's tailings management practices from research to implementation. The Canadian Mining and Metallurgical Bulletin. **90**: 39-44.

Liu Y.B, Caughill, D.L., Shaw W., Lord, E., Burns, R., and Scott, J.D. 1996. Volume reduction of oil sands fine tails utilizing nonsegregating tailings. Proceedings of Tailings and Mine Waste '96 Conference, Colorado State University, Fort Collins, Colorado, Jan 16-19.

Majid, A., Sparks, B.D., Ripmeester, J.A. 1990. Characterization of Insoluble Organic Matter Associated with Non-Settling Clay Minerals from Syncrude Sludge Pond Tailings. Fuel. **69**:145-150.

Mikula, R.J., Payette, C., Munoz, V., Lam, W.W. 1991. Microscopic Observation of Structure in Oil Sands Sludge. The Petroleum Society of CIM and AOSTRA 1991 Technical Conference, Banff, Alberta, April 21-24, 1991. Paper no. 91-120.

Mikula, R.J., Angle, R.Z., Kan, J., and Xu, Y. 1993. Factors that Determine Oil Sands Sludge Properties. Division Report WRC 93-40 (CF). CANMET, Energy, Mines and Resources Canada.

Mikula, R.J., Kasperski, K.L., Burns, R.D., MacKinnon, M.D. 1996*a*. Nature and Fate of Oil Sands Fine Tailings in Suspensions: Fundamentals and Applications in the Petroleum Industry. *Edited by* L.L. Schramm. pp. 677-723

Mikula, R.J. 1996*b*. Personal Communication. CANMET, Devon, Alberta.

Mitchell, J.K. 1993. Fundamentals of Soil Behaviour, 2nd Edition. John Wiley & Sons Inc. 437p.

Mitchell, J.K. 1960. Fundamental aspects of thixotropy in soils. Journal of Soil Mechanics Foundations Divisions American Society of Civil Engineers. **86**(3): 19-52.

Morgenstern, N.R. and Scott, J.D. 1994. Geotechnics of Fine Tailings Management. Geoenvironment 2000, ASCE Specialty Conference, New Orleans, February 24-26, 1995.

Pane, V. and Schiffman, R.L. 1997. The permeability of clay suspension. Geotechnique **47**(2): 273-288.

Sawyer, C.N., McCarty, P.L., Parkin, G.F. 1994. Chemistry for Environmental Engineering, 4th Edition. McGraw-Hill Inc. 658p.

Scott, J.D. and Dusseault, M.B. 1982. Behaviour of Oil sands Tailings Sludge. Proceedings, 33rd Annual Technical Meeting of the Canadian Institute of Mining and Metallurgy, Calgary, Alberta, June 1982. Paper no. 82-33-85. 19 p.

Scott, J.D., Dusseault, M.B., and Carrier III, W. David. 1985. Behaviour of the Clay/Bitumen/Water Sludge System from Oil sands Extraction Plants. Applied Clay Science, 1:207-218.

Scott, J.D., Liu, Y., and Caughill, D.L. 1993. Fine Tails Disposal Utilizing Nonsegregating Mixes. Proceedings, Oil Sands - Our Petroleum Future Conference, Edmonton, Alberta, April 4-7, 1993. F18. 19p.

Shaw, R.C., Schramm, L.L, and Czarnecki, J. 1996. Suspension in the Hot Water Floatation Process for Canadian Oil Sands in Suspensions: Fundamentals and Applications in the Petroleum Industry. *Edited by* L.L. Schramm. pp. 639-675.

SOSG (Suncor Oil Sand Group Limited). 1996. Suncor Steepbank Mine Application Second Request for Supplemental Information. Report to Alberta Environmental Utility Board.

Stahl, R. P. 1996. Dry Land Reclamation of Fine Mine Waste. PhD. Thesis, University of Alberta, Department of Civil Engineering, Edmonton, Alberta, Canada. 297 p.

Suthaker, N.N. 1995. Geotechnics of Oil Sand Fine Tailings. PhD. Thesis, University of Alberta, Department of Civil Engineering , Edmonton, Alberta, Canada. 223 p.

Suthaker, N.N., Scott, J.D. 1996*a*. Syncrude Phosphogypsum CT Standpipe Tests to Determine the Segregation Boundary. Report to Syncrude Canada Limited.

Suthaker, N.N., Scott, J.D. 1996*b*. Syncrude Agricultured Grade Gypsum Composite
Tailings; Part 1: Standpipe tests to determine the optimum additive,
Part 2: Standpipe tsts to determine the segregation boundary,
Part 3: Multilayer standpipe tests to determine the water release and to model the Syncrude 1995 NST field demonstration,
Part 4: Standpipe tests to determine the initial permeability and compressibility.
Report to Syncrude Canada Limited.

Suthaker, N.N. 1997. Personal Communications. Geotechnical and Geoenvironmental Engineering Department, University of Alberta, Edmonton, Alberta.

Tan, K.H. 1993. Principles of Soil Chemistry, 2nd Edition. Marcel Dekker Inc. 362p.

van Olphen, H. 1977. An Introduction to Clay Colloid Chemistry, 2nd Edition. John Wiley & Sons Inc. 301p.

Yong, R.N. and Sethi R.N., 1978. Mineral Particle Interaction Control of Tar Sand Sludge Stability. Journal of Canadian Petroleum Technology. 17:76-83.

Appendix 1: Sample Calculations

1. To calculate wet mass required for hydrometer test:

Solids content of MFT = 27.5%
mass of dry solids required = 50g

let X be the mass of total MFT wet mass
let a be the mass of total MFT dry mass

$$S(\%) = \frac{a}{X}$$

$$X = \frac{50g}{0.275}$$

$$\boxed{X = 181.8g}$$

181.8g of MFT is mixed with 2.5g of Calgon and stirred for 5 minutes.

2. Making kaolinite or silica flour slurries at approximately 28% solids content

For **100g** of slurry and at **28%** solids content:

$S(\%) = \frac{a}{X}$, where a is the mass of dry solids and X is the mass of wet soil soil material

$$28\% = \frac{a}{100g}$$

$$a = 0.28(100g)$$

Mass of kaolinite clay or silica flour required = **28g**

$$X = \text{water} + 28g$$

$$= 100g - 28g$$

Mass of deionized water required = **72g**

3. Exchangeable Sodium Ratio

a) ESR = 0.015 SAR

$$\text{SAR} = \frac{[Na]}{\sqrt{\frac{[Ca]+[Mg]}{2}}}$$, [] is expressed in meq/L

and meq/L = (mg/L)/(atomic weight/charge of the ion)

if [Na] is 600ppm, [Ca] is 200ppm, and [Mg] is 30ppm:

$$\begin{aligned}\text{SAR} &= \frac{\frac{600}{23}}{\sqrt{\frac{200/20 + 30/12.2}{2}}}\\ &= \frac{26.1}{2.5}\\ &= 10.5\\ \text{ESR} &= 0.015(10.5)\\ &= \mathbf{0.16}\end{aligned}$$

b) to calculate the amount of NaOH and $CaSO_4$ required to make a slurry with ESR >> 0.1

For ESR >> 0.1, let ESR = 2

ESR = 0.015 SAR

The author is aware that K_G in the Gapon equation should be less than 0.015 $(\text{mmol/L})^{-1/2}$ since SAR of the kaolinite clay slurry is greater than 30. For this SAR, it is necessary to determine K_G experimentally to predict ESR of the slurry accurately. However, the purpose of this exercise is not to obtain an exact ESR for the slurry but to obtain a kaolinite clay system that has a dispersed clay strucutre. Hence an ESR of 2.0 was chosen which provides a large factor of safety. The Gapon equation is only used as a guide to approximate the concentrations of NaOH and $CaSO_4 \bullet 2H_2O$ that would result in a dispersed clay structure.

$$\text{SAR} = \frac{0.01}{0.015} = \frac{[Na]}{\sqrt{\frac{[Ca]+[Mg]}{2}}}$$

$$133.3 = \frac{[Na]}{\sqrt{\frac{[Ca]+0}{2}}}$$

$$\left[0.667\left(\sqrt{\frac{[Ca]}{2}}\right)\right]^2 = ([Na])^2$$

$$17768.9\left(\frac{[Ca]}{2}\right) = ([Na])^2$$

$$\boxed{8884.4[Ca] = [Na]^2} \qquad \text{(A1)}$$

The concentration of Na and Ca are expressed in meq/L:

$[Na] = \frac{x}{23}$ $\quad [Ca] = \frac{y}{{}^{40}\!/_{2}}$, where x and y are the concentration of Na and Ca respectively expressed in mg/L or ppm.

Replace equation (A1) with the concentration of Na and Ca expressed in meq/L:

$$\frac{x}{23} = 94.3\left(\frac{y}{20}\right)^{\frac{1}{2}} \qquad \text{(A2)}$$

Therefore for 100mL of kaolinite or silica flour-deionized water slurry:
if x = 5000ppm = **0.5g/100mL**, then from equation (A2), y = 106ppm = **0.01g/100mL**.

4. MFT (SY-22) Separation Process

Syncrude pond water is added to 15L of MFT with solids content of 27.5% to achieve a solids content of approximately 6.5%.

For 100mL of MFT = 107g, therefore 15L = 16.1kg

$S(\%) = \frac{a}{X}$, where a is the mass of dry solids and X is the mass of wet soil soil material

$$27.5\% = \frac{a}{16.1kg}$$
$$a = 4.4kg$$

Then for 6.5% solids content:

$$6.5\% = \frac{4.4kg}{X}$$
$$X = 68.1kg = \text{pond water} + 4.4kg$$

Pond water required = **63.7*kg***

5. Fines Content

Following the standpipe test, samples of tailings were collected to determine the solids and fines content. The sequence of which the samples were taken collected for solids and fines content is illustrated as follow:

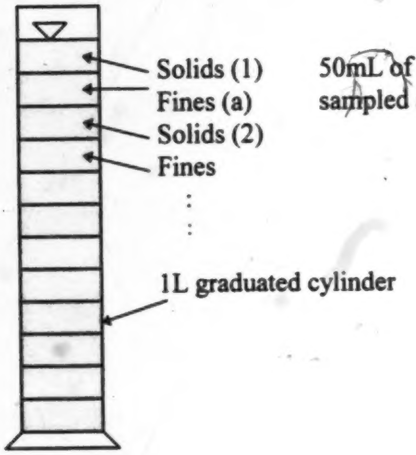

50mL of solids or fines content samples were sampled alternately throughout the cylinder.

For fines content (a), take the average of the solids content (1) and (2):
Average $S(\%)$ = 38.0%

Initial total wet mass of sample, *r*, collected for fines content determination	= 52.3g
Mass of material retained on the #325 sieve	= 13.3g

Let Z be the initial total dry solids of the sample taken for fines content determination.

It is assumed that the solids content of the sample collected for fines content determination is the average solids content of the sample above and below.

$$38\% = \frac{Z}{52.3g}$$
$$Z = 19.9g$$

$$\text{Fines content (\%)} = \frac{Z-r}{Z} \text{ x } 100\%$$

$$= \frac{19.9-13.3}{19.9} \text{ x } 100\%$$

$$= \mathbf{33.2\%}$$

6. *Sands(%)* and SFR

$$\textit{Sands (\%)} = 100\% - \text{Fines content}$$
$$= 100\% - 33.2\%$$
$$= \mathbf{66.8\%}$$

$$\text{SFR} = \frac{66.8\%}{33.2\%}$$
$$= \mathbf{2.0}$$

7. Clay Mineral Fraction (CMF)

a) Clay content obtained from hydrometer test:
This tailings sample has 50% solids content and 20% fines content. The MFT has 55% clay size material and 95% of the MFT are <45μm. The beach sand has 4% clay size material, 5.6% of the sand are <45μm and 89.4% solids content.

Total wet mass of MFT = 511g
Mass of dry solids in this MFT = 511g x 27.3%
= 139.5g
Mass of dry solids <45μm in this MFT = 139.5g x 95%
= 132.5g

Total wet mass of beach sand = 813g
Mass of dry solids in this sand = 813g x 89.4%
= 726.8g
Mass of dry solids <45μm in the sand = 726.8 x 5.6%
= 40.7g

Total dry solids in the tailings mix = 139.5g + 726.8g
= 866.3g

Percent of total dry solids <45μm found in MFT

$$= \frac{132.5}{866.3} \text{g} \times 100\% \qquad \text{(A3)}$$

= 15.3%

Percent of total dry solids <45μm found in the sand

$$= \frac{40.7}{866.3} \text{g} \times 100\% \qquad \text{(A4)}$$

= 4.7%

Clay Mineral Fraction of the tailings (%)
= (A3) x (% clay size material in MFT) +
(A4) x (% clay size material in beach sand)

= (15.3% x 55%) + (4.7% x 4%)
= **8.6%**

b) CMF obtained from methylene blue test

The methylene blue test was performed by the McMurray Resources Ltd. (Research and Testing).

$$\text{CMF (\%)} = \frac{0.006\,MB\#+0.04}{14}$$

, where *MB#* is the methylene blue number obtained through methylene blue test provided by the McMurray Resources (Research and Testing) Ltd.

8. Initial Void Ratio

$$e_i = \frac{G_s(1-S\%)}{S\%}$$

$G_s = 2.6$ (for MFT and sand mixer)

for $S\% = 50\%$

$$e_i = \frac{2.6(1-0.5)}{0.5}$$

$$= \mathbf{2.6}$$

9. F/(F+W) and C/(C+W)

For a tailings with

Fines content = 16.8%

Solids content = 53.6%

Clay content (determined by hydrometer test)= 36%

CMF = 3.8%

Sands = 83.2%

$$F/(F+W) = \frac{16.8\%(53.6\% / 100\%)}{(16.8\%(53.6\% / 100\%)) + (100\% - 53.6\%)} \text{ x } 100\%$$

$$= \mathbf{16.25\%}$$

"C" in C/(C+W) is the total amount of clay size material in the tailings. Therefore,

C = CMF x Solids content

C = (3.8%/100%) x 53.6%

= 2.0%

$$C/(C+W) = \frac{2.0\%}{2.0\% + (100\% - 53.6\%)} \text{ x } 100\%$$

$$= \mathbf{4.2\%}$$

10. *Clay/Water* and *Clay/Sands* ratio

The clay content of in these ratio does not include the clay size material in the MFT and the beach sand used in making CT. It was simplified that 100% of the MFT material was < 45μm, and 36%, 55% or 70% of the MFT was clay size material.

Using the example in **9.**:

$$Clay/Water = \frac{\underline{(36\%/100\%) \times (16.8\%/100\%) \times 53.6\%}}{100\% - 53.6\%}$$

$$= \mathbf{0.07}$$

$$Clay/Sand = \frac{\underline{(36\%/100\%) \times (16.8\%/100\%) \times 53.6\%}}{(83.2\%/100\%) \times 53.6\%}$$

$$= \mathbf{0.07}$$

11. Segregation Index (SI)

The weighted average of a tailings for a standpipe test is first calculated before determining the SI. This table shows the solids content, sampling heights, normalized heights, SI and weighted average of the tailings that has 55% solids content, and 15% fines content with 36% clay size material.

Table A.1: Table used for calculating SI

Solid Content (%)	Sampling Height (mL)	Sampling Height (cm)	H/Hf	SI	Weighted Ave. S(%)
37.3	565	17.0	1	26.73	3.79
71.1	450	13.5	0.80	0.11	13.16
73.9	356	10.7	0.63	n/a	13.08
75.0	250	7.5	0.44	0.06	13.68
75.2	150	4.5	0.27	0.00	13.30
75.9	50	1.5	0.09	0.58	10.07
				27.49	**67.09**

a) Weighted average solids content:

at $H/H_f = 1$, $S_{weighted}\%$ $= S\%\left(\frac{h_i - h_{i-1}}{2}\right)$

$$= 37.3\%\left(\frac{1.0 - 0.8}{2}\right)$$

$$= \mathbf{3.79\%}$$

at $H/H_f = 0.8$, $S_{weighted}\%$
$$= S\%\left(\frac{h_{i+1} - h_i}{2} + \frac{h_i - h_{i-1}}{2}\right)$$
$$= 71.1\%\left(\frac{1.0 - 0.8}{2} + \frac{0.8 - 0.63}{2}\right)$$
$$= \mathbf{13.16\%}$$

the above step is repeated until the last row of data:

at $H/H_f = 0.09$, $S_{weighted}\%$
$$= S\%\left(\frac{h_{i+1} - h_i}{2}\right)$$
$$= 75.9\%\left(\frac{0.27 - 0.09}{2}\right)$$
$$= \mathbf{10.07\%}$$

The total weighted average was then calculated by summing the weighted average at each height.

From SI was calculated using the following equation:

$$SI = \frac{\Sigma\left|(S_i - S_{ave}) * \left[\left(\frac{\frac{H_{i+1}}{H_f} - \frac{H_i}{H_f}}{2}\right) - \left(\frac{\frac{H_i}{H_f} - \frac{H_{i-1}}{H_f}}{2}\right)\right]\right|}{S_{ave}} * 100\%$$

S_i is the solids content at the sampling height (cm) "i", S_{ave} is the total weighted average, and H_f is the sampling height (cm) recorded immediately after the standpipe test.

"n/a" is denoted as a negative number which is excluded in the calculation.

12. Cavity Expansion Test

Figure A-1 and A-2 show the output data for the Cavity Expansion Test for the two day old MFT and the MFT treated with 2500g/m^3 of LGG. The latter sample was also left undisturbed for two days.
Three readings were taken and they were labelled as "a", "b", "c". These points were approximately 120° from each other.

The output (V) was converted to psi using the following calibration:
y = 0.0115 + 0.054658x, where x is the difference between the peak voltage and

the base of the curve at which it begins to rise towards the peak.

Cu_{peak} (Pa) = y(0.75)(6895)
the peak strength is taken at 75% of the maximum bubble shear strength and the strength is converted to Pa from psi by multiplying the y value with 6895.

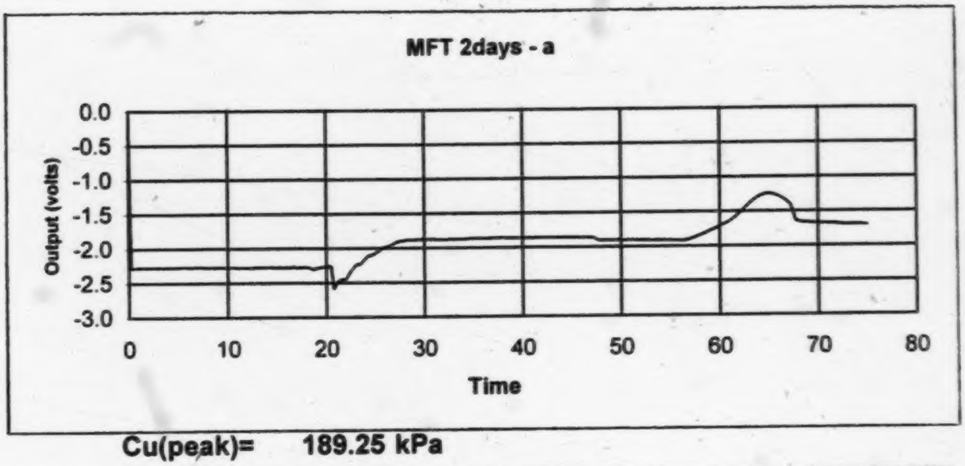

Cu(peak)= 189.25 kPa

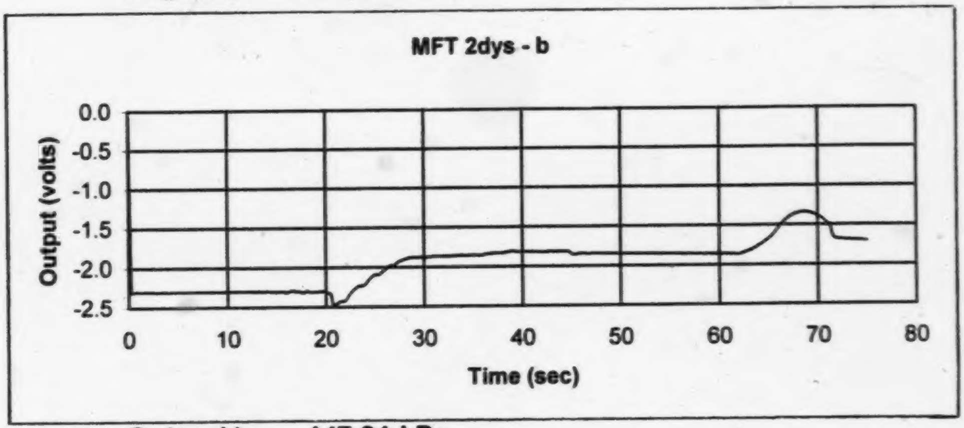

Cu(peak)= 147.24 kPa

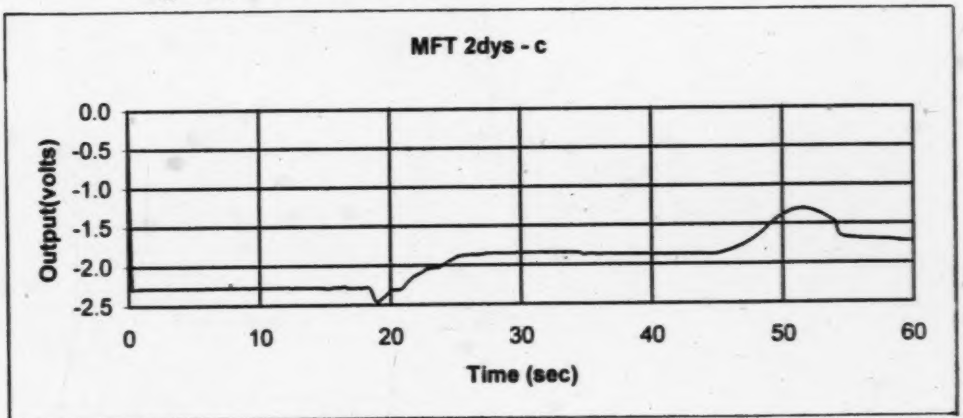

Cu(peak)= 161.13 kPa

Figure A-1: Output data for Cavity Expansion Test on two day old MFT (SY-22).

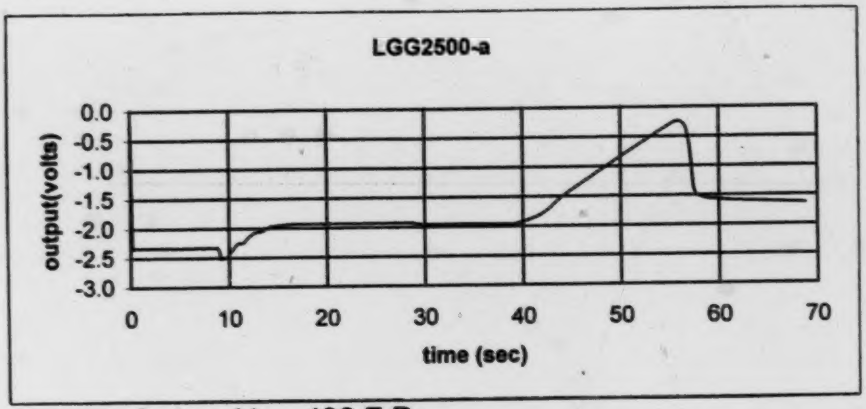

Cu(peak)= 483.7 Pa

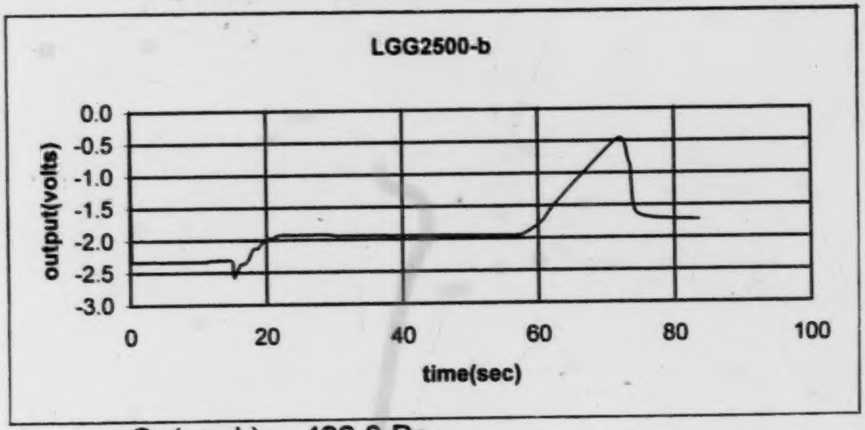

Cu(peak)= 422.3 Pa

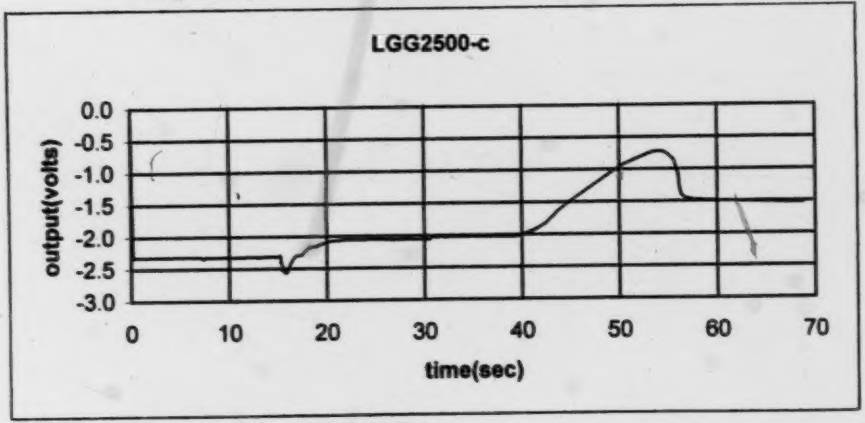

Cu(peak)= 355.2 Pa

Figure A-2: Output data for Cavity Expansion Test on MFT treated with 2500g/m^3 of LGG